Mechanisms of epithelial morphogenesis and integrity during *Nematostella vectensis* development and *Shigella* pathogenesis

BY

ASHLEIGH E FRITZ

Submitted to the graduate degree program in Cell Biology and Anatomy and the Graduate Faculty of the University of Kansas in partial fulfillment of the requirements for the degree of Doctor of Philosophy.

_____

Matthew C. Gibson, Ph.D., Co-Chair

_____

William H. Kinsey, Ph.D., Co-Chair

_____

Lane K. Christenson, Ph.D.

_____

Jennifer L. Gerton, Ph.D.

_____

Brenda J. Rongish, Ph.D.

Date Defended: March 28, 2014

The Dissertation Committee for Ashleigh E Fritz
certifies that this is the approved version of the following dissertation:

Mechanisms of epithelial morphogenesis and integrity during *Nematostella vectensis* development and *Shigella* pathogenesis

_____
Matthew C. Gibson, Ph.D., Co-Chair

_____
William H. Kinsey, Ph.D., Co-Chair

Date approved: April 4, 2014

Abstract

The transition to animal multicellularity involved the evolution of single cells organizing into sheets of tissue. The advent of tissues allowed for specialization and diversification, which led to the formation of complex structures and a variety of body plans. These epithelial tissues undergo morphogenesis during animal development, and the establishment and maintenance of their polarity and integrity is crucial for homeostasis and prevention of pathogenesis. This architecture is dynamically maintained through a variety of cellular processes including the regulation of intracellular transport, cytoskeletal modulation, and cell adhesion. While studies in established model organisms and cell culture have contributed to our current knowledge of these processes, evolutionary and *in vivo* perspectives are largely lacking. Our efforts to gain a better understanding of epithelial biology have centered around two main themes: 1) Ancient mechanisms of morphogenesis during animal development and 2) Modulation of epithelial architecture during pathogenesis.

First, to address the ancient mechanisms of epithelial morphogenesis, we examine tentacle development in the cnidarian *Nematostella vectensis* as a model of outgrowth formation. Through drug treatments, transcriptional analysis and imaging experiments, our study identifies molecular and cellular mechanisms that act during elongation of the tentacles and body column. At the onset of tentacle development, we observe an ectodermal placode that forms at the oral end of the animal, which is transcriptionally patterned into four tentacle buds. Subsequently during morphogenesis, our results show that cell shape changes and cell rearrangements act during elongation

of the bud into a mature tentacle. In the body column during elongation, we also observe a period of oriented cell divisions along the oral-aboral axis. Together, our results reveal ancient cellular and molecular mechanisms of epithelial morphogenesis during development in an early-branching metazoan.

Second, to explore alterations in epithelial architecture and integrity during bacterial pathogenesis, we express a *Shigella* bacterial virulence protein, VirA, in *Drosophila* and vertebrate tissue. Previous reports on the function of VirA have only employed *in vitro* and cell culture assays, so the function of VirA in an epithelial context remains largely unknown. Through *in vivo* expression and imaging experiments, we show that VirA expression in *Drosophila* disrupts epithelial architecture and cell polarity, with no discernible effects on microtubule stability. In the *Drosophila* salivary gland and eye imaginal disc, cells expressing VirA round and lose polarity markers. We observe a similar apical cell rounding phenotype when VirA is expressed in chick neural tube, implying a conserved mechanism of VirA function in vertebrates. Finally, we demonstrate a mislocalization of Rab11 in VirA expressing epithelia, suggesting a potential defect in vesicle trafficking. Taken together, our results reveal a novel function for VirA in disruption of cell polarity or adhesion, possibly through vesicle trafficking, leading to a breakdown of epithelial integrity facilitating the pathogenesis of *Shigella* in the human intestinal epithelium.

Acknowledgements

This dissertation and my doctoral degree would not have been possible without the support and encouragement of many people. First, I would like to thank my advisor, Dr. Matthew Gibson. Over the course of my graduate career, you have taught me to ask meaningful questions, conduct informative experiments, and communicate my science effectively. Additionally, I am grateful that you allowed me the freedom to work on system not yet established in the lab and on a project I thought was stimulating. Also, I would like to thank Dr. Aissam Ikmi for all of the meaningful discussions on my experiments, science, and writing. Furthermore, I appreciate all the other current and past members of the Gibson Lab. Thank you not only for your feedback on my projects and presentations, but also for your support and friendship both in and outside of the lab.

Next, I would like to thank my committee members, Drs. Lane Christenson, Jennifer Gerton, William Kinsey, and Brenda Rongish for their feedback and support during my graduate career. Thank you all for attending meetings, reading my proposal and dissertation, and providing me with thought provoking questions and suggestions that have contributed to my research. I would also like to especially thank Brenda for always being supportive, helpful, and available when I have questions or need anything. Additionally, I would like to thank Drs. Doug Wright and Peggy Petroff for all of their assistance, guidance, and encouragement during my graduate studies in the Department of Anatomy and Cell Biology.

Further, all of the experiments in this dissertation could not have been completed without the generous support of the Stowers Institute for Medical Research and the core facilities. Thank you to Diana Baumann and the Aquatics facility members for maintaining and taking such great care of our *Nematostella* population. Additionally, I appreciate all the work Chris Seidel and Ariel Paulson put into analysis of the microarray results. I would also like to thank the Molecular Biology core for carrying out the microarray experiment. Lastly, I am grateful for the efforts of Teri Parmley and the members of the Tissue Culture facility for culturing and transfecting HeLa cells.

I would also like to thank my undergraduate mentors and professors who motivated me to pursue a graduate degree in science. I am grateful for the fantastic undergraduate education, which prepared me for the challenge of doctoral research. I would like to specifically thank Drs. Brent Buckner and Diane Janick-Buckner and Anne Bergey for your encouragement and mentoring during my undergraduate career.

Last, but definitely not least, I would like to especially thank my family and friends. My family has always encouraged me to succeed and has taught me to hold myself to high expectations. Without this, I would not be where I am today. While many of my friends and family have not been directly involved in my research or experiments, you all have personally supported me and helped me to stay motivated throughout my doctoral career. Not only have you taken the time to listen to my problems and struggles, but also you have celebrated my accomplishments, all the while providing constant encouragement; for all of this, I am extremely grateful.

Table of Contents

List of figures and tables

Chapter 1: Introduction

The transition to animal multicellularity involved single cells organizing into tissue sheets. The formation of tissues allowed for the evolution of more complex structures and the diversity of body plans that exist among animals. Thus, epithelia are a common and defining feature of all metazoan animals, which allow for tissue morphogenesis during the development of organs and structures and serve as barriers to body compartments and pathogens from the outside environment. This tissue type is characterized by its distinctly apical-basal polarized, adherent cells (reviewed in Fristrom, 1988). The research during my graduate career has focused on two main topics: 1) Ancient mechanisms of epithelial morphogenesis during development of a basal metazoan and 2) How epithelial architecture and integrity are altered during pathogenesis. Accordingly, the introduction to this dissertation concentrates on these themes by first covering the fundamentals of epithelial tissue polarity and architecture. Subsequently, I explore the topics of mechanisms of epithelial morphogenesis during animal development and epithelial integrity during bacterial pathogenesis.

Epithelial tissue polarity and architecture

Cell polarity, adhesion, and tissue architecture

To study the processes of morphogenesis and integrity of epithelial tissue, we must first understand how these tissues are polarized and assembled into sheets. Epithelial cells' ability to self-organize into tissue sheets is based on their apical-basal polarization. Adherent cells orient with the apical surfaces towards the outside environment or lumen. The basal surface generally contacts a secreted extracellular matrix, the basal lamina. Polarized epithelial cells contain two main domains along the apico-basal axis: apical and basolateral. Each membrane domain has a specific composition containing distinct sets of proteins and is physically separated by junctional complexes. The establishment and maintenance of polarity involves various cellular processes including polarized vesicle trafficking, polarity protein localization, and physical separation of the domains by the junctions.

Studies in *Drosophila* and vertebrate model systems have revealed differences between their junctional architecture (Figure 1.1). These junctions and their associated proteins assist in the functions of paracellular barrier, adhesion, linking the membrane to the cytoskeleton, and the establishment and maintenance of polarity. At the most apical region of the lateral membrane in *Drosophila* is the subapical region (SAR) or marginal zone, which is devoid of junctions and functions in cell polarity (Tepass, 1996). Apical protein determinants including Crumbs, Atypical Protein Kinase C (aPKC), and Par3 (Bazooka in *Drosophila*) are localized here (Tepass, 1996; Wodarz et al., 2000). Just

Figure 1.1 – Epithelial cell junctions in *Drosophila* and vertebrates

Schematic representation of the epithelial cell junctions in *Drosophila melanogaster* and vertebrates from Macara (2004). In *Drosophila*, there are two main apical junctions: the adherens junctions (zona adherens) and the more basally localized septate junctions. Vertebrates instead have apical tight junctions and more basal adherens junctions. Each junction localizes a different subset of proteins including those involved in the establishment and maintenance of polarity.

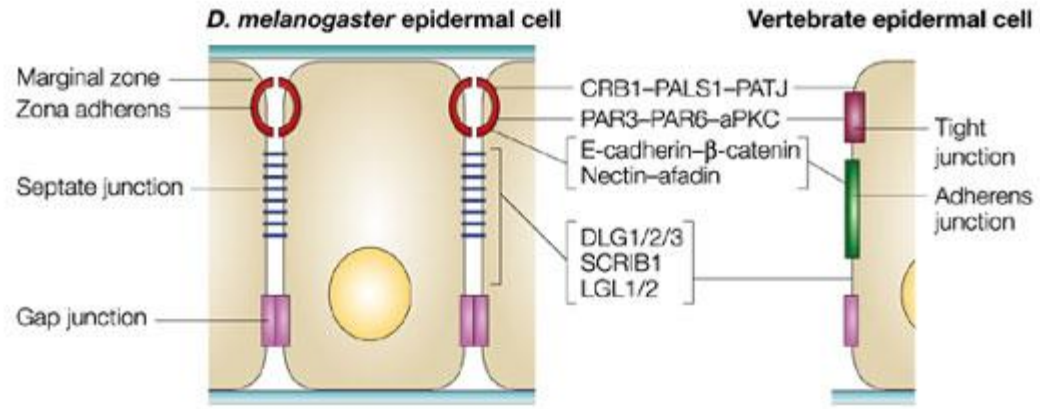
D. melanogaster epidermal cell
Vertebrate epidermal cell
Marginal zone
Zona adherens
Septate junction
Gap junction
CRB1–PALS1–PATJ
PAR3–PAR6–aPKC
E-cadherin–β-catenin
Nectin–afadin
DLG1/2/3
SCRIB1
LGL1/2
Tight junction
Adherens junction

Figure 1.1

basal to the SAR lie the adherens junctions or zonula adherens, which are sites of localization for E-cadherin and β-catenin (the homolog is Armadillo in *Drosophila*). Additionally, adherens junctions play an important role in linking the membrane to the actin cytoskeleton (Tepass and Hartenstein, 1994). Immediately basal of the adherens junctions in *Drosophila* are the septate junctions, which assist in the paracellular barrier function and polarization of the epithelial cell (Lamb et al., 1998; Genova and Fehon, 2003). Polarity proteins including Discs large (Dlg), Lethal giant larvae (Lgl), and Scribble (Scrib) localize at the septate junctions (Bilder et al., 2000; Bilder and Perrimon, 2000; reviewed in: Bilder, 2001; Tepass et al., 2001; Knust and Bossinger, 2002). In vertebrate epithelia, there are no septate junctions, but instead tight junctions. Tight junctions similarly play a role in barrier function and polarity, but are located apically in a region similar to the *Drosophila* SAR (reviewed in: Tsukita et al., 2001, Knust and Bossinger, 2002, and Tsukita and Furuse, 2002). Located basal to the tight junctions in vertebrate epithelia are the adherens junctions. Additional lateral membrane junctions in both vertebrate and invertebrate epithelia are gap junctions, which allow the transmission of ions and small molecules between neighboring cells (reviewed in Phelan and Starich, 2001). Desmosomes, which are lateral membrane junctions that link the cytoskeletal intermediate filaments of cells, exist in vertebrates, but not invertebrates (reviewed in Hynes and Zhao, 2000 and Delva et al., 2009). The maintenance of cell polarity and junctional architecture must be regulated during both morphogenesis and homeostasis.

Rab GTPase mediated vesicle trafficking in epithelial cells

To establish and maintain polarity, proteins must be localized to specific subcellular sites. One way to achieve this is delivering vesicle cargo with particular proteins to distinct structures in the cell, such as junctions, lateral membranes, or apical membranes. Thus, vesicle trafficking is essential for the maintenance of polarity, barrier function, and cell signaling, secretory and endocytic pathways amongst other functions. Additionally, the loss of proper polarity or trafficking can lead to pathogenesis from external sources and various diseases including cancer. Rab GTPases are a major regulator of vesicle trafficking in eukaryotic cells. This class of small GTPases act as molecular switches and alternate between active and inactivate states. There are more than 60 different Rab GTPase proteins in humans and over 30 in *Drosophila* (Pereira-Leal and Seabra, 2001; reviewed in: Zerial and McBride, 2001; Schwartz et al., 2007; Zhang et al., 2007). While localizing to distinct membrane domains, these GTPases recruit effector proteins to organize most of the intracellular traffic in eukaryotic cells (Chavrier et al., 1990).

Rab GTPases generally exist in two different states: an active, GTP bound and inactive, GDP bound state (Figure 1.2A). In the inactive state, the GDP-Rab complex is stabilized by the GDP dissociation inhibitor protein (GDI), which can additionally function in Rab recycling and delivery to the correct membrane compartment (Matsui et al., 1990; Ullrich et al., 1993; Soldati et al., 1994; Ullrich et al., 1994). Guanine nucleotide exchange factors (GEFs) facilitate the release of GDP in order to allow binding of GTP, and therefore, assist in the conversion to an active Rab GTPase (Delprato et al., 2004; reviewed in Barr and Lambright, 2010). In the active state, the

Rab GTPase hydrolyzes its bound GTP, which converts it back into the GDP bound, inactive state; this reaction is catalyzed by the GTPase-activating proteins (GAPs) (Haas et al., 2007). There is also an associated conformational change in the Rab proteins between the GTP and GDP bound states (Stroupe and Brunger, 2000). Rab effector proteins generally prefer the GTP bound (active) state, although exceptions do exist (Shirane and Nakayama, 2006).

Within the cell cytosol is a highly complex system of intracellular compartments and transport between them (Figure 1.2B). While it is not completely understood how Rab GTPases are targeted to the correct membrane, some data suggest that GDI displacement factors in the membrane recognize specific Rab-GDI complexes and facilitate the removal of the GDI allowing the Rab GTPase to associate with the membrane (Soldati et al., 1994; Sivars et al., 2003; Ohya et al., 2009). However, some recent data from experiments that anchor mislocalized GEFs suggest that these proteins may also play a role in the localization of Rab GTPases (Gerondopoulos et al., 2012; Blumer et al., 2013).

Rab11, which is known to be localized on recycling endosomes (Calhoun and Goldenring, 1996; Ren et al., 1998; Casanova et al., 1999), has more recently been implicated in the regulation of cell polarity, adhesion, and epithelial integrity (Figure 1.2C). It was reported that Rab11 mediated trafficking is important for E-cadherin recycling and targeting to the adherens junctions in both *Drosophila* and mammalian cells (Langevin et al., 2005; Lock and Stow, 2005; Desclozeaux et al., 2008). Further, studies in *Drosophila* have implicated the necessity of Rab11 for the maintenance of cell polarity and epithelial integrity (Roeth et al., 2009; Xu et al., 2011).

Figure 1.2 – Rab GTPase mediated vesicle trafficking in epithelial cells

(A-C) Schematic representation of Rab GTPases and their mediation of vesicle trafficking in epithelial cells adapted from Stenmark (2009). (A) Rab proteins generally exist in an active (GTP bound) or inactive (GDP bound) form. Guanine nucleotide exchange factor proteins (GEFs) convert the inactive into an active state by releasing the GDP from the Rab protein, so GTP can bind. Conversely, GTPase activating proteins (GAPs) stimulate the hydrolysis of the bound GTP to inactivate the Rab protein. (B) An epithelial cell showing the complicated network of vesicle trafficking and the Rab proteins associated with the various types of intracellular vesicles and compartments. (C) Rab11 is found on recycling endosomes and is important in trafficking proteins to the apical membrane.

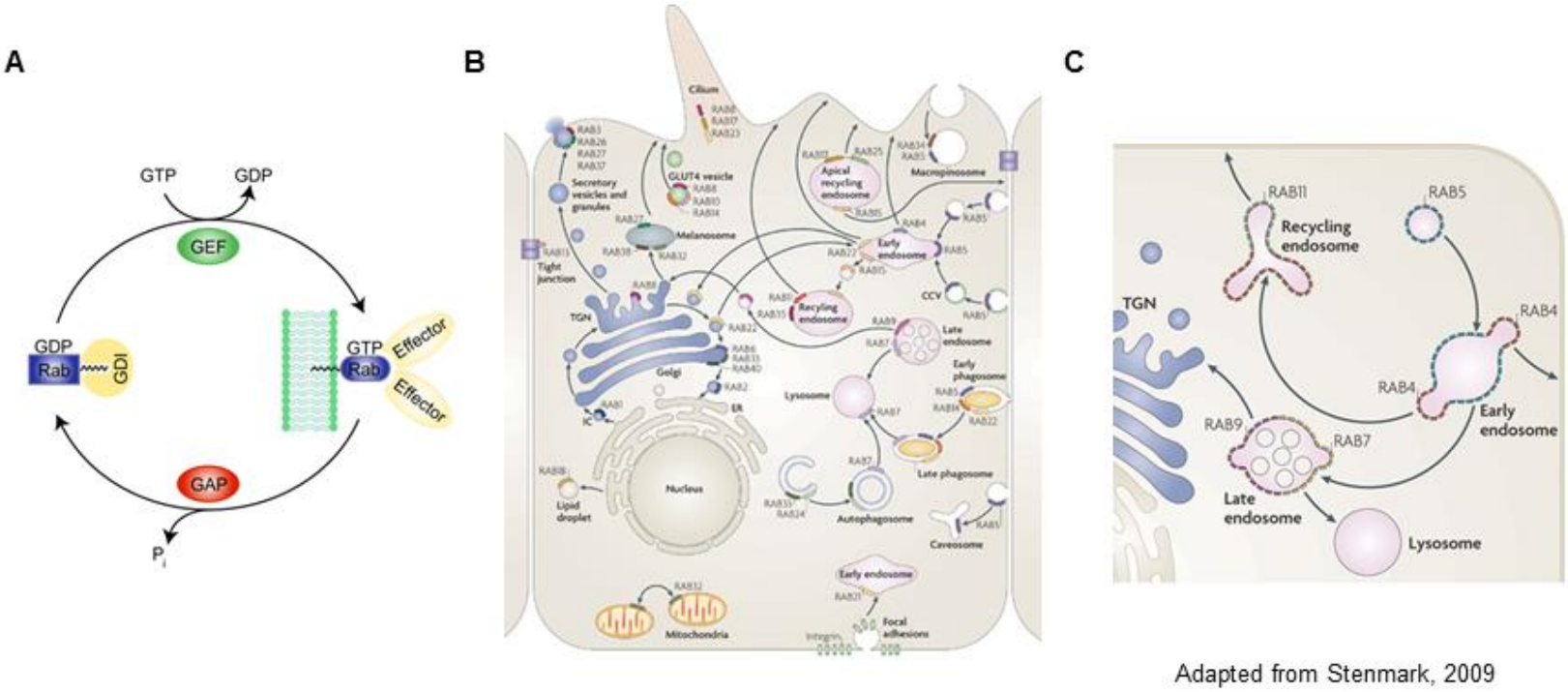

Adapted from Stenmark, 2009

Figure 1.2

Epithelial morphogenesis during development and evolution

During embryonic development in most animals, individual blastomeres become polarized and adhere to each other to form an epithelial sheet. This sheet of cells, generally formed by the blastocyst stage or during cellularization, will contribute to the germ layers and give rise to adult organs and structures. During development, morphogenetic processes drive changes in the shape of epithelial sheets that give rise to these adult formations.

Mechanisms of epithelial morphogenesis during animal development

During animal development, epithelial tissues are patterned and undergo morphogenesis to form a diversity of body plans, organs, appendages, and structures. Studies in bilaterian model organisms, such as mouse, chick, *Xenopus*, and *Drosophila*, have identified several processes that drive morphogenesis, three of which I will highlight here. First, changes in the shape of epithelial cells can increase or decrease the surface area of an epithelial sheet. With a reduction in the apico-basal axis of cells, the surface area of the sheet will increase; this occurs during *Xenopus* epiboly and *Drosophila* wing morphogenesis (Figure 1.3A; Keller, 1980; reviewed in Fristrom, 1988). Conversely, columnarization, thickening of cells with an increase in the apico-basal axis, occurs in some follicle cells during oogenesis in *Drosophila* (Figure 1.3A; Zarnescu and Thomas, 1999). Second, oriented cell divisions can result in directional expansion of a tissue. One example of this is germband extension in the *Drosophila* embryo where cells preferentially divide along the anterior-posterior axis (Figure 1.3B; da Silva and

Vincent, 2007). Oriented cell divisions also play a role during zebrafish gastrulation, where a subset of cells in the epiblast divide along the anterior-posterior axis during elongation (Concha and Adams, 1998). Third, cell intercalation and convergent extension act to shape developing embryos through a combination of tissue and cellular movement. These morphogenetic movements result in the narrowing and elongation of a sheet of cells (Figure 1.3C). The best described example of convergent extension occurs in the mesodermal cells during *Xenopus* gastrulation (Keller, 1978; Keller et al., 1992; Shih and Keller, 1992). However, this process has also been described in the epithelium of the *Drosophila* embryo during germband extension and in ascidian epithelia during notochord development (Irvine and Wieschaus, 1994; Munro and Odell, 2002).

At the tissue level, placodes are primordial structures that precede morphogenesis during the development of multiple organ and appendage structures. These thickened epithelial structures are molecularly patterned through signaling pathways and gene expression before being elaborated into an adult structure (Figure 1.3D). The ectodermal appendages of vertebrates originate from placodes, including teeth, feathers, and scales (reviewed in Pispa and Thesleff, 2003). Additionally, the sensory placodes contribute to development of the eye lens and inner ear (reviewed in Baker and Bronner-Fraser, 2001; Streit, 2007). However, placodes have not only been described in vertebrate model organisms; they are known to contribute to the development of the *Drosophila* trachea and imaginal discs (Franch-Marro et al., 2006; reviewed in Fristrom, 1988). More recently, placodes have been studied in the context of ascidian sensory organs (Manni et al., 2004). Nevertheless, most of our current

Figure 1.3 – Mechanisms of epithelial morphogenesis during development

(A-C) Schematic representations of cellular processes that drive morphogenesis of epithelial sheets during development. Cell shape changes (A), including flattening and columnarization, act to increase or decrease the surface area of an epithelial sheet. Oriented cell divisions (B) can result in directed expansion of a tissue. Cell intercalation and convergent extension (C) act to narrow and elongate a cell sheet. **(D)** At the tissue level, thickened epithelial placodes serve as primordia that are patterned and subsequently undergo morphogenesis to form adult organs and structures, including teeth, the eye lens, and the *Drosophila* wing.

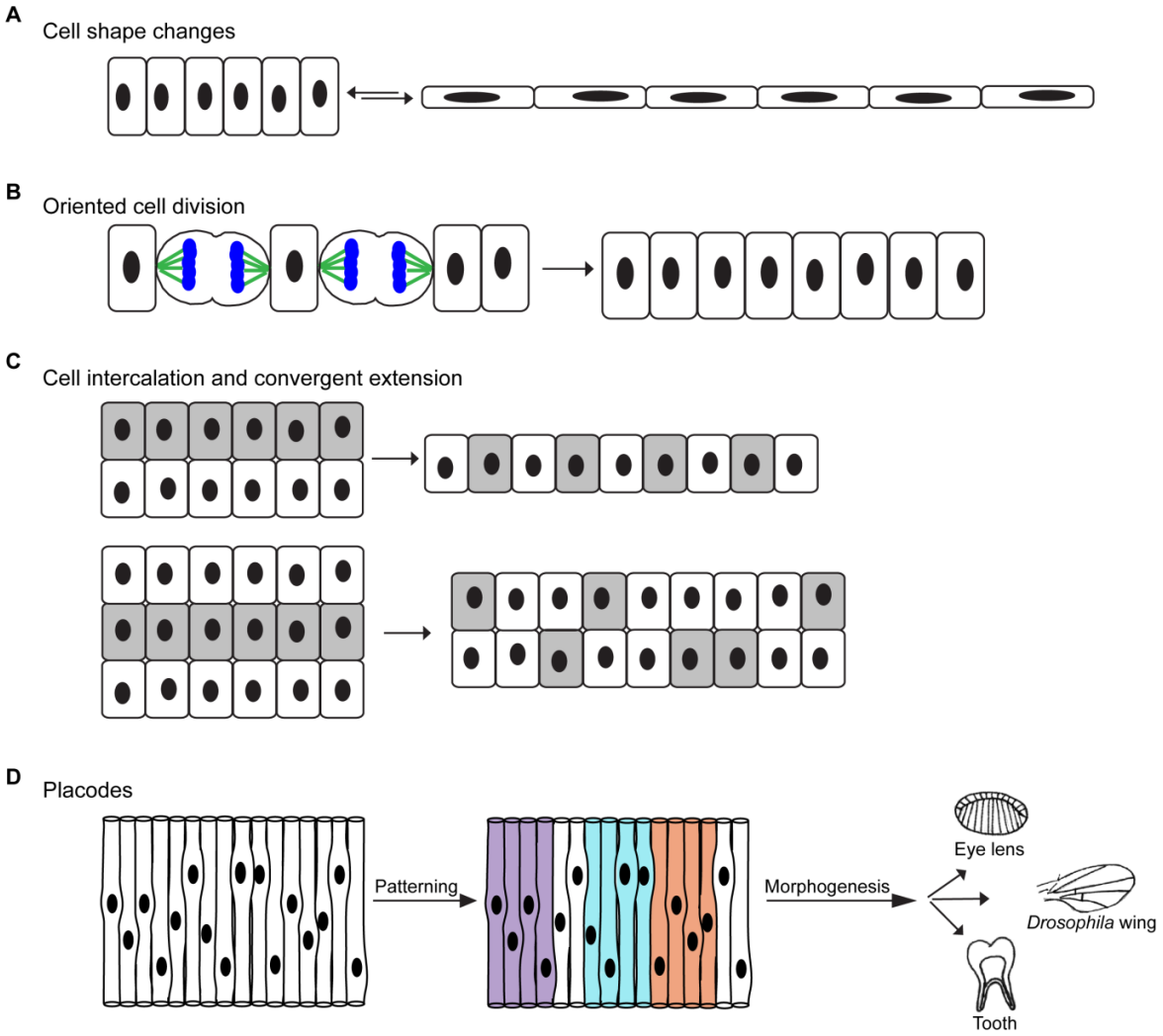
A
Cell shape changes
B
Oriented cell division
C
Cell intercalation and convergent extension
D
Placodes
Patterning
Morphogenesis
Eye lens
Drosophila wing
Tooth

Figure 1.3

knowledge about the molecular and cellular mechanisms involved in these morphogenetic processes has been elucidated in select bilaterian model systems.

Nematostella vectensis as a model system for exploring ancient mechanisms of epithelial morphogenesis

Genome content

To explore the ancient mechanisms of morphogenesis, we use the basal metazoan *Nematostella vectensis*, a sea anemone and an emerging model system. This model is being used as a powerful tool in the evolution and development field to explore the evolution of the germ layers (Wikramanayake et al., 2003; Martindale et al., 2004; Technau, 2010), signaling pathways (Kusserow et al., 2005; Rentzsch et al., 2006; Matus et al., 2007; Matus et al., 2008; Kumburegama et al., 2011; Marlow et al., 2012), the nervous system (Marlow et al., 2009; Nakanishi et al., 2012), and axial patterning (Finnerty, 2003; Wikramanayake et al., 2003; Rentzsch et al., 2006; Saina et al., 2009; Sinigaglia et al., 2013). With the advantage of its phylogenetic position, as the sister group to the bilaterians, cnidarians provide evolutionary insight into the developmental mechanisms used by higher organisms (Figure 1.4; Collins et al., 2006; Putnam et al., 2007; Dunn et al., 2008; Hejnol et al., 2009). The genome of *Nematostella* has been sequenced, which revealed a surprising similarity in the organization and content of its genome with that of higher organisms, including humans (Putnam et al., 2007). It is estimated to be around 450 Mbps in size and contain around

Figure 1.4 – Metazoan phylogeny

Phylogeny showing the major classes of metazoan organisms as well as their closest unicellular ancestor, Choanoflagelata. Dotted lines indicate positions that are currently still debated at the base of the metazoan tree. The 'Non-Bilateria' includes Ctenophora (comb jellies), Porifera (sponges), Placozoa (*Trichoplax*), and Cnidaria. Cnidaria is broadly divided into Anthozoa (sea anemones and corals) and Medusozoa (*Hydra* and jellyfish). Bilateria includes Deuterostomia (ex. echinoderms and vertebrates), Lophotrochozoa (ex. flatworms and mollusks), and Ecdysozoa (ex. *Drosophila* and *C. elegans*).

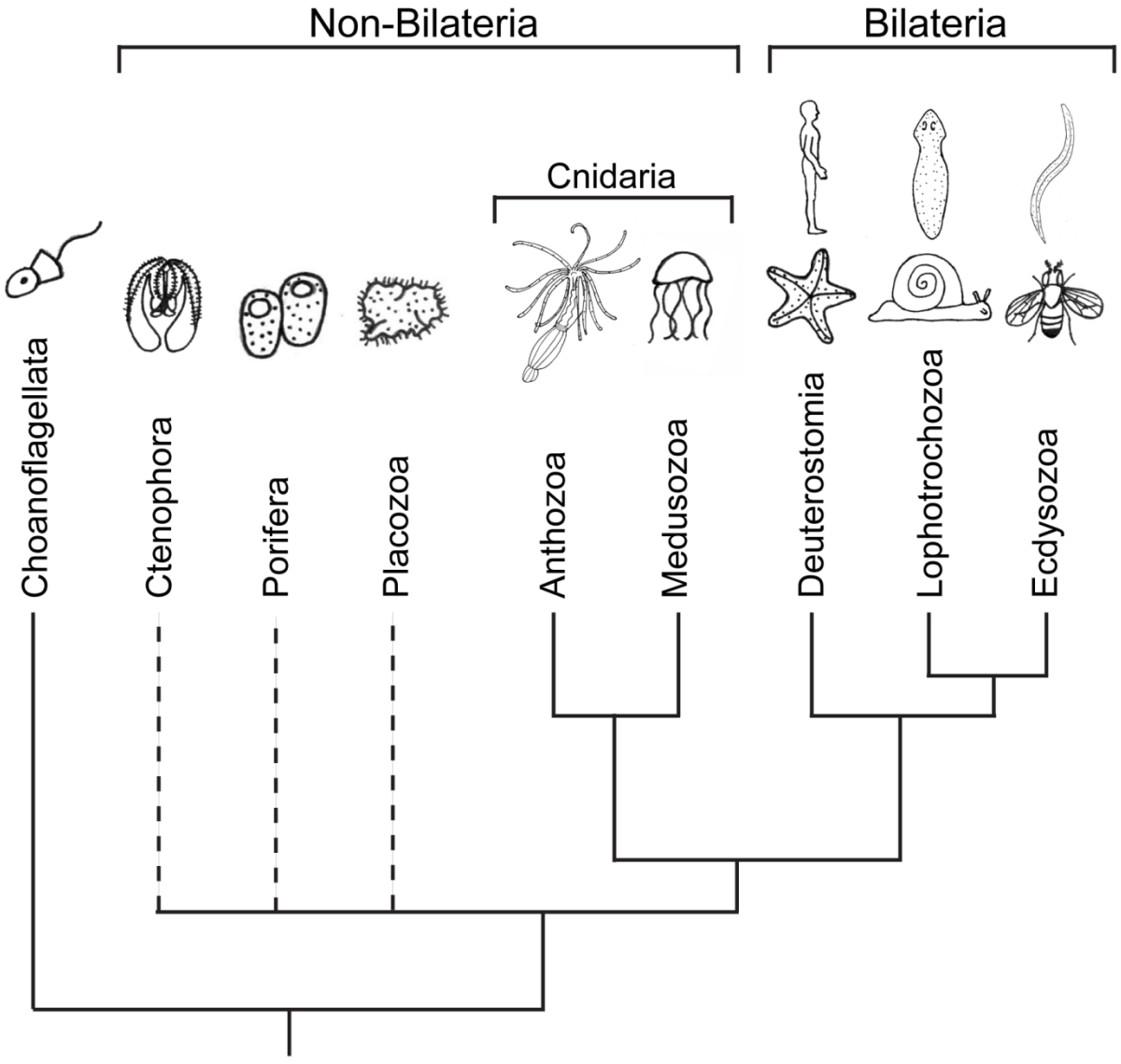
Non-Bilateria
Bilateria
Cnidaria
Choanoflagellata
Ctenophora
Porifera
Placozoa
Anthozoa
Medusozoa
Deuterostomia
Lophotrochozoa
Ecdysozoa

Figure 1.4

18,000 genes (Putnam et al., 2007). Additionally, *Nematostella*'s genome contains more orthologs of human genes than some of the more closely evolutionarily related organisms; this even includes genomes of established model systems such as *Drosophila* and *C. elegans*. Furthermore, it also contains orthologs of genes known to contribute to various human diseases (Sullivan and Finnerty, 2007). Since the genome is similar to that of higher bilaterians, *Nematostella* contains many of the genes and signaling pathways known to be involved in developmental processes of these organisms; this includes a Hox gene cluster (Finnerty and Martindale, 1999; Chourrout et al., 2006), Fibroblast Growth Factors (FGFs; Matus et al., 2007), Bone Morphogenetic Proteins (BMPs; Rentzsch et al., 2006), Hedgehog (Hh) proteins (Matus et al., 2008), Wnts (Kusserow et al., 2005), and Notch pathway members (Marlow et al., 2012). Given that the *Nematostella* genome is so similar to that of vertebrates, it suggests that the genome has retained the complexity of the bilaterian-cnidarian common ancestor (eumetazoan ancestor). Additionally, the genomes of many currently used model organisms, like fly and worm, seem to have undergone genome condensation, losing many genes during evolution, and are generally regarded as 'derived' examples.

Since the *Nematostella* genome has been sequenced, more techniques and tools can be used to explore development and other processes. As previously discussed, comparative genomics can be used to compare genes of *Nematostella* with those of other species. Currently, tools are being developed and used for reverse genetics in this organism. This includes knockdown with antisense morpholinos (Rentzsch et al., 2008; Genikhovich and Technau, 2011; Nakanishi et al., 2012;

Sinigaglia et al., 2013; Wolenski et al., 2013), expression of mRNA (Tsukita and Furuse, 2002; Rentzsch et al., 2006; Rentzsch et al., 2008; Kumburegama et al., 2011; Layden et al., 2012; Marlow et al., 2012; Rottinger et al., 2012; Layden et al., 2013), and generation of transgenic animals (Renfer et al., 2010; Nakanishi et al., 2012).

Lifecycle of *Nematostella*

Nematostella are simple and inexpensive to culture in the lab through their entire reproductive cycle (Hand and Unlinger, 1992; Stefanik et al., 2013). They can be maintained in artificial sea water, and adults are fed *Artemia* nauplii, brine shrimp larvae. An established spawning protocol allows us to easily obtain large numbers of animals on a regular basis (Fritzenwanker and Technau, 2002b; Stefanik et al., 2013). This protocol includes changes in light, temperature, and diet that induce the animals to reproduce sexually. Using this protocol, spawning can be induced at a desired time to have embryos for microinjection or other experiments. In addition, the association of egg masses with females permits their isolation during spawning; there are no morphological differences between male and female individuals. These segregated females are kept separate from males, so the timing of fertilization can be controlled.

In addition to a sexual mode of reproduction, *Nematostella* can also reproduce asexually. Asexual reproduction can occur by two different methods of transverse fission: physal pinching and polarity reversal (Reitzel et al., 2007). During physal pinching, the animal constricts at the aboral end, which leads to separation of this portion from the rest of the adult animal. This aboral fragment is able to develop into a separate adult animal. Polarity reversal occurs by the development of a new oral pole

at the aboral tip. The animal will constrict its body column between the two new oral ends to produce two separate adults. Additionally, *Nematostella* can regenerate after being cut transversely, providing the potential for regeneration studies using this organism (Reitzel et al., 2007).

In the laboratory, we most often spawn *Nematostella* sexually to obtain large numbers of animals for experiments as described above (Hand and Unlinger, 1992; Fritzenwanker and Technau, 2002b). Fertilization occurs externally after females and males have released eggs and sperm, respectively (Figure 1.5). The embryo undergoes several rounds of chaotic cell division, becoming a blastula and then gastrulating. This key developmental event, gastrulation, results in the formation of two germ layers, the ectoderm and endoderm. After gastrulation, there is a swimming planula larval phase. The planula larva settles and further growth and differentiation take place to form the four-tentacle primary polyp. Interestingly, development to this stage does not involve feeding, but subsequent growth and tentacle addition requires nutrition.

Body plan

The bauplan of the adult polyp consists of a cylindrical body column with eight mesenteries and a pharynx, mouth, and approximately 16 tentacles at the oral end of the animal (Figure 1.6). The ectoderm and endoderm are separated by a layer of mesoglea, extracellular matrix. Even though the body plan is very simple, *Nematostella* has about 20 types of differentiated cells including myoepithelial cells, secretory cells, nerve cells, and nematocysts (reviewed in Erwin, 2009). Cnidarians are early-branching

Figure 1.5 – Life cycle of *Nematostella vectensis*

Nematostella adults release eggs and sperm into the water. Fertilized embryos undergo chaotic cell division, gastrulate to form two germ layers, and develop into a swimming planula larva. The larva settles and undergoes metamorphosis to form a four-tentacle primary polyp. Primary polyps begin feeding, grow, and add additional tentacles as they mature to the adult stage.

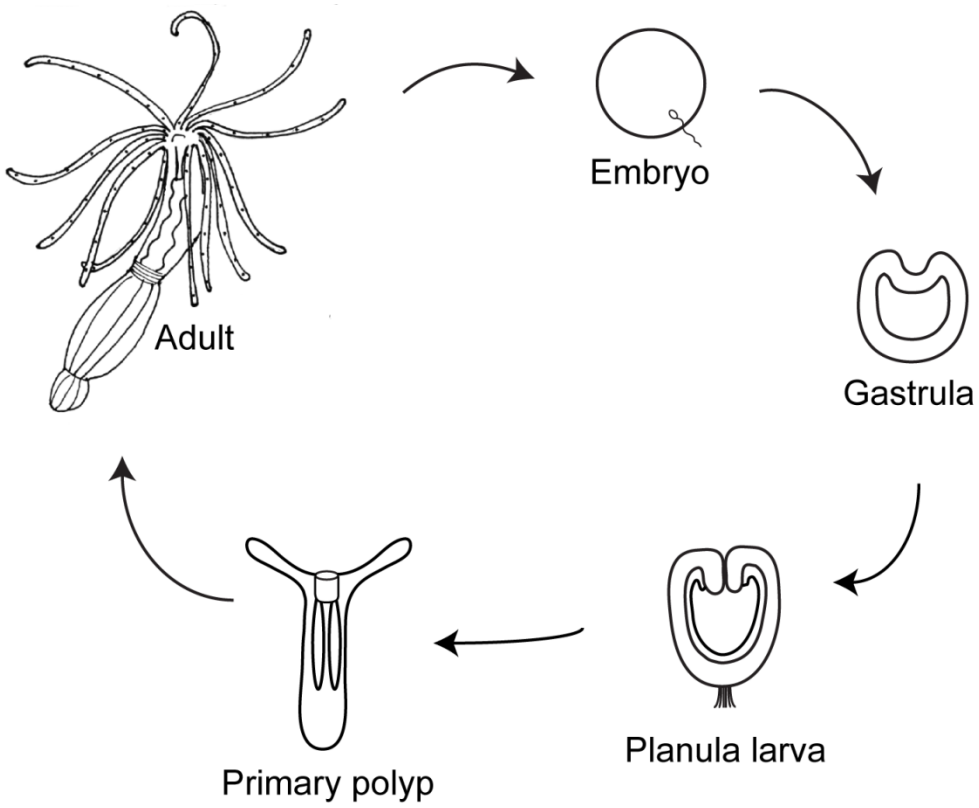

Figure 1.5

Figure 1.6 –*Nematostella* adult anatomy

Adult *Nematostella* polyp (12 tentacle stage) on the left with structures labeled on the right. At the oral end of the animal is the head containing a mouth and radiating tentacles. The tentacles are used for prey capture and feeding. The mouth opening leads into the pharynx, which opens into the body cavity. Ingestion of food, expulsion of waste, and spawning all occur through the mouth opening. The tube-shaped body column houses the eight mesenteries. The aboral end of the animal is referred to as the foot.

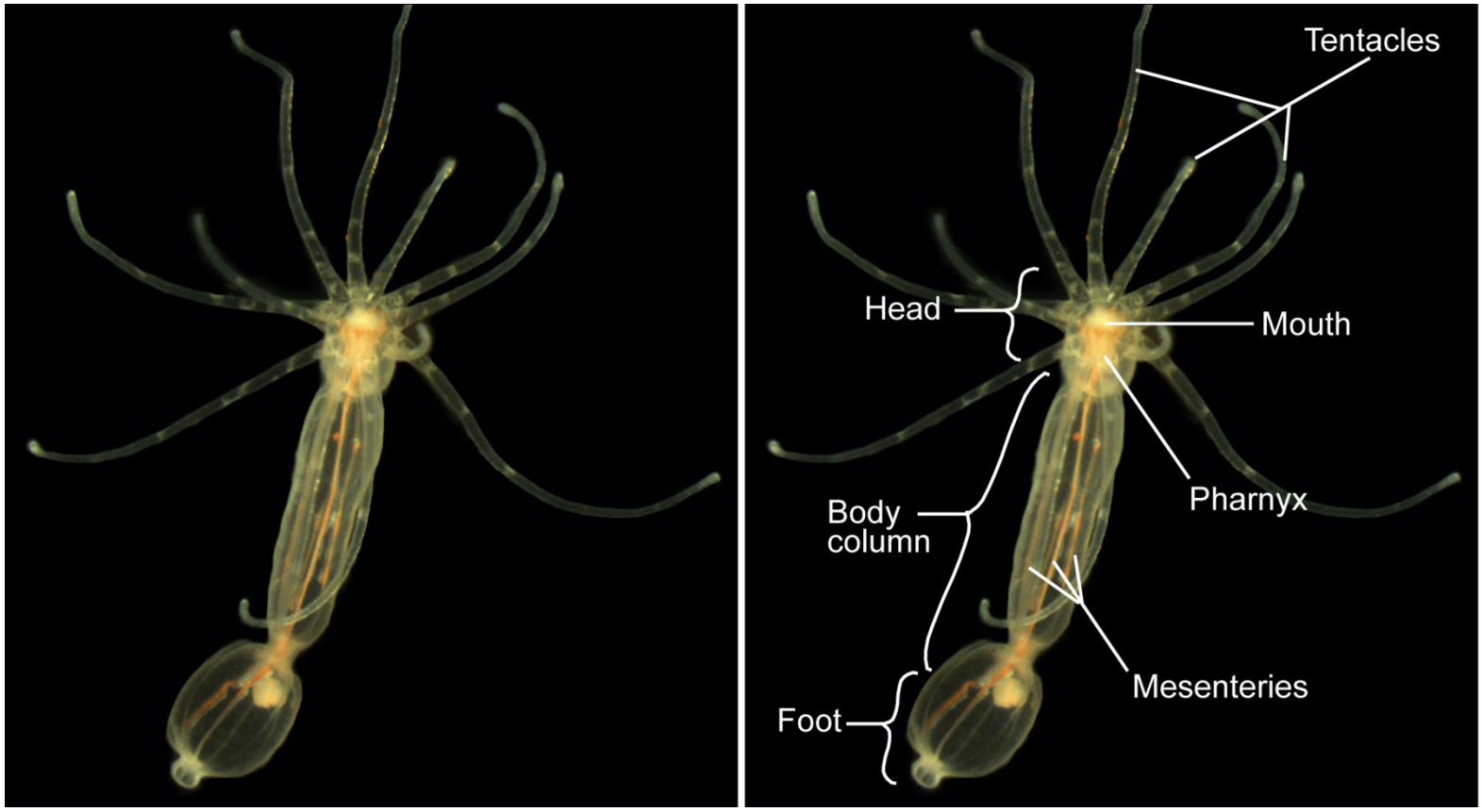
Tentacles
Head
Mouth
Pharnyx
Body column
Mesenteries
Foot

Figure 1.6

metazoan animals with defined appendage structures, tentacles. *Nematostella* uses its tentacles to capture prey and feed. These appendages can also be articulated and retracted into the body. They contain numerous cell types including nematocysts, spirocytes, and myoepithelial cells, and are innervated (Marlow et al., 2009; Renfer et al., 2010). Ctenophores might also have appendage-like structures, but the phylogenetic position of this group is still being debated (Schram, 1991; Nielsen et al., 1996; Collins, 1998; Zrzavy et al., 1998; Kim et al., 1999; Peterson and Eernisse, 2001; Ryan et al., 2013).

Epithelial morphogenesis in basal metazoans

Ancient mechanisms of epithelial morphogenesis in basal metazoan animals are largely unknown. Most of our current knowledge comes from studies of organisms within the cnidarian clade. The cnidarians are phylogenetically divided into two main groups: Anthozoa (sea anemones and corals) and Medusozoa (jellyfish and *Hydra*) (Collins, 2002; Marques and Collins, 2004; Collins et al., 2006; Daly et al., 2007; Kayal et al., 2013). Mechanisms of morphogenesis in *Nematostella*, an anthozoan cnidarian, have only been explored in the context of gastrulation. Gastrulation occurs by invagination in *Nematostella*, where the epithelial cells at the blastopore undergo cell shape change, constriction at the apical apex to form bottle cells (Magie et al., 2007; Kumburegama et al., 2011).

Within the broad Medusozoa, *Hydra* has been a subject of laboratory study for over 250 years. During this time, many scientists have used *Hydra* to investigate topics

including reproduction, regeneration, and stem cell biology. Recently, the genome of *Hydra magnipapillata* has also been sequenced (Chapman et al., 2010). Due to the lack of an inducible spawning protocol, most studies in *Hydra* examine development and morphogenesis in the light of regeneration, asexual budding, and adult maintenance. Epithelial morphogenesis in *Hydra* has largely been studied in the context of asexual budding. At the initiation of bud formation on the body column, there is a thickening of the epithelial cells along their apico-basal axis, which flatten as the bud forms (Gelei, 1925; Graf and Gierer, 1980). Additionally, during bud evagination, clusters of cells intercalate into elongated arrays of cells (Philipp et al., 2009). It has also been shown that cells in the ectoderm have oriented cell divisions along the oral-aboral axis; however, the endoderm cells have oriented cell divisions as well that are oriented perpendicular to the body axis (Shimizu et al., 1995). These oriented cell divisions are not thought to play a role during elongation or bud formation.

Another emerging hydrozoan cnidarian model, *Clytia hemisphaerica*, has also recently been used to study development in a basal metazoan (Houliston et al., 2010). This medusozoan model has a lot of potential since there is an established spawning protocol, and the genome is currently being sequenced (Roosen-Runge, 1970; Carre and Carre, 2000; Houliston et al., 2010; Verlhac et al., 2010). In *Clytia*, cell intercalation is also thought to play a role in larval elongation along the oral-aboral axis (Momose et al., 2012).

To study ancient mechanisms of epithelial morphogenesis, we used *Nematostella* tentacle development as a model of organ or appendage formation. This process has not been previously described or studied in *Nematostella*. While tentacle

formation has not been well addressed in developing hydrozoan cnidarians, some data from these systems has shed light on the processes of tentacle maintenance and regeneration. *Hydra* adults have constantly dividing cell populations in both germ layers that continually replace the cells of its body (Campbell, 1967b; David and Murphy, 1977; Yaross et al., 1986; Dubel et al., 1987). These include proliferating epithelial cells as well as interstitial stem cells (i-cells), which give rise to neuronal cells (including nematocytes), gland cells, and germ cells (David and Murphy, 1977; Bosch and David, 1987; reviewed in Bode, 1996). In the apical portion of the body column, these cells migrate toward the head (Figure 1.7A). A subset of these cells enters the tentacle zone and becomes specified by an unidentified morphogenetic gradient originating from the hypostomal organizer region. Once a cell is specified to become part of the tentacle, division ceases, and then it is able to differentiate (Takahashi et al., 2005). The mature tentacles are continuously repopulated in this fashion with the oldest cells being sloughed off the distal tip of the tentacles.

There have been some studies on the molecular mechanisms that underlie *Hydra* tentacle maintenance and regeneration. Ectopic activation of canonical Wnt signaling, by drug treatment, is sufficient to induce tentacle formation all along the body column (Philipp et al., 2009). As another example, Hym-301, a novel *Hydra* protein, has been shown by gain- and loss-of-function experiments to regulate the number of tentacles that form during asexual budding and regeneration (Takahashi et al., 2005). Unfortunately, all of these studies are based on experiments using budding (asexual reproduction) or regenerating *Hydra*, NOT on experiments investigating the normal developmental process as a result of embryogenesis.

Figure 1.7 – Cnidarian tentacle maintenance in *Hydra* and *Clytia*

(A) Schematic representation of adult *Hydra* tentacle maintenance adapted from Smith et al. (2000). Proliferating epithelial cells (*orange dots*) and interstitial stem cells (*teal dots*) in the body column move upward toward the head. In the tentacle zone, they receive a signal secreted from the hypostome (organizer), which informs them of their tentacle fate. Cells differentiate and migrate to form the epithelial cells (*peach ovals*) and nematocytes (*purple ovals*) of the tentacles. Cells of the tentacle are continuously repopulated, and the oldest cells are sloughed off of the tentacle tips. **(B)** Schematic representation of *Clytia* adult tentacle maintenance and nematocyte differentiation/maturation adapted from Denker et al. (2008). Stem cells (*yellow*) in the tentacle bulb proliferate to give rise to the differentiating nematoblasts (*orange*). These cells continue to develop (maturing nematoblasts; *red*) into the mature nematocytes (*purple*) as they migrate along the tentacle.

.

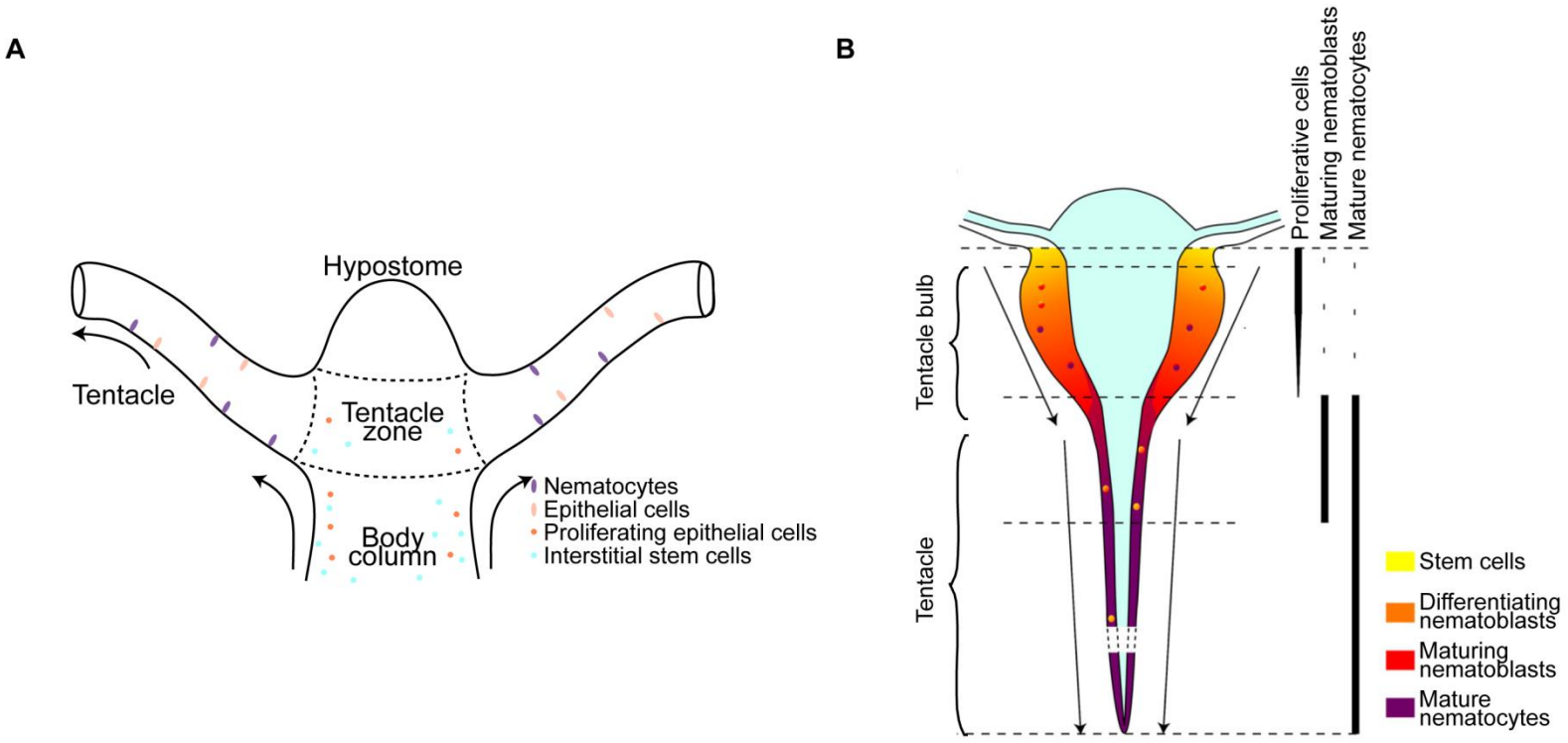
A
Hypostome
Tentacle
Tentacle zone
Body column
Nematocytes
Epithelial cells
Proliferating epithelial cells
Interstitial stem cells
B
Proliferative cells
Maturing nematoblasts
Mature nematocytes
Tentacle bulb
Tentacle
Stem cells
Differentiating nematoblasts
Maturing nematoblasts
Mature nematocytes

Figure 1.7

Even though tentacle development has not yet been addressed in *Clytia*, one study has shed light on the process of tentacle maintenance in the adult medusa (Denker et al., 2008). There seems to be a mechanism of tentacle population similar to that of *Hydra* (Figure 1.7B). At the base of each tentacle is a specialized structure called the tentacle bulb. Here, there are localized regions of stem cell proliferation, which produce cells that differentiate to form the nematoblasts, mature into the nematocytes, and migrate to populate the tentacles (Denker et al., 2008). While the homology of polyp and medusa tentacles has not been addressed, these two hydrozoan examples appear to have similar mechanisms of tentacle maintenance where specific populations of proliferating progenitor cells differentiate and migrate to give rise to the non-proliferative tentacle cells.

Even though *Hydra* and *Nematostella* are both members of Cnidaria, they are thought to be very evolutionary distant from one another. The distance of their divergence is similar to the protostome – deuterostome split (Putnam et al., 2007). Therefore, *Hydra* and *Nematostella* are just as evolutionary distant as flies and humans. The *Hydra* genome has undergone condensation and lost genes that were present in the eumetazoan ancestral genome (Chapman et al., 2010). Additionally, there are differences in their development. *Hydra* development is devoid of a larval stage, and the polyp develops directly from the embryo by hatching from a cuticle (Martin et al., 1997; Bottger et al., 2006). Further, interstitial stem cells (i-cells) have not been identified outside of the Medusozoa. Together, this information suggests that the processes of tentacle development and homeostasis between these two cnidarian organisms might be very different.

Disruption of epithelial integrity during pathogenesis

Another important role of epithelia is the maintenance of their polarity and integrity in the prevention of disease. As a barrier against the environment, they are essential for defense against pathogenic bacteria. However, bacteria have evolved a variety of protein tools that they use to evade the host immune system and infect, reproduce, and spread. These pathogenic bacteria can gain access to the body by several routes, one of which is fecal-oral. This can happen when sanitary conditions are not present and food and water become contaminated with sewage. Therefore, the intestinal epithelium plays a major role in the defense of pathogens and the immune system. One of its functions is to act as a barrier between the body and the gut contents, so the bacteria must first cross this barrier or obtain access to the epithelial cells.

To explore the mechanisms of bacterial modulation of host epithelial architecture, we are using a virulence effector, VirA, from *Shigella flexneri*, a gram negative bacterium. *Shigella* is a human specific pathogen that infects through the fecal-oral route and causes inflammation and destruction of the human intestinal epithelium. The ingestion of only 100 bacteria is enough to illicit an infection resulting in bacillary dysentery (DuPont et al., 1989). *Shigella* is a major threat to human health with 80 million cases a year worldwide resulting in 700,000 deaths; 90 percent of these cases are in developing nations (WHO, 2005). There is currently no vaccine to prevent the spread of this disease.

Shigella flexneri pathogenesis

After ingestion, *Shigella* must gain access to its host by crossing the intestinal epithelial barrier. Bacteria are initially transported across the host gut epithelium by microfold cells (M cells), which are specialized immune cells that constantly sample the gut contents for antigens (Figure 1.8; Wassef et al., 1989; reviewed in Sansonetti et al., 1996). After passing through the M cell to the basal side of the epithelium, the resident macrophages engulf the bacteria. *Shigella* is able to escape degradation by the macrophage by inducing its cell death (Zychlinsky et al., 1992). The bacterium is then free to infect and spread through the basolateral surfaces of the intestinal epithelial cells (Mounier et al., 1992). This ultimately results in breakdown of the epithelial barrier and diarrhea. Using a type III secretion system (T3SS), *Shigella* secretes and injects effector proteins into host cells that can alter various aspects of host cell biology including the cytoskeleton, immune response, and intracellular signaling cascades, enabling the bacteria to replicate and spread (reviewed in Schroeder and Hilbi, 2008 and Parsot, 2009).

Bacterial modulation of epithelial architecture

Studies from bacterial pathogens have revealed effector protein functions in altering tissue integrity. One of the strategies is modulation of the apical junctions to facilitate infection (reviewed in Kim et al., 2010). *Clostridium difficile*, an intestinal bacterial pathogen, is known to secrete toxins, toxin A and toxin B, which disrupt tight junctions by dissociating integral proteins (including Occludin, ZO-1, and ZO-2) from

these sites (Nusrat et al., 2001; Chen et al., 2002). Also, *Vibrio cholera*, the bacteria that causes cholera, secretes Hemagglutinin protease, which has been shown through cell culture assays to degrade the extracellular domain of Occludin, a tight junction component (Wu et al., 2000b). *Bacteroides fragilis*, a commensal gut bacteria that can become pathogenic, also secretes a protease, Fragilysin, which affects adherens junctions by cleaving the extracellular domain of E-Cadherin (Wu et al., 1998). Additionally, bacterial effectors are known to modulate intracellular trafficking through activation or inactivation of Rab GTPases; this has mainly been studied for the functions of establishing a replicative niche and avoiding autophagy (reviewed in Ham et al., 2011).

VirA structure and function

One of these effector proteins that *Shigella* injects into the gut epithelial cells using its T3SS is the effector protein, VirA. From ΔVirA mutant bacterial infection assays, VirA is known to be essential for the effective infection and spreading of *Shigella* (Uchiya et al., 1995). This protein belongs to the EspG family, which includes EspG and EspG2 from enteropathogenic *Escherichia coli* (EPEC) and enterohaemorrhagic *Escherichia coli* (EHEC; Elliott et al., 2001; Smollett et al., 2006). Based on *in vitro* data and cell culture assays, VirA was initially reported to be a cysteine protease that cleaved microtubules by binding Tubulin heterodimers (Yoshida et al., 2002; Yoshida et al., 2006). This function was thought to assist the bacteria in

Figure 1.8 – *Shigella flexneri* pathogenesis

Schematic representation of *Shigella* pathogenesis adapted from Schroeder and Hilbi (2008). *Shigella* bacteria present in the gut lumen as a consequence of ingestion are internalized by M cells during surveillance of the gut contents, which allows the bacteria to pass through the epithelium. On the basal side, they are engulfed by macrophages. Through a variety of mechanisms, they ultimately cause apoptosis of the macrophage and are then able to infect and spread through the basolateral side of the colonic epithelium. *Shigella* pathogenesis eventually destroys the epithelial integrity.

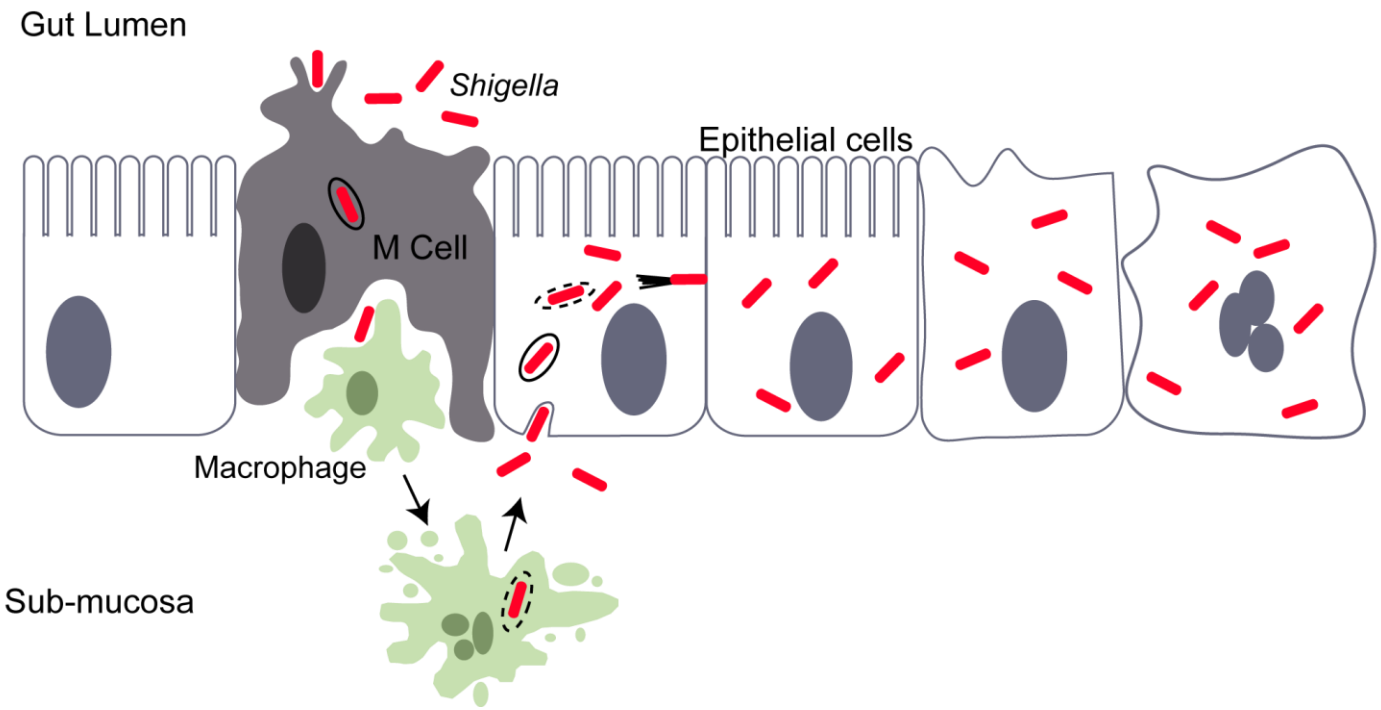
Gut Lumen
Shigella
Epithelial cells
M Cell
Macrophage
Sub-mucosa

Figure 1.8

intracellular movement. However, more recent studies that also reported the crystal structure of the VirA protein have refuted this claim (Davis et al., 2008; Germane et al., 2008). These findings, centered on the protein's structure and inability to reproduce similar results, reopen the question of the function of VirA during *Shigella* pathogenesis.

Recent reports have suggested various new functions for VirA (Clements et al., 2011; Bergounioux et al., 2012; Dong et al., 2012). Yeast two hybrid data reported by Clements et al. (2011) suggest that VirA binds to a golgi resident membrane protein, GM130. Additionally, Clements et al. (2011) reports that secretion by HeLa cells expressing VirA was significantly reduced by a secreted embryonic alkaline phosphatase (SEAP) assay. In another recent study using ΔVirA mutant bacteria, HeLa cell culture and *in vitro* biochemical assays, Bergounioux et al. (2012) report that VirA acts to increase Calpain protein levels by causing degradation of its inhibitor, Calpastatin. Since Calpains have a variety of cellular substrates, the authors suggest that the increase in Calpain may assist in infection through cytoskeletal elements and degradation of p53 to reduce host cell death. Additionally through biochemical and cell culture assays, Dong et al. (2012) report that VirA acts as a Rab1 GAP, which results in inactivation of the Rab1 protein. The authors suggest that this functions in *Shigella*'s ability to escape autophagy in host cells. While these studies report various potential functions for VirA in *Shigella* pathogenesis, they all use *in vitro* biochemistry and cell culture assays; none explore the function of VirA in the context of an *in vivo* tissue. Our study of VirA expression in *Drosophila* epithelia and chick neural tube is the first to examine its function in an epithelial tissue, which is more similar to where it would be expressed in a human host. Further, our results shed light on a mechanism where

bacteria effector proteins could alter host cell polarity to disrupt epithelial integrity during pathogenesis.

Summary

The evolution of epithelial tissues allowed for specialized function and thus, the amazing diversity of animal body plans. These polarized, adherent sheets must maintain their integrity during morphogenesis and homeostasis. This is regulated by a multitude of cellular processes including vesicle transport, cytoskeletal modulation, and cell adhesion. While much has been uncovered from studies in *Drosophila*, chick, *Xenopus*, mouse, and tissue culture, there are still large gaps in our knowledge of these processes, especially outside of these systems. The work in this dissertation focuses on filling knowledge in two of these unknown areas: mechanisms of epithelial morphogenesis in a basal metazoan and the modulation of epithelial polarity and integrity during bacterial pathogenesis.

What are the ancient mechanisms for epithelial morphogenesis?

Our efforts to understand metazoan development have largely been limited to a select set of bilaterian model organisms. With the recent advances in sequencing technology and the subsequent addition of sequenced genomes, more models are constantly emerging. One of these, *Nematostella vectensis*, is becoming more established for the study of development and evolution. In chapter 2, we take advantage of this simple organism to observe the processes of epithelial morphogenesis during the tentacle development, as a model for organ or appendage outgrowth. Our results not only establish the initial report on this process, but also lead to many other questions in developmental and regenerative biology.

How is epithelial architecture modulated by bacteria during pathogenesis?

Epithelial tissues are not only important during development of organs and structures,

but also the maintenance of their polarity and integrity is essential for the prevention of diseases, such as cancer and infections. Much is still unknown as to the function of bacterial effector proteins and how they hijack the endogenous cellular processes to their own advantage. It was not our initial intent to study bacterial pathogenesis in a developmental biology lab. We originally sought to use VirA as a tool for severing microtubules in distinct subcellular locations. However, our observations of *Shigella* effector protein, VirA, expression in a tissue context highlight the importance of *in vivo* experiments. While previous studies have only examined the function of VirA in cell culture and *in vitro* assays, ours is the first to use an *in vivo* tissue system and has shed light on potential cellular and tissue level mechanisms for pathogenesis.

Chapter 2: Mechanisms of tentacle morphogenesis in the sea anemone *Nematostella vectensis*

Abstract

Evolution of the capacity to form secondary outgrowths from the principal embryonic axes was a crucial innovation that potentiated the diversification of animal body plans. Nevertheless, precisely how such outgrowths develop in early-branching metazoan species remains poorly understood. Here we demonstrate that three fundamental processes contribute to embryonic tentacle development in the cnidarian *Nematostella vectensis*. First, a pseudostratified ectodermal placode forms at the oral pole of developing larvae and is transcriptionally patterned into four tentacle buds. Subsequently, Notch signaling-dependent changes in apico-basal epithelial thickness drive elongation of these primordia. In parallel, oriented cell rearrangements revealed by clonal analysis correlate with shaping of the elongating tentacles. Taken together, our results define the mechanism of embryonic appendage development in an early-branching metazoan, and thereby provide a novel foundation for understanding the diversification of body plans during animal evolution.

Introduction

During development, changes in epithelial cell shape and cell number are central to the formation of organs and appendage structures. Studies of epithelial morphogenesis in bilaterian model systems have identified four basic mechanisms that initiate and drive organ and appendage outgrowth. First, changes in cell shape can dramatically alter the surface area of an epithelial sheet. For example, epithelial cells reduce the length of their apico-basal axis during wing morphogenesis in *Drosophila* and epiboly in *Xenopus*, resulting in increased surface area (Keller, 1980; Fristrom, 1988). Second, oriented cell division has been shown to direct tissue expansion during germband extension in *Drosophila* and primitive streak elongation in chick (Wei and Mikawa, 2000; da Silva and Vincent, 2007). Third, cell intercalation or convergent extension can longitudinally extend a tissue, such as during *Drosophila* embryonic germband extension and gastrulation in *Xenopus* (Keller, 1978; Irvine and Wieschaus, 1994). Fourth, many organ and appendage structures initiate morphogenesis as thickened epithelial placodes. In vertebrates, these include ectodermal appendages such as teeth, feathers, and scales, as well as the sensory placodes that give rise to structures like the eye lens and inner ear (Baker and Bronner-Fraser, 2001; Pispa and Thesleff, 2003; Streit, 2007). Placodes are not only a vertebrate innovation; these structures also contribute to the development of *Drosophila* trachea and imaginal discs, as well as sensory organs in ascidians (Fristrom, 1988; Manni et al., 2004; Franch-Marro et al., 2006). Nevertheless, most of our current knowledge about the molecular and cellular mechanisms involved in these morphogenetic processes has been elucidated in select bilaterian model systems.

To identify ancient pre-bilaterian mechanisms of epithelial morphogenesis, we are studying tentacle development in the cnidarian sea anemone, *Nematostella vectensis* (Collins et al., 2006; Putnam et al., 2007; Dunn et al., 2008; Hejnol et al., 2009). Cnidarians are among the earliest branching metazoans with defined appendage structures used for prey capture and feeding. The adult *Nematostella* polyp exhibits 16 tentacles at the oral end of the animal, providing an ideal system to investigate mechanisms of epithelial morphogenesis during appendage development and regeneration. Furthermore, despite a deceptively simple diploblastic body plan, the *Nematostella* genome exhibits similar organization and content to that of vertebrates (Putnam et al., 2007). Accordingly, the genome encodes many proteins known to be involved in appendage development of arthropods and vertebrates; including a Hox gene cluster (Finnerty and Martindale, 1999; Chourrout et al., 2006), Fibroblast Growth Factors (FGFs) (Matus et al., 2007), Bone Morphogenetic Proteins (BMPs) (Rentzsch et al., 2006), Hedgehog (Hh) proteins (Matus et al., 2008), Wnts (Kusserow et al., 2005), and Notch pathway members (Marlow et al., 2012). At present, however, the contribution of these pathways to *Nematostella* tentacle development is largely unknown.

Cnidarians are broadly subdivided into two clades, Anthozoa (including sea anemones and corals) and the medusazoans (jellyfish and *Hydra* species; Collins et al., 2006). Previous studies in hydrozoan systems have examined the origin of cells that populate and maintain tentacles. In these cases, tentacle growth was primarily studied in the context of adult homeostasis, regeneration, and budding, but not as a result of embryonic development. In *Hydra*, interstitial stem cells (i-cells) and epithelial cells in

the oral pole of the body column proliferate and move progressively up towards the tentacle zone (Campbell, 1967a; Campbell, 1967b; David and Challoner, 1974; David and Gierer, 1974; Bouillon, 1994). Once in the tentacle zone, they receive signals secreted from the hypostomal organizer (Broun and Bode, 2002), stop dividing, differentiate, and migrate into the tentacle (Campbell, 1967b; Holstein et al., 1991). A similar mechanism is observed in the jellyfish, *Clytia*. In this case, populations of cells proliferate in a bulb at the base of the tentacle and then differentiate and move further into the tentacle itself (Denker et al., 2008). Although the degree of homology of polyp and medusa tentacles is still unclear, these two examples suggest a common mechanism in hydrozoans, wherein tentacle growth and maintenance is driven by migration of progenitor cells that only proliferate outside of the tentacle.

Here, we show that the mechanism of *Nematostella* tentacle development does not involve localized cell proliferation as in Hydrozoa, but rather formation of a thickened ectodermal placode followed by changes in epithelial cell shape and cell arrangement along the oral-aboral axis. In a broader context, our findings hint at the ubiquity of fundamental aspects of epithelial morphogenesis throughout animals, and also define the formation of thickened epithelial placodes as a common initiating mechanism underlying outgrowth from the main body axes during animal development.

Materials and Methods

Nematostella culture and differential interference contrast (DIC) imaging

Animals were raised at 16°C in 12 parts per thousand (ppt) artificial seawater (Sea Salt; Instant Ocean). Adult populations were spawned using an established protocol (Hand and Unlinger, 1992; Fritzenwanker and Technau, 2002a). For imaging, planula larvae through four-tentacle primary polyps were relaxed in 7% $MgCl_2$ (Sigma) in artificial seawater for ten minutes and fixed in 4% paraformaldehyde (Electron Microscopy Sciences) in artificial seawater for one hour at room temperature. Fixed specimens were washed three times in PTw (PBS with 0.1% Tween-20; Sigma), incubated in 87% glycerol (Sigma), mounted on glass slides, and imaged on a Leica SP5 confocal microscope.

EdU incorporation in planula and primary polyps

Animals in artificial seawater were incubated with EdU (300 μM from a stock dissolved in DMSO) for 15 minutes (Click-it Alexa Fluor 488 kit; Molecular Probes) as previously reported in Meyer et al. (2011). After incorporation, animals were relaxed in 7% $MgCl_2$ in artificial seawater for ten minutes, fixed in cold 4% paraformaldehyde and 0.2% glutaraldehyde (Electron Microscopy Sciences) in artificial seawater for 90 seconds, and then 4% paraformaldehyde for one hour at room temperature. Specimens were washed three times in PBS and permeabilized in PBT (PBS with 0.5% TritonX-100; Sigma) for 20 minutes. The reaction cocktail was prepared based on the

Click-it kit protocol and incubated with the animals for 30 minutes. After three washes in PBS, the samples were labeled with Hoechst 34580 (1 μg/mL; Molecular Probes) in PBT overnight at 4°C. Animals were imaged on a Leica SP5 confocal microscope and z-stacks were made using Leica Application Suite Advanced Fluorescence software (LAS AF).

Immunohistochemistry, RNA in situ hybridization, and imaging

Animals were fixed and stained according to a protocol adapted from Genikhovich and Technau (2009a). After fixation animals were stained with primary (mouse anti-α-Tubulin; Sigma; 1:1000) and secondary antibodies (goat anti-mouse IgG Alexa Fluor 488; Molecular Probes; 1:500). Phalloidin (2 units/mL; Alexa Fluor 546 Phalloidin; Molecular Probes) was used to label F-Actin. Nuclei were counterstained with Hoechst 34580 (1 μg/mL; Molecular Probes). Animals were imaged on a Leica SP5 confocal microscope with LAS AF software.

For DAPI staining to mark cnidocytes, animals were fixed in 4% paraformaldehyde with 10 mM EDTA for one hour (Szczepanek et al., 2002; Marlow et al., 2009). They were washed four times in PBS and stored at 4°C. Before staining, animals were washed three times in PBT (PBS + 0.2% TritonX-100 + 0.1% BSA) and then incubated with DAPI (28 μM; Invitrogen) in PBT overnight at 4°C. After staining, animals were washed at least seven times in PBT. Animals were imaged as described above. DAPI was excited with both the UV and 488 confocal lasers.

RNA *in situ* probes were designed to cover at least 500 or more nucleotides. Regions were amplified from cDNA translated from total RNA (isolated from mixed stages of animals with the RNeasy Mini Kit; Qiagen) using the standard protocol of the OneStep RT-PCR kit (Qiagen) and the primers listed in supplementary material Tables S2 and S3. Gene fragments were cloned into the TOPO-PCR4 sequencing vector (Invitrogen). Antisense probe was synthesized by *in vitro* transcription (MEGAScript kit; Ambion) driven by T3 or T7 RNA polymerase with DIG incorporation (Roche). Probes were ethanol precipitated and resuspended in hybridization buffer to a concentration of 50 ng/μL. RNA *in situ* hybridization was carried out according to the protocol of Genikhovich and Technau (2009b). Briefly, animals were fixed in 0.2% glutaraldehyde and 3.7% formaldehyde (Sigma) in artificial seawater for 90 seconds and then in 3.7% formaldehyde in artificial seawater for one hour at room temperature. They were then washed, dehydrated in methanol (Sigma), and stored in methanol at -20°C until needed. Probes were hybridized to the animals for between 16 and 48 hours at 65°C. Animals were imaged on an Axiovert 200 widefield microscope (Zeiss) with an Axiocam HRc camera using AxioVision software.

Microinjection

Unfertilized eggs were first dejellied in 4% Cysteine solution (in artificial seawater, pH = 7.4-7.6) for 10 minutes and then washed three times in artificial seawater (Fritzenwanker and Technau, 2002a). Following dejellying, eggs were fertilized and injected with linearized ubiquitin-GFP plasmid (Mark Martindale; Kewalo

Marine Laboratory; Honolulu, HI, USA) at 30 ng/μL using Femtojet express (Eppendorf). Injected eggs were raised at room temperature in the dark and fixed at specific developmental stages for phalloidin staining: embryos (24 hours), early planula larvae (two days), late planula larvae (four days) and primary polyps (seven to eight days).

Drug treatment of planula larvae

Prior to Cytochalasin D (Cyto D; Calbiochem) treatment, animals were raised for 10 days at 16°C in artificial seawater. 1 μM Cyto D was applied in 0.1% DMSO in artificial seawater for 48 hours at room temperature in the dark. Concurrently, control animals were incubated in 0.1% DMSO in artificial seawater. Animals were fixed, stained, and imaged as described above. Phenotypes were quantified by the percentage of animals that developed tentacles. For quantification of body column ectoderm thickness, animals from three independent experiments were measured using LAS AF software (Leica). Statistics were done using a Student's t-test.

Prior to DAPT (Sigma) treatment, animals were raised for eight days after spawning at 16°C in artificial seawater. They were incubated in 20 μM DAPT with 0.1% DMSO in artificial seawater for two days at room temperature in the dark. In parallel, control animals were incubated with 0.1% DMSO in 12 ppt artificial seawater.

Phenotypes following Cyto D or DAPT treatment were quantified by the percentage of animals that developed tentacles. To quantify the thickness of the body column ectoderm, measurements were taken from three independent experiments using LAS AF software. Statistical analyses were calculated using a Student's t-test.

Microarray design and data analysis

Total RNA was extracted from dissected animals using the miRNeasy kit (Qiagen) with Trizol (Invitrogen). RNA quality was verified using a Bioanalyzer 2100 with Pico Total RNA chips (Agilent). RNA was amplified and labeled with Cyanine 3-CTP or Cyanine 5-CTP (Quick AMP Labeling Kit; Agilent). The array was designed in October of 2008 and comprised a 43,803 60-mer probe set targeting 43,787 sequences consisting of 20,456 JGI predictions and EST clusters, 16,816 StellaBase predictions, and 6,515 UniGene predictions, EST clusters, and mRNAs. This probe set was submitted to Agilent for their 4x44k platform under design ID: 022085. Further details are available upon request. Microarray data were analyzed in the R environment. The linear modeling package Limma (Smyth, 2004) was used to derive gene expression coefficients and calculate p-values. P-values were adjusted for multiple hypothesis testing using the method of Benjamini and Hochberg (1995). Genes were considered differentially expressed if they had adjusted p-values of less than 0.05 and an expression ratio of at least 2-fold in a given comparison. The data and array platform have been deposited in GEO under the accession numbers: GSE45588 and GPL16896.

Results

Cell proliferation is not spatially patterned in developing tentacles

Tentacle development in anthozoans has not been described in detail, and we therefore outlined the basic stages of this process in *Nematostella*. In early planula larvae, the first visible step in tentacle development was transition of the oral ectoderm to a thickened, epithelial placode (Figure 2.1A,E). In slightly later stages, the first four tentacle buds arose from within this region (Fig. 2.1B,F, brackets), and subsequently, grew out from the body (Figure 2.1C,G) and elongated into the four juvenile tentacles (Figure 2.1D,H). At this stage, planula larvae settled and further growth and differentiation took place to form the four-tentacle juvenile polyp. Concurrent with tentacle elongation, we noted that the body column also progressively elongated along the oral-aboral axis (Figure 2.1C,D). Additionally, the endoderm thinned along with the ectoderm, although this cell layer was not as rigidly organized (Figure 2.2). Importantly, all developmental events to this point took place in the absence of feeding, while the subsequent addition of tentacles and their growth were nutrient-dependent (data not shown).

A general theme emerges from previous analyses of tentacle maintenance in adult hydrozoan cnidarians, wherein specific populations of proliferating progenitor cells stop dividing, differentiate, and migrate into the tentacles (Campbell, 1967a; Campbell, 1967b; Holstein et al., 1991; Denker et al., 2008). Still, given the substantial evolutionary distance between Hydrozoa and the more basal Anthozoa

Figure 2.1 – Stages of tentacle development in *Nematostella*

(A-H) DIC images with (A-D) lateral views and (E-H) oral views of animals during tentacle development at sequential stages: early planula (A,E), budded planula (B,F), growing tentacles (C,G), and primary polyp (D,H). *Nematostella* has two cells layers: the ectoderm and endoderm (A). Buds arise within the oral placodal ectoderm, indicated by brackets (B). These buds elongate from the body (C-D, G-H) to form the four primary polyp tentacles (D,H). The oral pole is represented by the asterisks and is oriented to the right in all lateral images. Scale bar in A represents 100 μm.

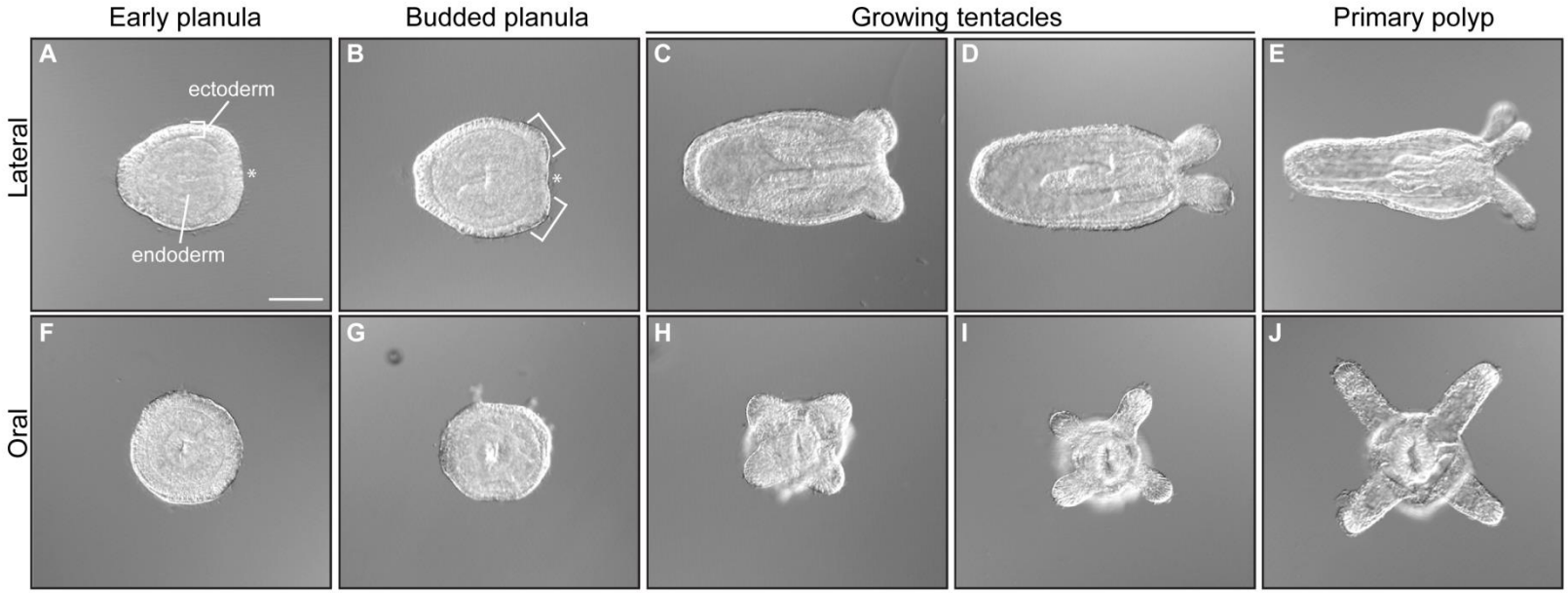
Early planula
Budded planula
Growing tentacles
Primary polyp
Lateral
Oral
A
B
C
D
E
F
G
H
I
J
ectoderm
endoderm
*
*

Figure 2.1

Figure 2.2 – Cell shape changes in the endoderm during development

(A-D) Animals at subsequent stages of development were stained with phalloidin to label F-Actin (Phalloidin; *green*) and Hoechst to label the nuclei (Hoechst; *red*). As the body column ectoderm progressively obtains a flattened morphology, the endoderm appears to make a similar transition. Yellow brackets denote the approximate thickness of the endodermal cell layer. The scale bar represents 10 μm.

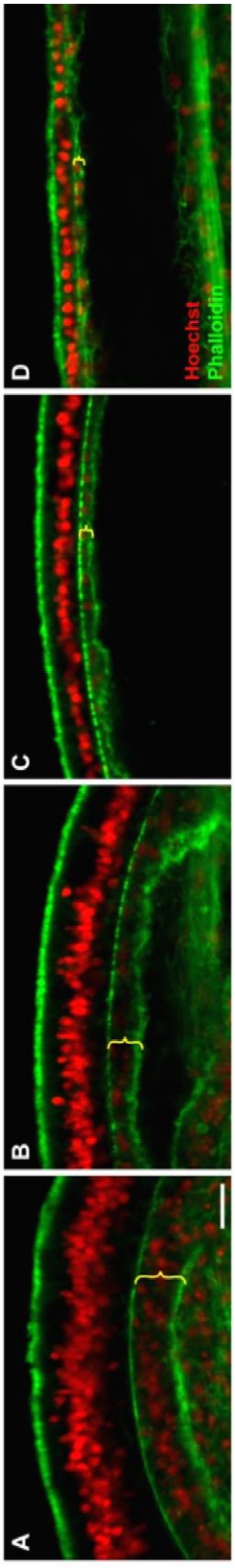

Figure 2.2

Figure 2.3 - Spatially uniform proliferation during tentacle development in *Nematostella*

(A-C) Confocal z-stacks of animals stained for EdU incorporation (*green*) and Hoechst (*red*) to visualize S-phase cells and nuclei, respectively, at sequential stages during tentacle development: early planula (A), budded planula (B), growing tentacles (C), and primary polyp (D). **(A'-D')** The EdU channel from the images in A-D shows that there are no spatially-restricted populations of proliferating cells. **(A"-D")** Magnification of the boxed regions from A'-D'. EdU positive cells can be seen in the growing and mature tentacles (see C" and D"). The outline of the animal is indicated (*dashed line*). Scale bar in A is 100 μm.

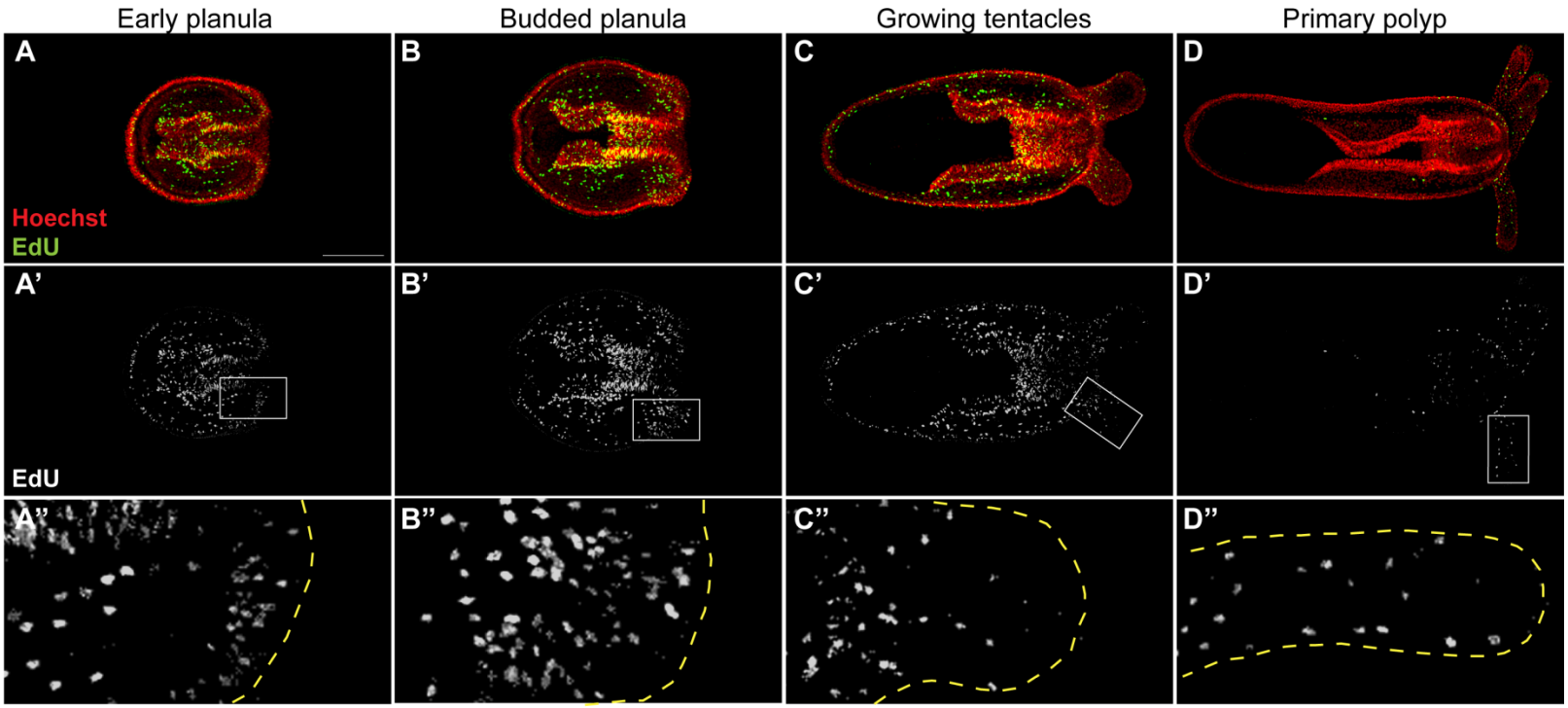
Early planula
Budded planula
Growing tentacles
Primary polyp
A
B
C
D
Hoechst
EdU
A'
B'
C'
D'
EdU
A"
B"
C"
D"

Figure 2.3

(Collins et al., 2006; Putnam et al., 2007), highly divergent mechanisms could govern tentacle morphogenesis in each group. To determine if *Nematostella* tentacle outgrowth or maintenance involves a similar mechanism of progenitor cell proliferation and migration, we isolated animals from the early planula through primary polyp stages and visualized S-phase incorporation of the nucleotide analog EdU. Throughout tentacle development, cell proliferation occurred in both the ectoderm and endoderm all along the body column (Figure 2.3A-D'). Unlike the previously studied hydrozoan systems, cell proliferation was not obviously localized to any specific region in the developing animal. Additionally, we observed EdU positive cells in the tentacle ectoderm at all stages analyzed, consistent with continuous heterogeneous proliferation throughout development (Figure 2.3A"-D").

Radical changes in the apico-basal thickness of ectodermal cells during tentacle elongation

While we did not identify localized domains of cell proliferation correlating with tentacle outgrowth, we did observe striking changes in the morphology of ectodermal epithelial cells during this process. To investigate this further, we tracked cytoskeletal dynamics using probes for both Actin and Tubulin. At the early planula stage before the initiation of tentacle development, cells in the body column and oral ectoderm constituted a thickened, pseudostratified epithelium (Figure 2.4A,E,I; Meyer et al., 2011). Just prior to tentacle bud formation, the oral ectoderm thickened in comparison

Figure 2.4 – Changes in ectodermal morphology during tentacle and body column elongation

(A-D) Confocal sections of whole animals stained with an antibody against α-Tubulin (α-Tub; *green*), phalloidin to visualize F-Actin (*red*), and Hoechst to label nuclei (*blue*) at sequential stages: early planula (A), budded planula (B), growing tentacles (C), and primary polyp (D). **(E-H)** Confocal sections of buds or tentacles at representative stages corresponding to A-D. Cells in the ectoderm change apico-basal dimension during tentacle development. **(I-L)** Similar cell shape changes are seen in the body column ectoderm at corresponding stages. **(I'-L')** F-Actin channel of I-L demonstrating the thickness of the ectoderm (brackets). **(I"-L")** Ectodermal cell cilia, as visualized by α-Tubulin staining, shorten during body column elongation. Brackets indicate length of cilia. **(M)** Quantification of body column and oral ectodermal thickness during elongation at stages that correlate with A-D. *P<0.001 (Student's *t*-test) **(N)** Quantification of cilia length from early planula and primary polyp stages. Error bars represent s.d.; n, number of individuals examined for each stage. Scale bars: 100 μm in D; 10 μm in H,L".

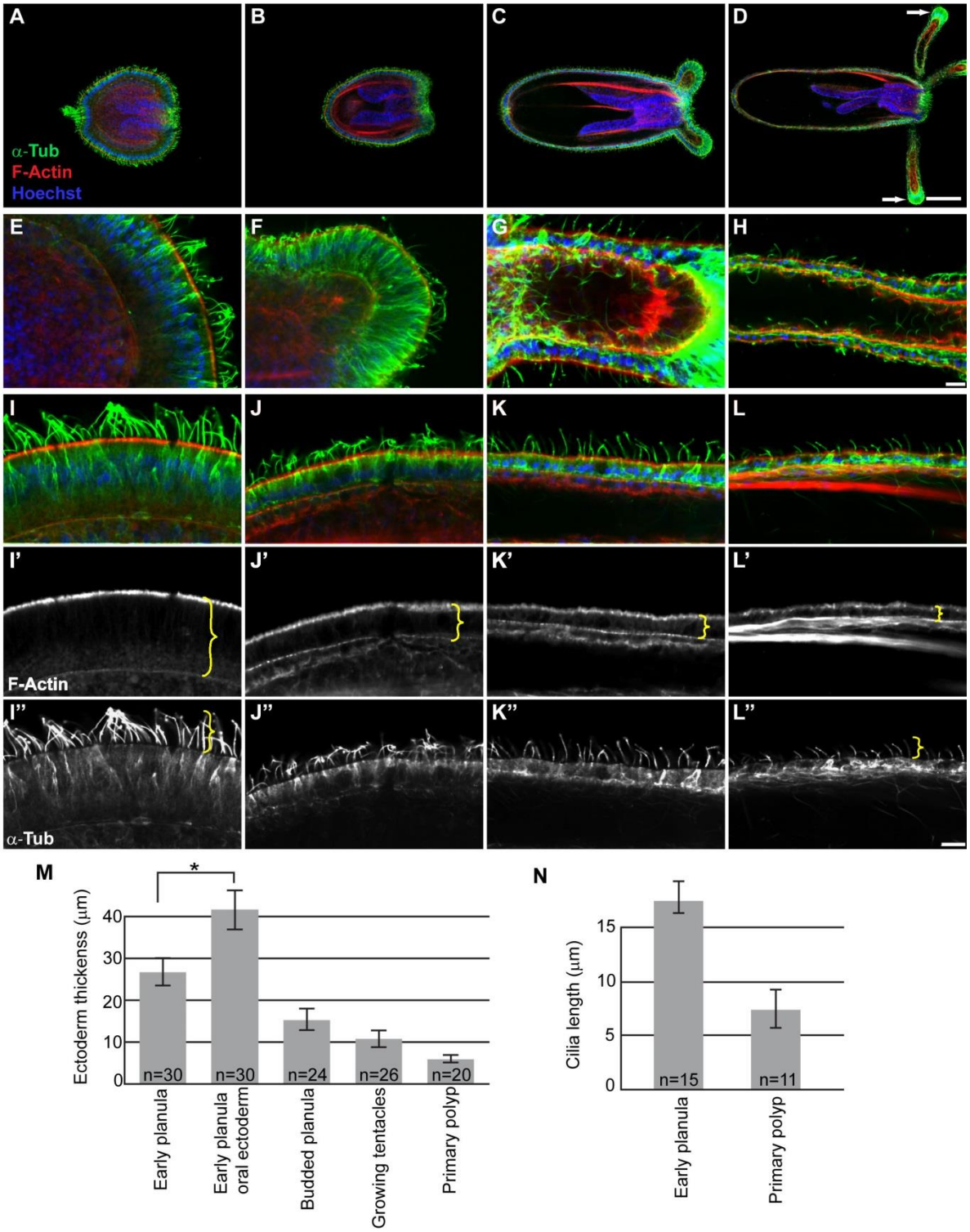
A
B
C
D
α-Tub
F-Actin
Hoechst
E
F
G
H
I
J
K
L
I'
J'
K'
L'
F-Actin
I''
J''
K''
L''
α-Tub
M
Ectoderm thickenss (μm)
0
10
20
30
40
*
n=30
n=30
n=24
n=26
n=20
Early planula
Early planula oral ectoderm
Budded planula
Growing tentacles
Primary polyp
N
Cilia length (μm)
0
5
10
15
n=15
n=11
Early planula
Primary polyp

Figure 2.4

to the body column, and the first four tentacle buds formed within this oral epithelial placode (Figure 2.4B,F; quantified in Figure 2.4M). As the buds elongated into tentacles, we observed a concomitant progression of the thickened, pseudostratified ectoderm into a simple columnar, then cuboidal and finally a more flattened morphology (Figure 2.4F-H). Interestingly, cells in the tentacle tips did not flatten (Figure 2.4D, arrows), perhaps allowing for a higher density of nematocysts used for prey capture. Similar cellular events were observed in the body column ectoderm during elongation of the oral-aboral axis (Figure 2.4I-L). Early in larval development the thickness of the body column ectoderm averaged 27.2 +- 3.2 μm, which thinned to an average of only 6.2 +- 0.9 μm by the primary polyp stage (Figure 2.4I'-L' and quantified in Figure 2.4M). Interestingly, during the progressive thinning of the ectodermal epithelium, the cilia associated with these cells also became progressively shorter (Figure 2.4I"-L", quantified in Figure 2.4N).

Actin dynamics are required for elongation of the body column and tentacles

The observations above suggest that changes in ectodermal cell shape could vastly increase the surface area of primary polyps, thereby representing a primary driver of tentacle outgrowth and the elongation of the body column. To functionally test the role of cell shape changes during elongation, we disrupted Actin polymerization with Cytochalasin D (Cyto D; 1 μM in 0.1% DMSO; Casella et al., 1981). For these experiments, animals were raised at 16°C for ten days post-fertilization, and then swimming planula were treated with Cyto D for 48 hours during the period of normal cell

Figure 2.5 – Cytochalasin D treatment of planula larvae inhibits ectodermal cell shape changes

(A-D) Confocal sections of whole mount animals stained with phalloidin to label F-Actin (*red*) and Hoechst to visualize nuclei (*green*). **(A'-D')** Magnified view of body column ectoderm from animals corresponding to A-D. Brackets indicate ectodermal thickness. Animals were treated at the planula stage (A,A'). Control animals elongated their body columns and grew tentacles (B,B'). Cytochalasin D (Cyto D)-treated animals were not able to elongate their body columns or grow tentacles (C,C'). This was accompanied by a lack of cell shape change in the ectoderm (compare C' with the control in B'). Animals recovered after Cyto D was washed off (D,D'). **(E)** Phenotypes of the Cyto D-treated animals were quantified by the percentage of animals that developed tentacles (*n*=66). **(F)** Apico-basal thickness of the body column ectoderm in Cyto D-treated animals. *P<0.001 (Student's *t*-test). The ectoderm of control, Cyto D-treated, and Cyto D-treated + wash animals was significantly thinner than at the start point. The Cyto D-treated animals had a significantly thicker body column ectoderm than controls. The treated + wash animals were able to thin the ectoderm to a thickness that was similar to controls. Error bars represent s.d.; n, number of individuals examined for each condition. Scale bars: 100 μm in A; 10 μm in A'.

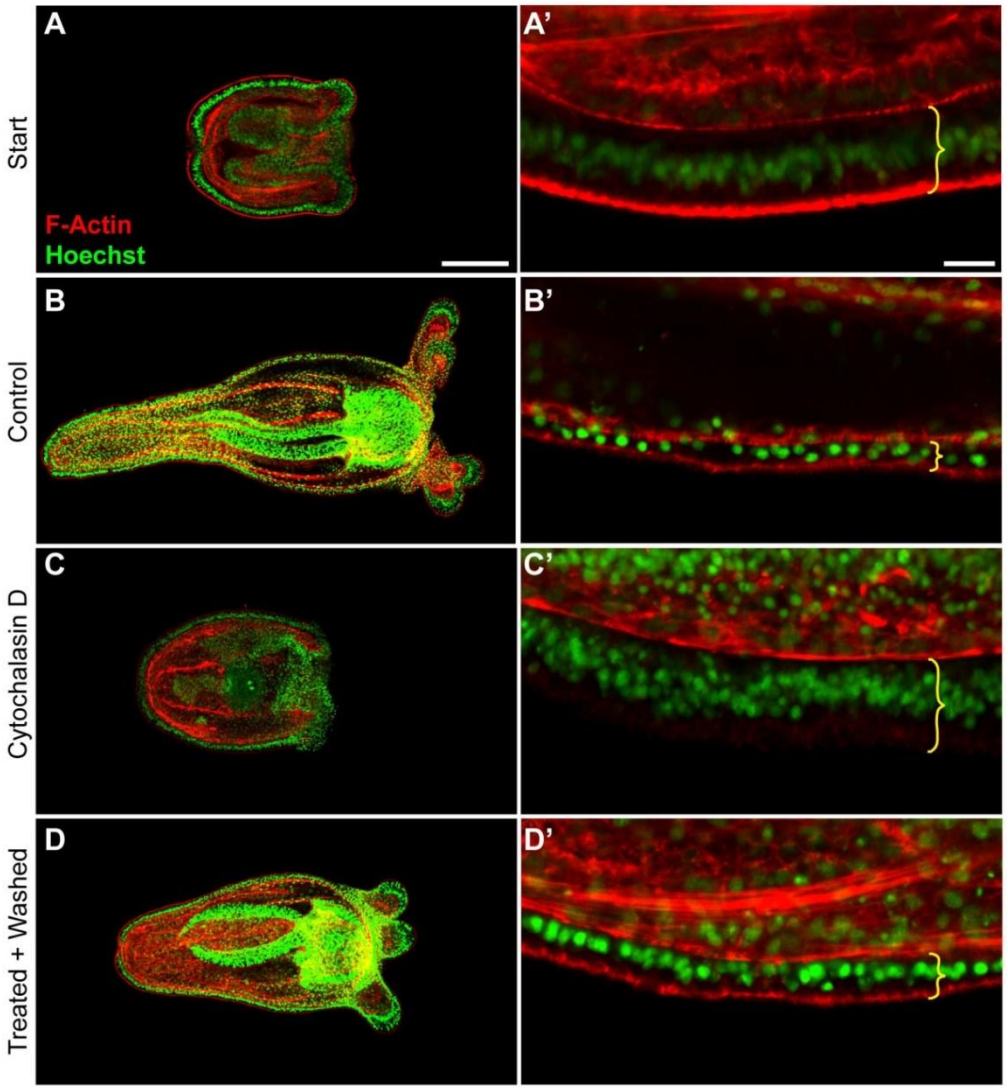
A
A'
Start
F-Actin
Hoechst
B
B'
Control
C
C'
Cytochalasin D
D
D'
Treated + Washed

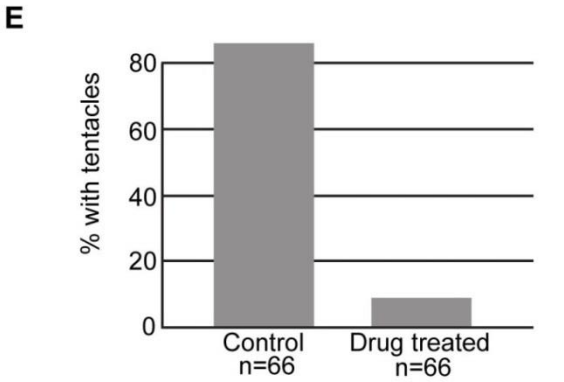
E
% with tentacles
80
60
40
20
0
Control
n=66
Drug treated
n=66

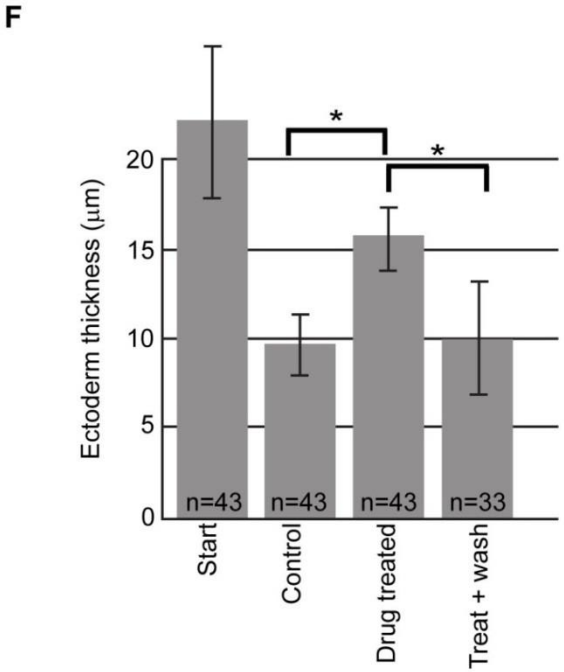
F
Ectoderm thickness (μm)
20
15
10
5
0
*
*
n=43
n=43
n=43
n=33
Start
Control
Drug treated
Treat + wash

Figure 2.5

Figure 2.6 – Cell proliferation is reduced with Cytochalasin D treatment

(A-B) Control (A-A') and Cyto D treated (B-B') animals were stained for EdU incorporation (EdU; *green*) and nuclei (Hoechst; *red*). While Cyto D animals still show some proliferation (B'), it is reduced as compared to controls (A'). Scale bar represents 100 μm.

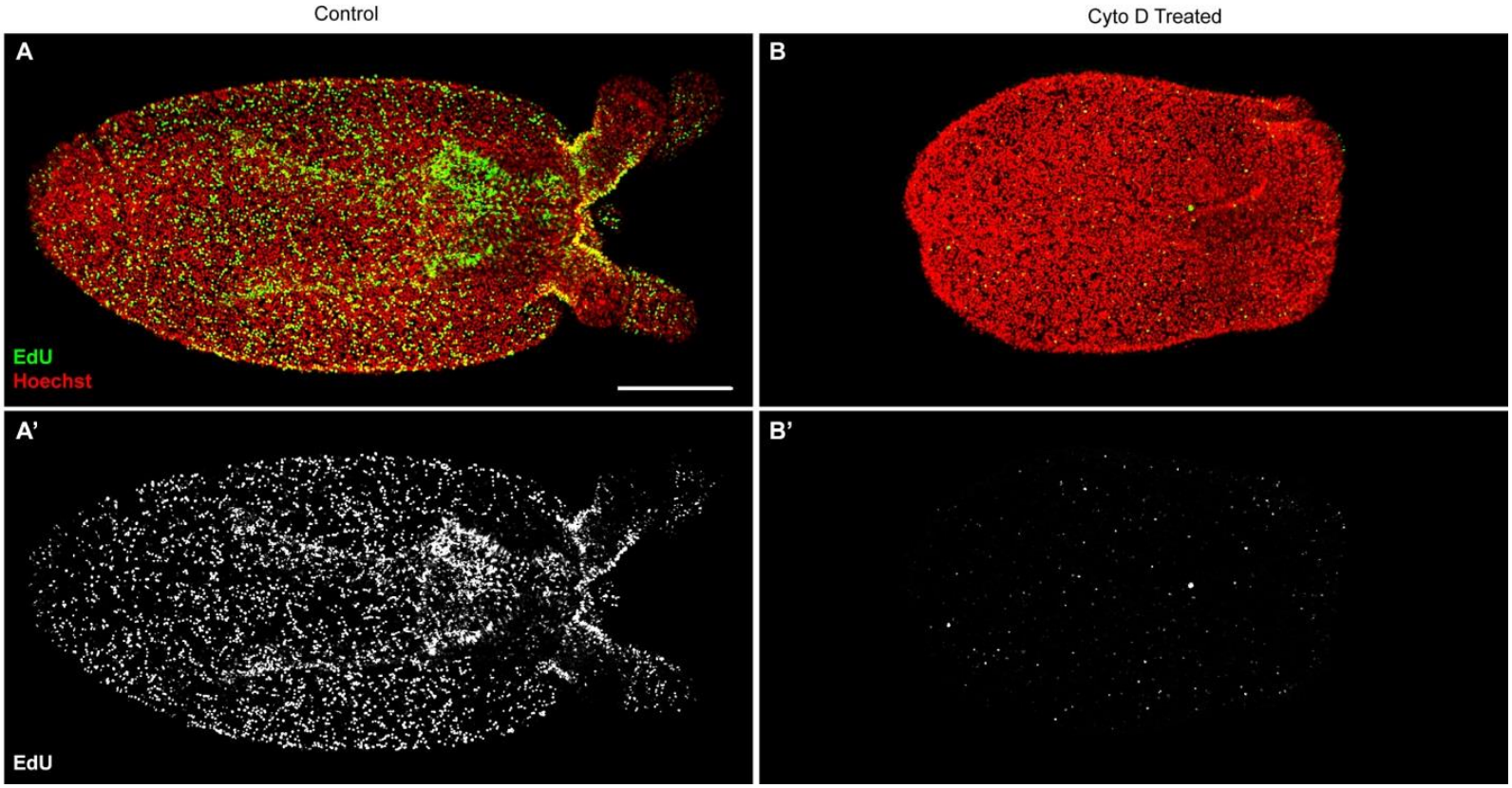

Figure 2.6

shape change and elongation (Figure 2.5A). Control animals elongated their body columns and formed growing tentacles in these two days (Figure 2.5B), but animals treated with Cyto D were unable to form tentacles or elongate the body column (Figure 2.5C, quantified in Figure 2.5E). These defects correlated with a block in epithelial morphogenesis. While the ectoderm of control animals thinned normally (Figure 2.5A', B'), drug treated animals retained a thickened, pseudostratified epithelium (Figure 2.5C', quantified in Figure 2.5F).

Additionally, we examined cell proliferation by EdU incorporation in the Cyto D treated and control animals. Although there was still some cell proliferation after Cyto D treatment, it was reduced compared to that in control animals (Figure 2.6). Intriguingly, upon removal of the drug treatment, these animals were able to continue development to become primary polyps (Figure 2.5D). These changes directly correlated with a thinning of the ectoderm into a more flattened epithelium as in controls (Figure 2.5D', quantified in Figure 2.5F). Combined, these results indicate that Actin polymerization is required for changes in ectodermal cell shape and the associated elongation of the body column and tentacles.

Elongation is directed by cell rearrangements and orientated cell division

While a dramatic reduction in apico-basal thickness of ectodermal cells can account for an increase in surface area of the entire animal, it cannot explain the directional expansion along the oral-aboral axis. To address how this is achieved, we used mosaic expression analysis. We microinjected one cell stage embryos with a

Figure 2.7 – Analysis of ectodermal cell clones during body column and tentacle elongation

GFP-marked cell clones (*green*) in representative animals stained with phalloidin to label F-Actin (*red*). Ectodermal surface views are shown. **(A,A')** Embryos exhibited irregular and largely isometric clone morphologies. **(B,B')** In early planula, the clone shape was not significantly different from that of the embryo. **(C,C')** By the late planula stage, cell clones appeared to elongate along the oral-aboral axis. The inset shows a clone of GFP-positive cells with both a rounded shape and a linear array of cells extending along the oral-aboral axis. **(D,D')** Primary polyps had highly elongated clone shapes. Asterisks indicate the position of the oral pole. Scale bars in A is 25 μm.

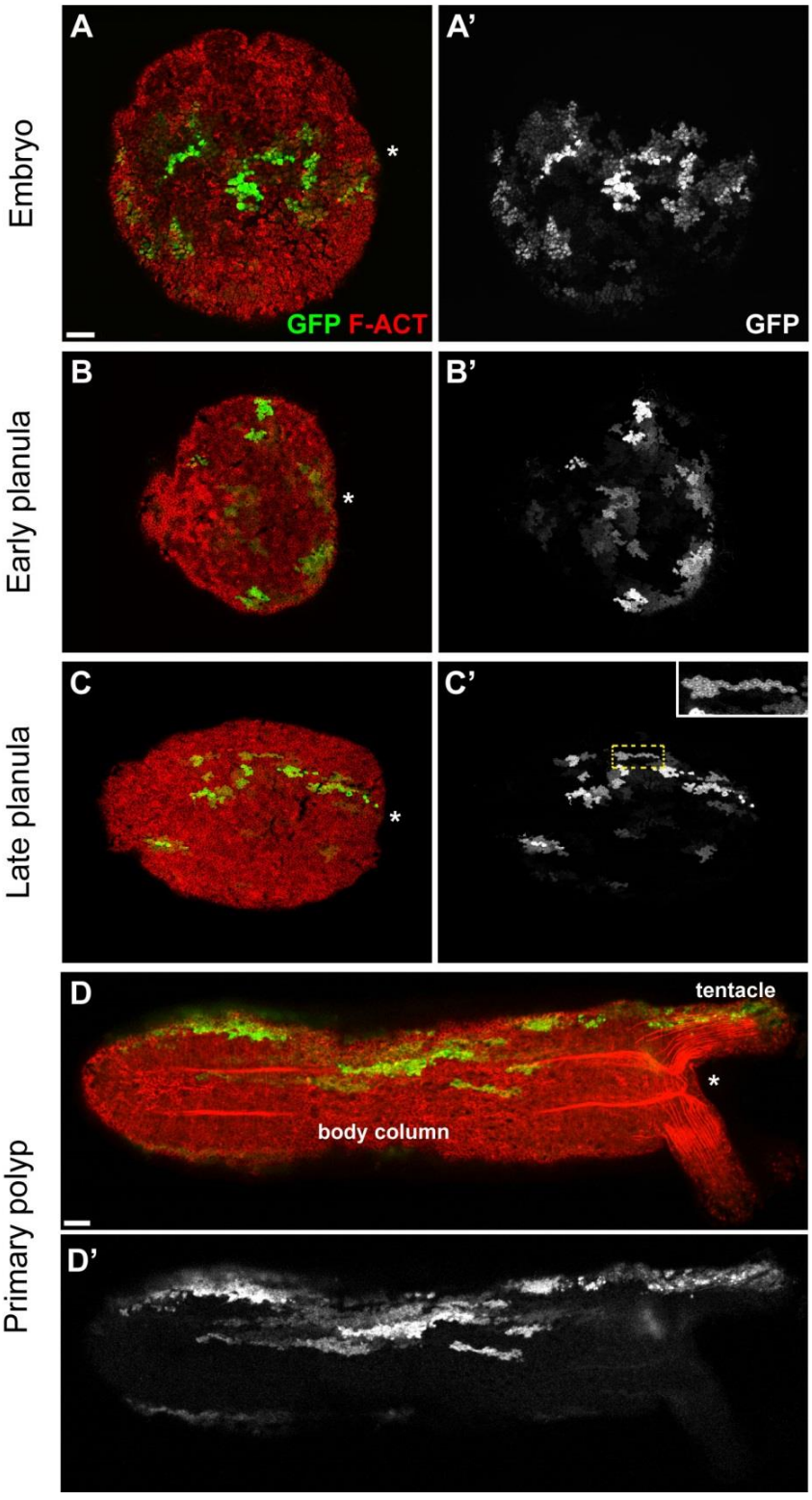
Embryo
Early planula
Late planula
Primary polyp
A
A'
GFP F-ACT
GFP
B
B'
C
C'
D
tentacle
body column
D'

Figure 2.7

Figure 2.8 - Additional examples of Ubiquitin-GFP injected animals showing the shape of ectodermal GFP-marked cell clusters during body column and tentacle elongation

(A-D) GFP-marked cell clones (GFP; *green*) in animals stained with phalloidin to label F-Actin (F-ACT; *red*) show additional examples of clone shape in embryos (A) and early planula larvae (B). Elongating cell clones appear in late planula larvae (C). Primary polyps exhibit highly elongated clones along the oral-aboral axis (D). Scale bars represent 25 μm.

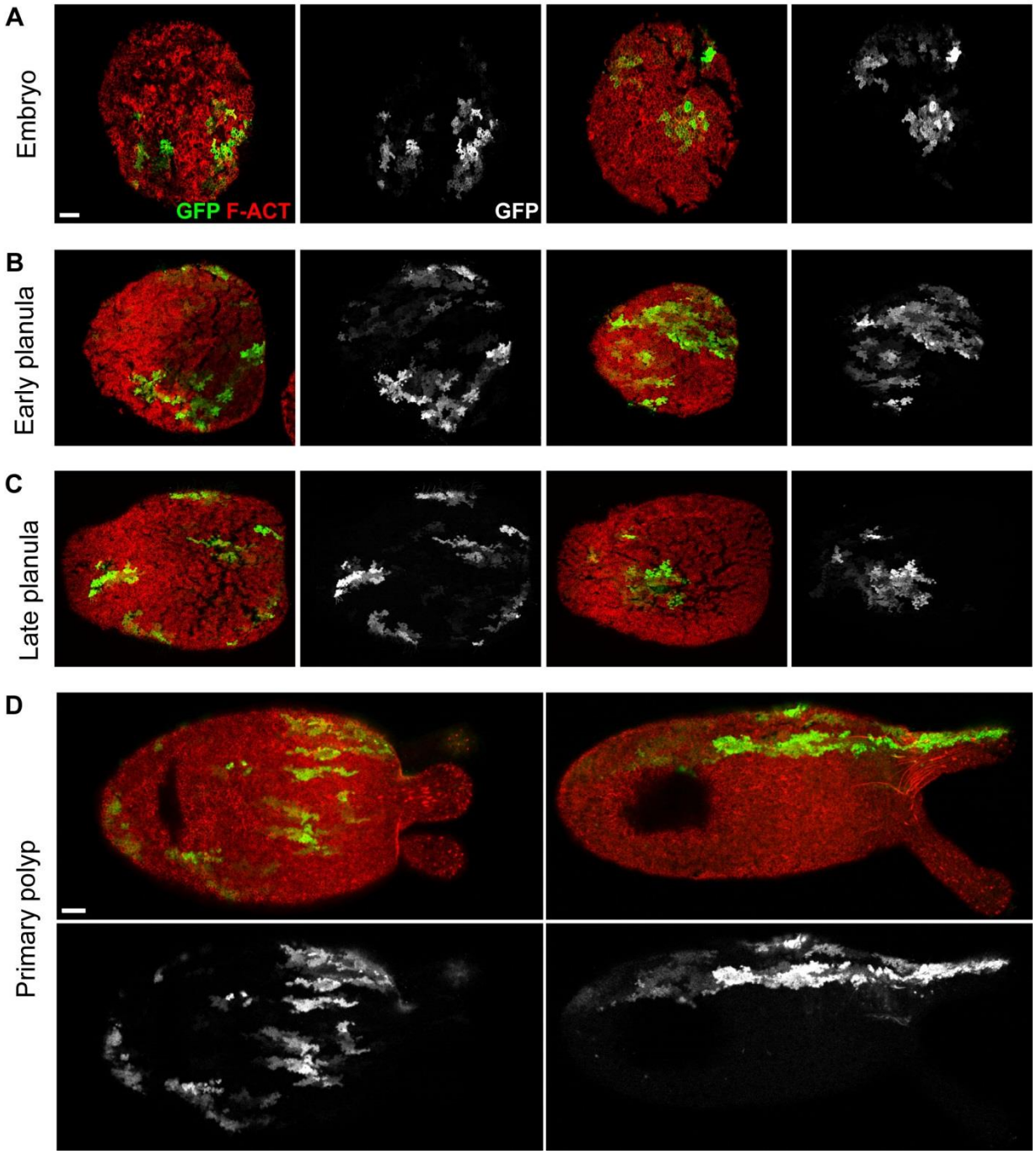
A
Embryo
GFP F-ACT
GFP
B
Early planula
C
Late planula
D
Primary polyp

Figure 2.8

construct expressing Green Fluorescent Protein (GFP) under the control of the *Nematostella ubiquitin* promoter, taking advantage of the resulting mosaic expression of GFP to observe the behavior of cell clones. Strikingly, there were clear changes in the shape of GFP-expressing clones at different stages of body column and tentacle elongation (Figure 2.7, Figure 2.8). At both embryonic and early planula larvae stages, animals had irregular but largely isometrically shaped GFP-expressing clones (Figure 2.7A-B'; Figure 2.8A,B). As late planulae began to undergo elongation of the body column and tentacles, we observed both irregularly-shaped and elongated clones (Figure 2.7C,C'; Figure 2.8C). Intriguingly, by the primary polyp stage almost all clones comprised linear arrays of cells stretching along the oral-aboral axis in both the body column and tentacles (Figure 2.7D,D'; Figure 2.8D).

The rearrangement of cell clones into linear oral-aboral morphologies could be explained by either cell rearrangements, such as convergent extension, or oriented cell division. To distinguish between these two possibilities, we analyzed the orientation of cell division during elongation of the body column and tentacles. In order to determine the angle of the spindle, animals from embryonic to primary polyp stages were stained to visualize microtubules and DNA, thus revealing orientation of metaphase and anaphase figures. The angle of the spindle was measured in degrees from the oral-aboral axis for the body column (Figure 2.9A,A'). While the spindle orientation early in development was random (Figure 2.10A-B), spindle orientations became biased along the oral-aboral axis during body column elongation (Figure 2.10C-F). As elongation progressed in the budded planula stage, this bias weakened and spindle orientation became more random (Figure 2.10G-I). Additionally, we measured the angles of mitotic

Figure 2.9 – Method for measurement of the orientation of cell division

(**A-A'**) During body column elongation, the angle between the mitotic spindle (*dashed yellow line*) and the oral-aboral axis (*solid yellow arrow*) was defined as the spindle angle. White arrowheads indicate mitotic figures. **(B-C)** In both developing buds (B-B') and tentacles (C), the angle of the spindle was measured from the proximo-distal axis (*solid white arrow*). This axis is parallel to the thickness of the bud and tentacle (*solid yellow lines*). Scale bars represent 25 μm.

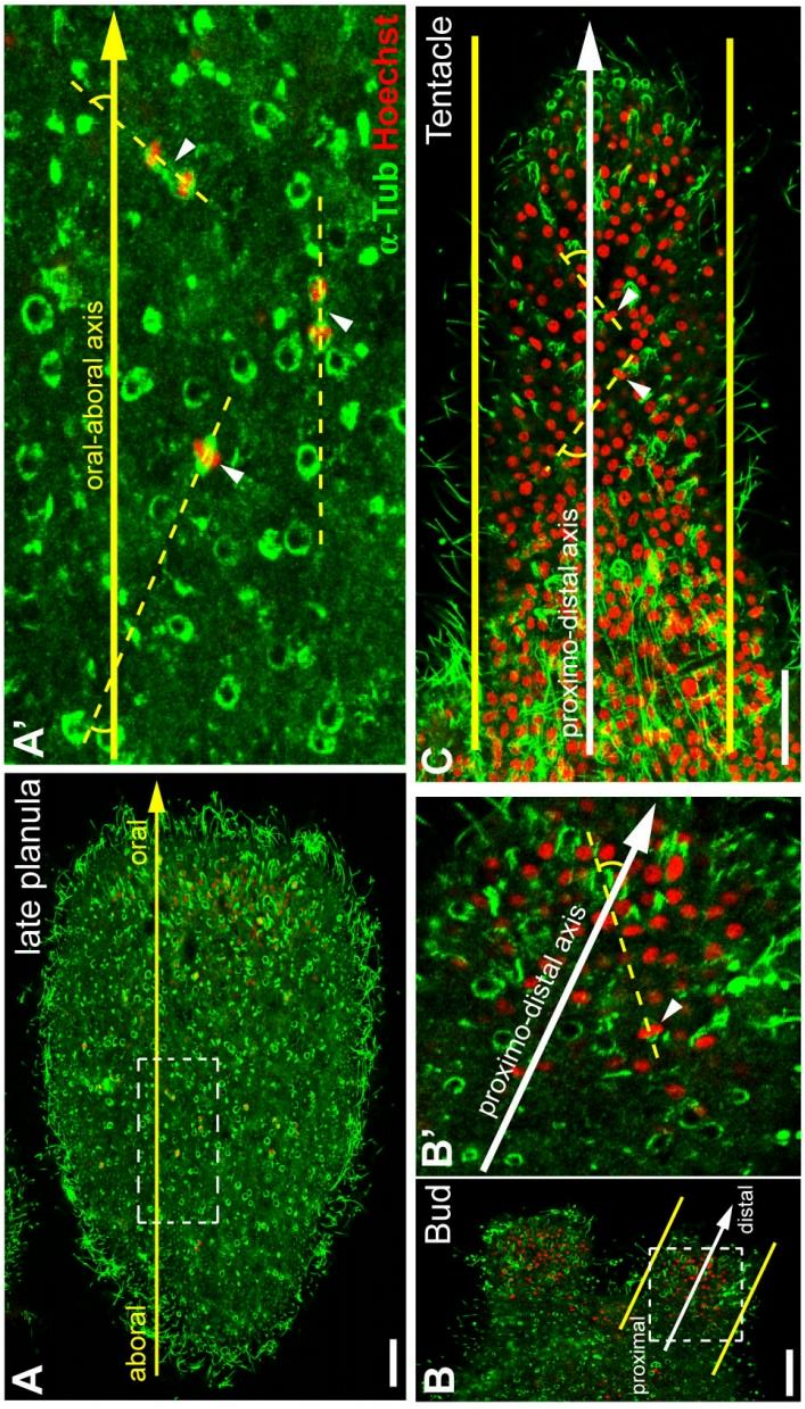
A
late planula
oral
aboral
A'
oral-aboral axis
α-Tub Hoechst
B
Bud
proximal
distal
B'
proximo-distal axis
C
Tentacle
proximo-distal axis

Figure 2.9

Figure 2.10 - Orientation of ectodermal cell division during *Nematostella* development

(A-I) Animals were stained for α-Tubulin to label mitotic spindles (*green*) and Hoechst to label nuclei (*red*). Orientation of the mitotic spindles was measured in embryos (A-B), early planula larvae (C-D), late planula larvae (E-F), budded planula larvae (G-H), and primary polyps (I). Asterisks indicate the oral pole. The boxed regions in A,C,E,G are magnified in A',C',E',G' to show detailed views of the ectoderm. Double headed arrows indicate mitotic figures as well as the orientation of the mitotic spindle. The angular deviation of the mitotic spindle was measured as degrees from the oral-aboral axis (B,D,F,H,I). n, number of mitotic figures used for quantification. Note the strong alignment of mitotic spindles along the oral-aboral axis in late planula stage animals (E-F). (**J-M**) Angular deviation of mitotic spindle alignment from the proximo-distal axis of tentacle buds (J-K) and mature tentacles (L-M). The boxed regions in J and L are magnified in J' and L'. The dashed line in J indicates the approximate boundary of the bud. The small green α-Tubulin-positive rings are nematocyst capsules. Scale bars: 25 μm.

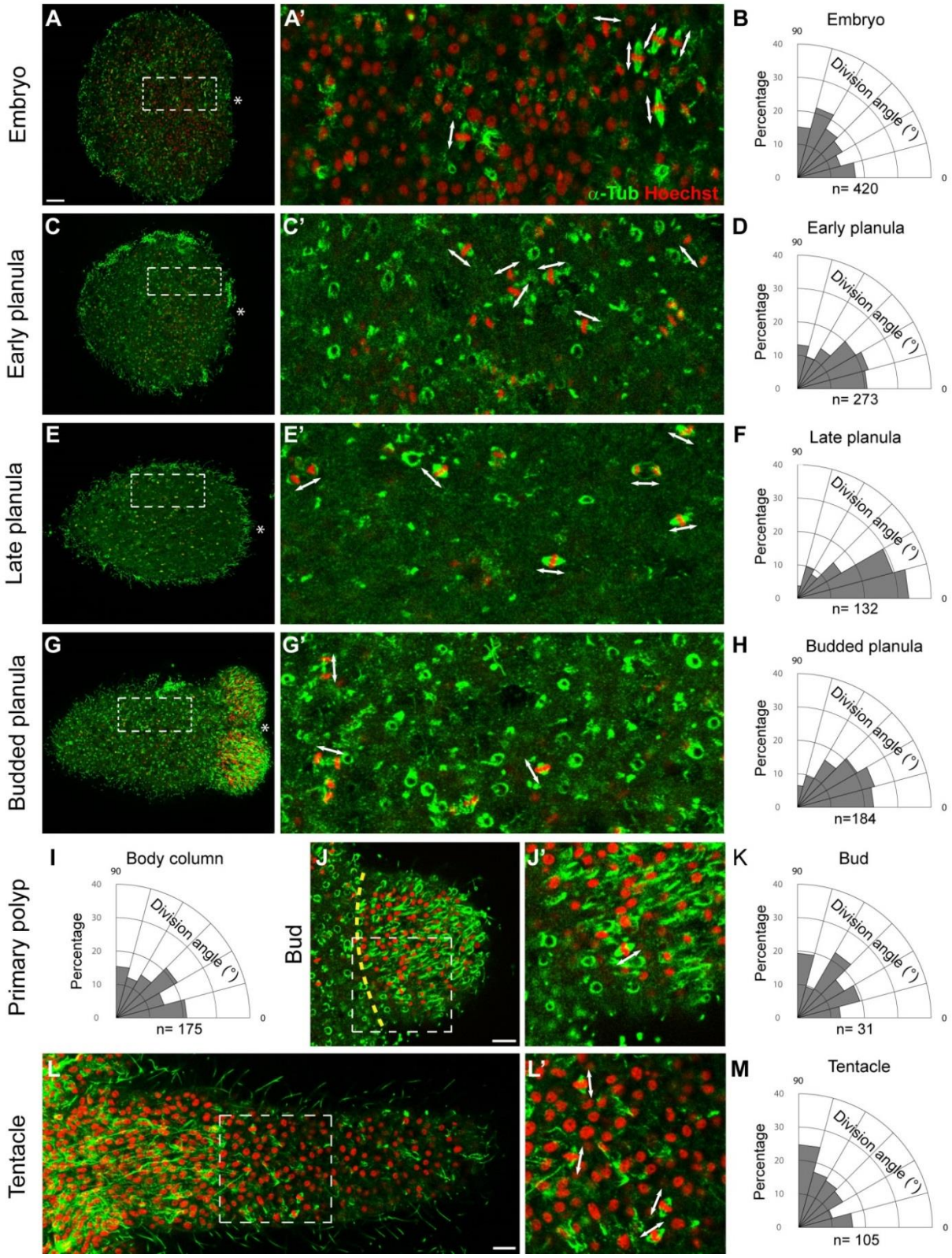
Embryo
Early planula
Late planula
Budded planula
Primary polyp
Tentacle
Bud
A
A'
α-Tub Hoechst
B
Embryo
Division angle (°)
Percentage
n= 420
C
C'
D
Early planula
n= 273
E
E'
F
Late planula
n= 132
G
G'
H
Budded planula
n=184
I
Body column
n= 175
J
J'
K
Bud
n= 31
L
L'
M
Tentacle
n= 105

Figure 2.10

spindles in the tentacle buds and tentacles in degrees from the proximo-distal axis (Figure 2.9B,C). Interestingly, here we did not observe any bias in spindle orientation (Figure 2.10J-M). Taken together, these results suggest that both cellular rearrangements and oriented cell division play a role in elongation of the body column. In developing tentacles, however, we found evidence for cellular rearrangements but did not observe a bias in mitotic spindle orientation.

Notch signaling is required for tentacle elongation

A relatively limited set of developmental signaling pathways regulate the patterning and morphogenesis of tissues and organs in all animals (Gerhart, 1999; Pires-daSilva and Sommer, 2003). Interestingly, the transmembrane receptor, Notch, and its ligand, Delta, are expressed orally and around the tentacle primordia in *Nematostella* larvae (Marlow et al., 2012). To investigate the role of Notch during tentacle morphogenesis, we modulated signaling using a pharmacological inhibitor, DAPT (Dovey et al., 2001; Kasbauer et al., 2007; Marlow et al., 2012). DAPT inhibits γ-secretase, the enzyme responsible for cleaving the Notch intracellular domain (NICD; Geling et al., 2002). We applied 20 μM DAPT in 0.1% DMSO to planula stage animals for two days during the expected period of body column and tentacle elongation (Figure 2.11A). As expected, control animals elongated their body columns and formed growing tentacles in these two days (Figure 2.11B,B'), morphogenetic events that were accompanied by changes in ectodermal cell shape (Figure 2.11B"). In direct contrast, DAPT treated animals failed to develop tentacles (Figure 2.11C, quantified in Figure

2.11D), and the oral ectoderm retained its thickened tentacle buds (Figure 2.11C'). Surprisingly, while normal morphogenesis of the tentacle ectoderm was blocked, DAPT treated animals exhibited normal thinning of the body column ectoderm and were still able to elongate their body columns along the oral-aboral axis (Figure 2.11C,C", quantified in Figure 2.11E). Additionally, cell proliferation and cnidocyte localization appeared unaffected (Figure 2.12 and Figure 2.13). These unexpected results demonstrate that epithelial shape changes in the body column and tentacular ectoderm are subject to distinct forms of upstream regulation. Specifically, disruption of Notch signaling did not affect the cell shape changes or elongation of the main body column, but did have a dramatic effect on cell shape change and elongation of the tentacles. These results further support the hypothesis that the cell shape change in the ectoderm is important for elongation, since the tentacle buds remained thickened and did not elongate from the body (Figure 2.11B', C').

Notch signaling generally acts through activation of downstream transcriptional targets, and we therefore sought to identify factors modulated by DAPT treatment. We examined the expression patterns of six previously identified tentacle domain markers and confirmed that the homeodomain transcription factor *OtxB* is expressed in developing tentacle buds and at the tips of tentacles in primary polyps (Mazza et al., 2007; Table 2.1; Figure 2.14A,B). In animals treated with DAPT for 48 hours at the planula stage, *OtxB* was no longer expressed in the tentacle buds. Instead, we observed *OtxB* misexpression in the oral pole of the mesenteries, which are internal endomesodermal structures (Figure 2.14C). These results imply a role for Notch signaling in regulating the expression of *OtxB*. None of the other genes we examined

Figure 2.11 – Notch signaling is required for tentacle elongation

(A-C) Confocal sections of whole animals stained with phalloidin to visualize F-Actin (*green*) and Hoechst to label nuclei (*red*). **(B',C')** Higher magnification confocal sections of the tentacle regions indicated by the larger boxes in B and C. **(B",C")** Higher magnification confocal sections of the body column ectoderm indicated by the smaller boxes in B and C. Animals were treated at the planula stage (A). Control animals had growing tentacles (B,B') and elongated body columns, which had undergone a cell shape change (B"). DAPT-treated animals remained budded and were not able to elongate tentacles (C,C'), but still elongated their body columns and underwent a cell shape change (C,C"). **(D)** The percentage of animals that developed tentacles in the presence and absence of DAPT. **(E)** Quantification of body column ectoderm thickness. Errors bars represent s.d.; n, number of individuals examined in each condition. *P<0.001 (Stendent's *t*-test). The body column ectoderm thickness was similar in control and DAPT-treated animals and significantly thinner than at the start point. Scale bars: 100 μm in C; 25 μm in C'; 10 μm in C".

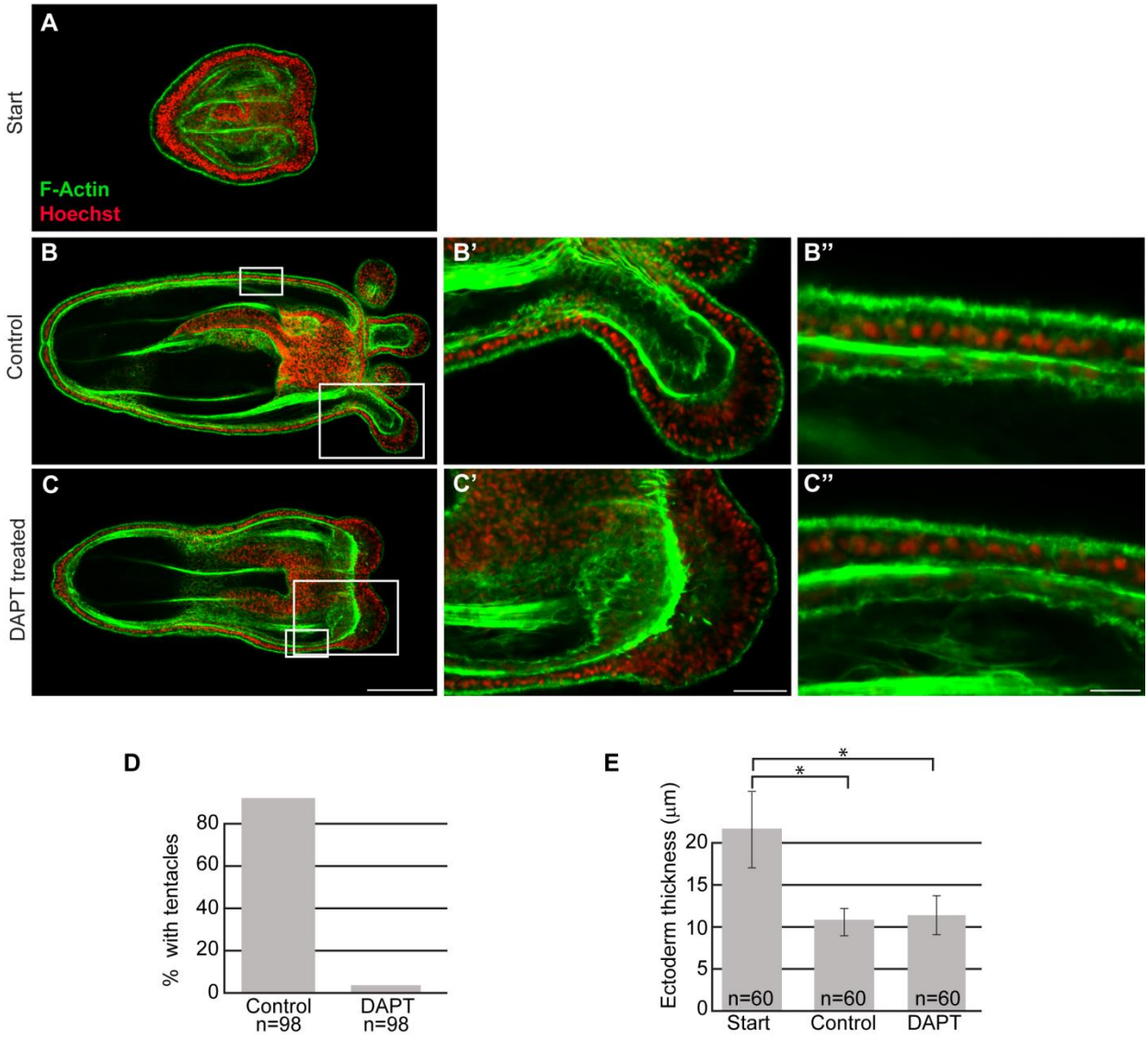
A
Start
F-Actin
Hoechst
B
B'
B''
Control
C
C'
C''
DAPT treated
D
% with tentacles
80
60
40
20
0
Control
n=98
DAPT
n=98
E
Ectoderm thickness (µm)
20
15
10
5
0
*
*
n=60
n=60
n=60
Start
Control
DAPT

Figure 2.11

Table 2.1: Genes screened by *in situ* hybridization after DAPT treatment

Sequence name	Accession	Expression Pattern Change?
ZicC	AB231868	no
OtxA	FJ824849	no
OtxB	FJ824850	yes
OtxC	FJ824851	no
Crossveinless-2	XM_001625111	no
Homeobrain	HM004558	no
Anthox2	AF085283.1	no
FoxL2	JGI: 82873608	no
Forkhead1	XM_001630267.1	no
Forkhead2	XM_001638841.1	no
Growth factor receptor	XM_001637818	no
G protein receptor	XM_001636348.1	no

Figure 2.12 – Cell proliferation is not affected by inhibition of Notch signaling

(A-B) Confocal stacks of animals stained for EdU incorporation (EdU; *green*) and nuclei (Hoechst; *red*) for Control (A) and DAPT treated (B) animals. (A'-B') EdU channel from A-B. DAPT treated animals still had many EdU positive cells (B'). The scale bar represents 100 μm.

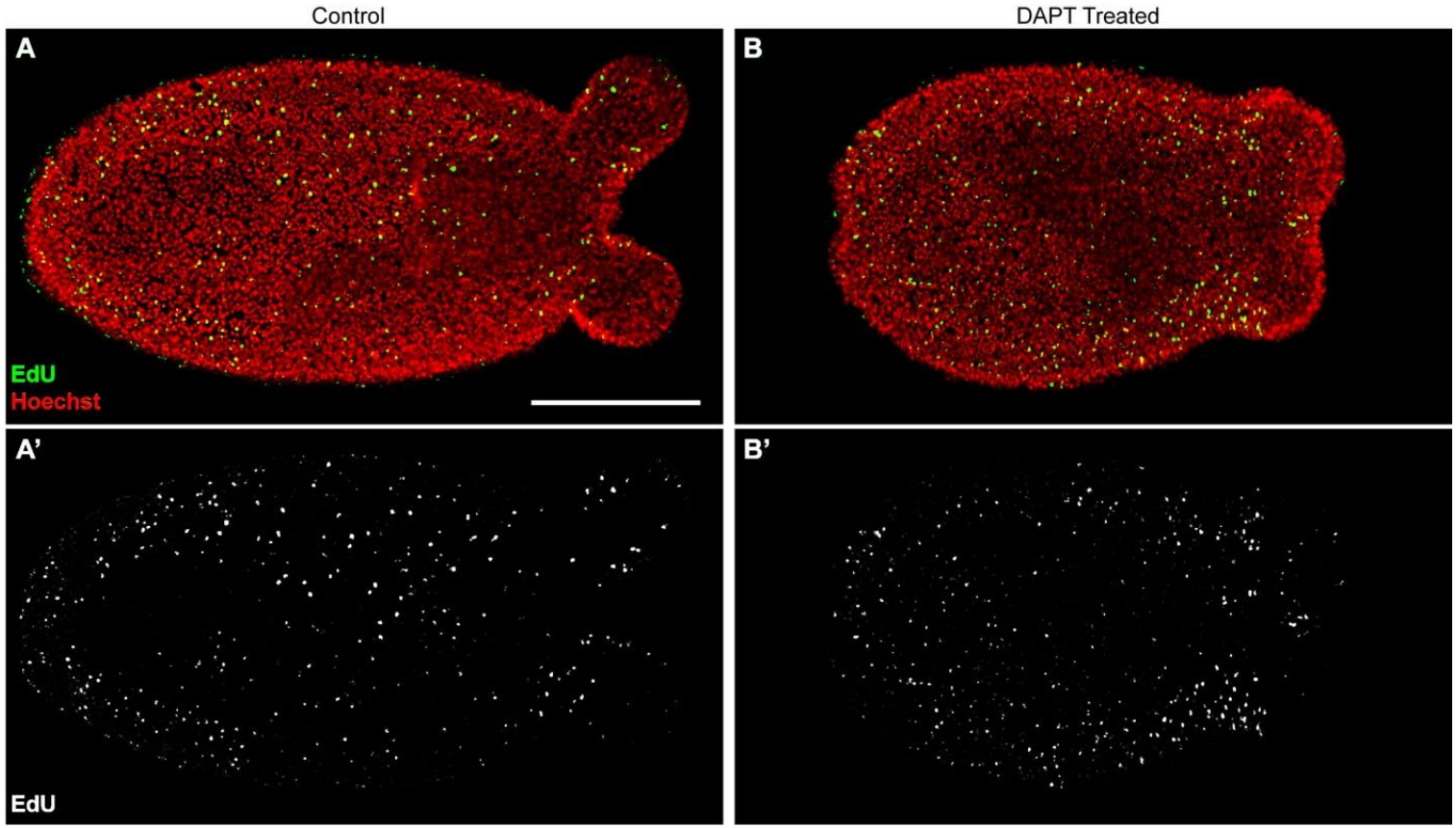

Figure 2.12

Figure 2.13 – Inhibition of Notch signaling during elongation did not dramatically alter cnidocyte localization

(A-C) Confocal stacks of animals stained with DAPI to visualize cnidocytes. Animals at the start of the experiment (A, A') had cnidocytes. Both control (B, B') and DAPT treated (C, C') animals had many cnidocytes all over their bodies. Red channel shows nuclei and cnidocytes excited by the UV laser. The green channel and bottom panel (A'-C') shows cnidocytes excited by the 488 laser. The scale bar represents 100 μm.

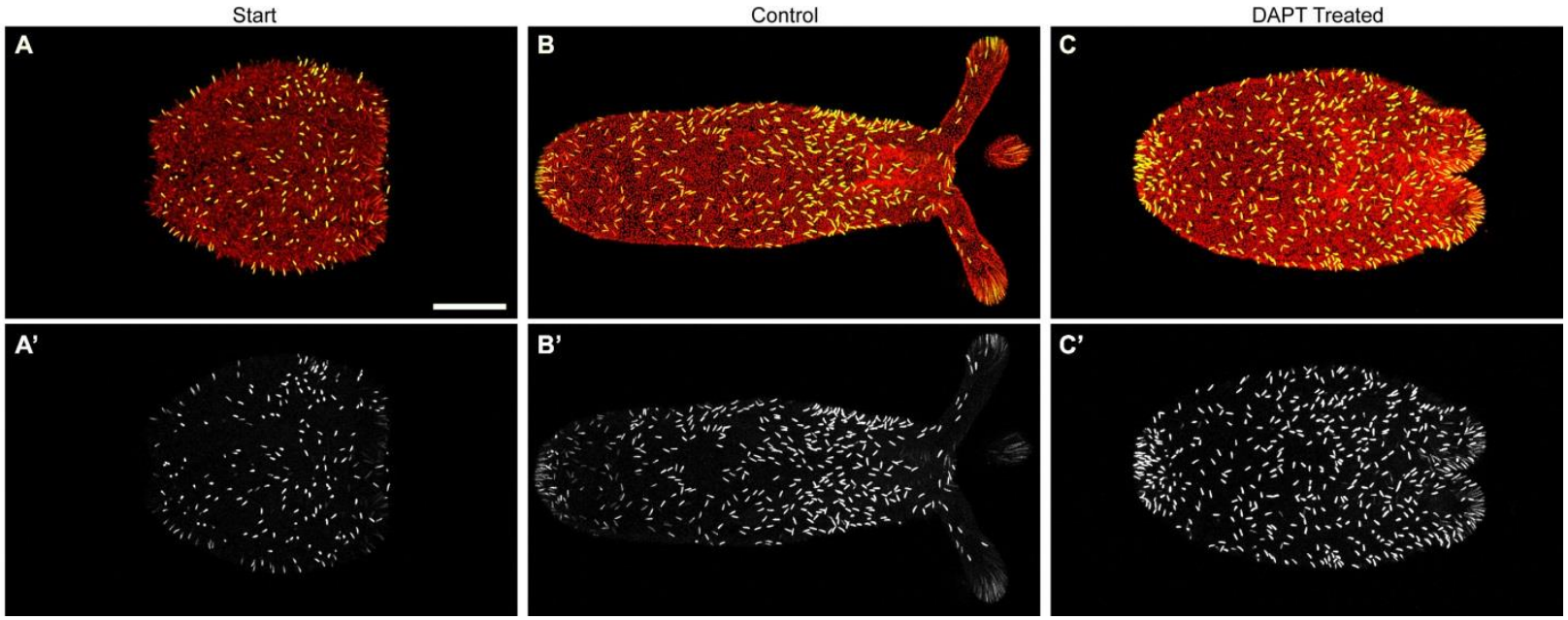

Figure 2.13

Figure 2.14 – *OtxB* expression is altered after inhibition of Notch signaling

(A-C) Oral (*top row*) and lateral (*bottom row*) views of RNA *in situ* hybridization with probes for *OtxB*. *OtxB* is normally expressed in the tentacle primordia (A) (Mazza et al., 2007) and then at the tips of the tentacles (C). It was also expressed at the aboral pole throughout development (A-B). After DAPT treatment, *OtxB* was misexpressed in the oral regions of the mesenteries, but aboral expression was maintained (C).

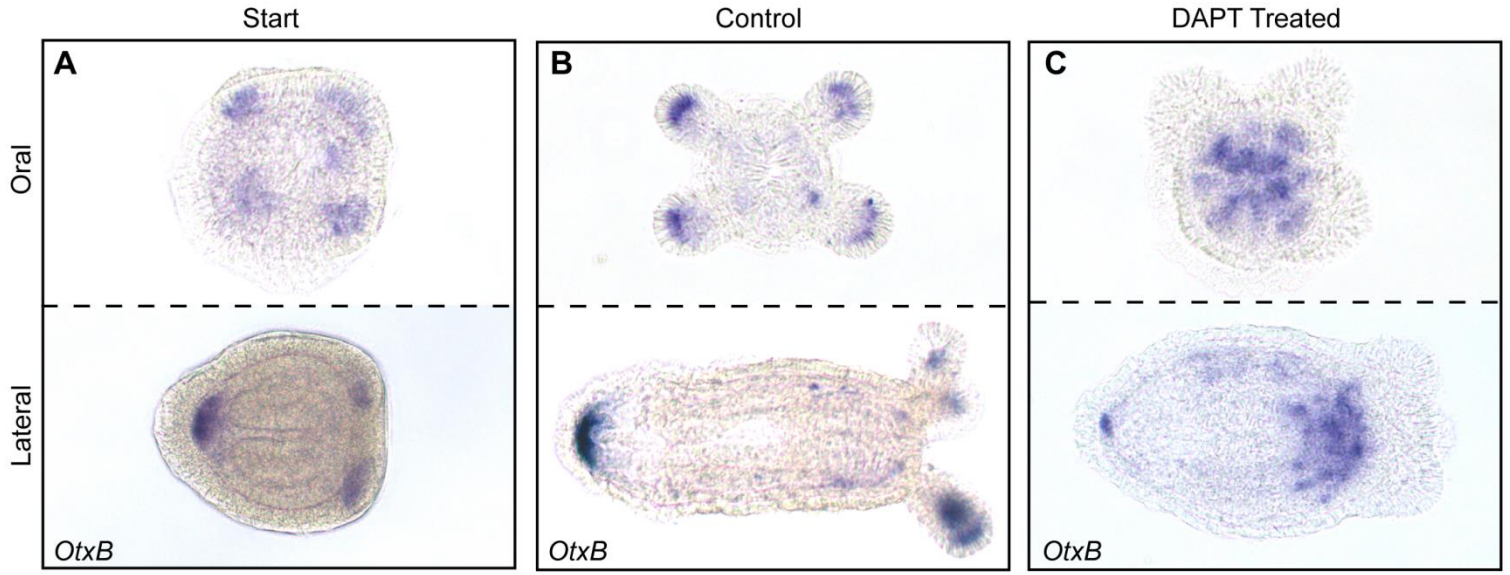

Figure 2.14

had detectable changes in localization of expression domain with DAPT treatment (Table 2.1), suggesting that tentacle patterning was not completely disrupted by inhibition of Notch. Additionally, we examined the expression patterns of Notch pathway components after DAPT treatment. *Notch*, *Delta*, and *HES3* did not appear to have qualitatively altered expression patterns (Figure 2.15). However, as expected, *HES3* levels were reduced after DAPT treatment (Figure 2.15C,F), and our results suggest that *Notch* and *Delta* are also downregulated after inhibiting the pathway (Figure 2.15A-B,D-E).

Unbiased identification of tentacle-specific genes by transcriptional profiling

To gain further insight into the transcriptional programs underlying tentacle morphogenesis and Notch signaling, we identified novel tentacle markers genes that could be used to screen for changes in their expression patterns following DAPT treatment. To take an unbiased approach, we designed a novel microarray from the sequences deposited in three publically available databases: Joint Genome Institute (JGI), National Center for Biotechnology Information (NCBI), and Stellabase (Sullivan et al., 2006; Sullivan et al., 2008). To identify genes potentially involved in tentacle initiation, outgrowth, and maintenance, we performed transcriptional profiling at three different stages: late planula larvae with tentacle buds, animals with growing tentacles, and four-tentacle polyps (Figure 2.16A). In each case, animals were microdissected with a sharp tungsten needle to isolate tentacle tissue from the rest of the larval body.

Figure 2.15 – Notch pathway components do not have altered expression patterns after DAPT treatment

(A-C) RNA *in situ* expression patterns of *NvNotch* (A), *NvDelta* (B) and *NvHES3* (C) in control animals. Expression of these transcripts was endodermal. Scale bar represents 100 μm. **(D-F)** Corresponding expression patterns in DAPT treated animals. All of the Notch pathway components had similar expression patterns in Control and DAPT treated animals. The DAPT treated animals may downregulate all of these genes as observed by reduced *in situ* staining.

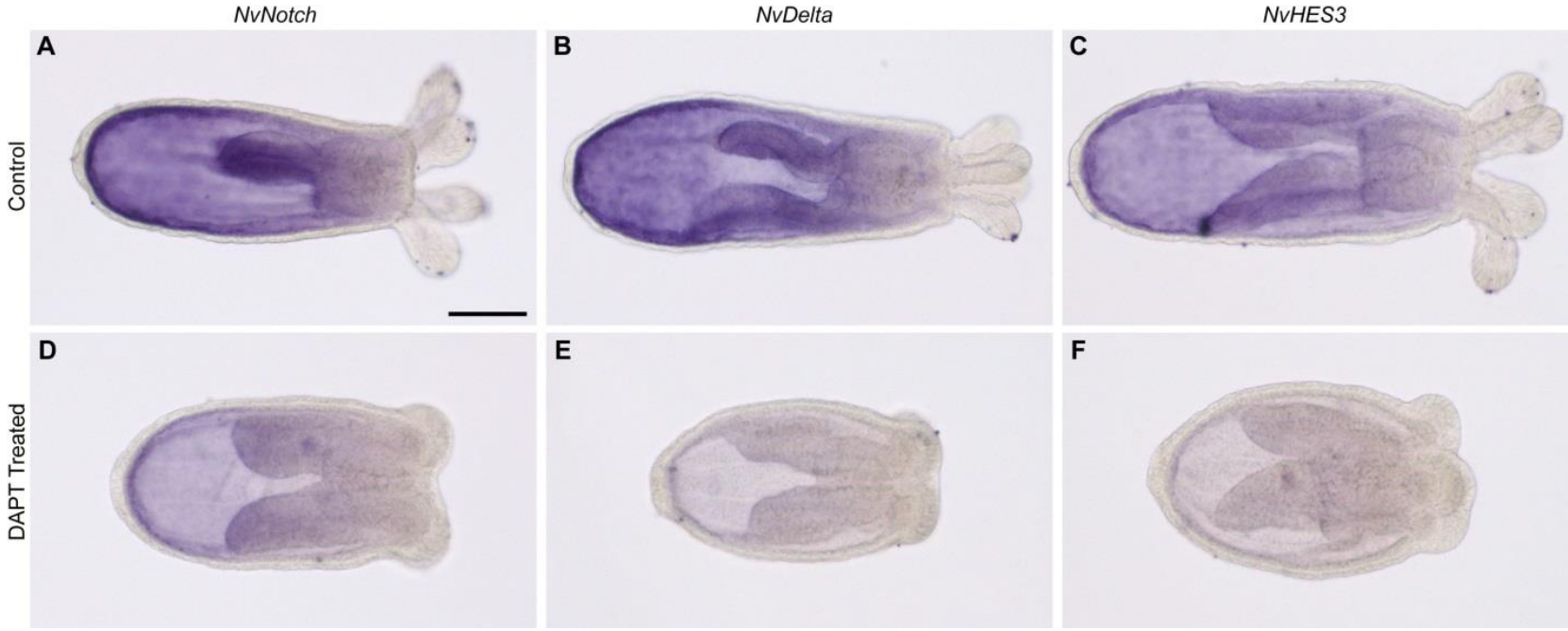

Figure 2.15

Figure 2.16 – An unbiased screen for novel tentacle markers

(A) The budded planula, growing tentacles and primary polyp stages were used to identify novel tentacle-specific genes by transcriptional profiling. Animals were dissected at the base of the tentacles (*dashed line*) and gene expression differences between the tentacle domain and corresponding body column were measured by custom microarrays in duplicate. **(B)** Venn diagram of the transcripts that were at least two fold upregulated in the oral/tentacle tissues from the three stages examined. A large proportion of tentacle-specific genes were common to all stages, suggesting an absence of major transcriptional changes underlying successive stages of development. **(C-E)** MA plots of normalized duplicate microarray analyses from budded planula (C), animals with growing tentacles (D), and primary polyps (E). Colored dots represent spots on the microarray. Duplicate experiments demonstrated consistent results.

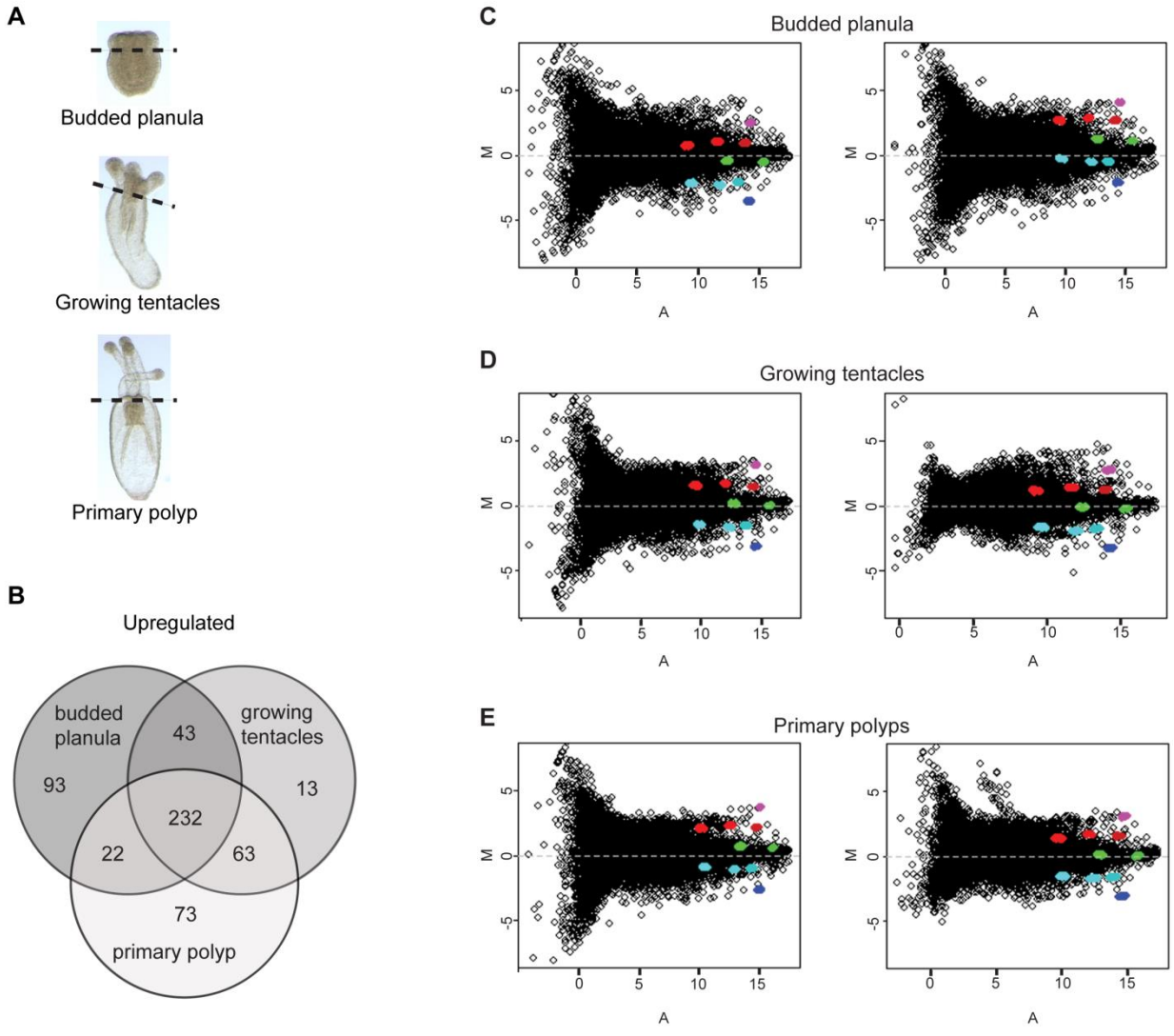
A
Budded planula
Growing tentacles
Primary polyp
B
Upregulated
budded planula
growing tentacles
primary polyp
93
43
13
232
22
63
73
C
Budded planula
D
Growing tentacles
E
Primary polyps
M
A

Figure 2.16

Each animal was bisected perpendicular to the main body axis at the base of the tentacles, generating cognate body column and oral- tentacle fragments (Figure 2.16A). RNA was isolated from each sample and subjected to a single round of amplification, dye labeling, and hybridization to a microarray chip in duplicate (Figure 2.16C-E). We found that many of the genes in the oral body portion were common among the different stages of development, suggesting they are consistently expressed during tentacle initiation, elongation and maintenance (Figure 2.16B).

For bioinformatics analysis of the results, highly differentially expressed sequences were manually subjected to BlastX search at NCBI to look for similarity to any known proteins in the non-redundant database. Additionally, the nucleotide sequence for each potential hit was blasted against the *Nematostella* EST database (NCBI) and EST clusters at JGI. Lastly, we used the protein sequence of candidate genes to identify conserved domains and to extract functional information using InterProScan from the European Bioinformatics Institute.

We chose 50 candidate genes to validate by RNA *in situ* hybridization. Attractive candidates included sequences with the highest fold change values or that contained transcription factor or signaling molecule domains. From these, we identified six genes that were not previously known to have tentacle domain expression patterns (Figure 2.17; Table 2.2). Two of these were previously identified genes, but were not known to have tentacle specific expression: *anthox2* (AF085283.1; Figure 2.17A; Finnerty et al., 2003; Ryan et al., 2006) and *foxL2* (JGI: 82873608; Figure 2.17B; Magie et al., 2005). Two more of these six contained forkhead domains, which we called *forkhead1* (XM_001630267.1; Figure 2.17C) and *forkhead2* (XM_001638841.1; Figure 2.17D). Of

Figure 2.17 – Novel transcriptional tentacle domain markers

(A-F) RNA *in situ* hybridization of tentacle marker genes identified from the microarray analysis. Most of these genes were expressed early in the oral placodal ectoderm before being expressed in the tentacle buds (A-C, F). *growth factor receptor-like* was expressed in the endoderm early, before exhibiting endodermal tentacle tip expression in primary polyps (E).

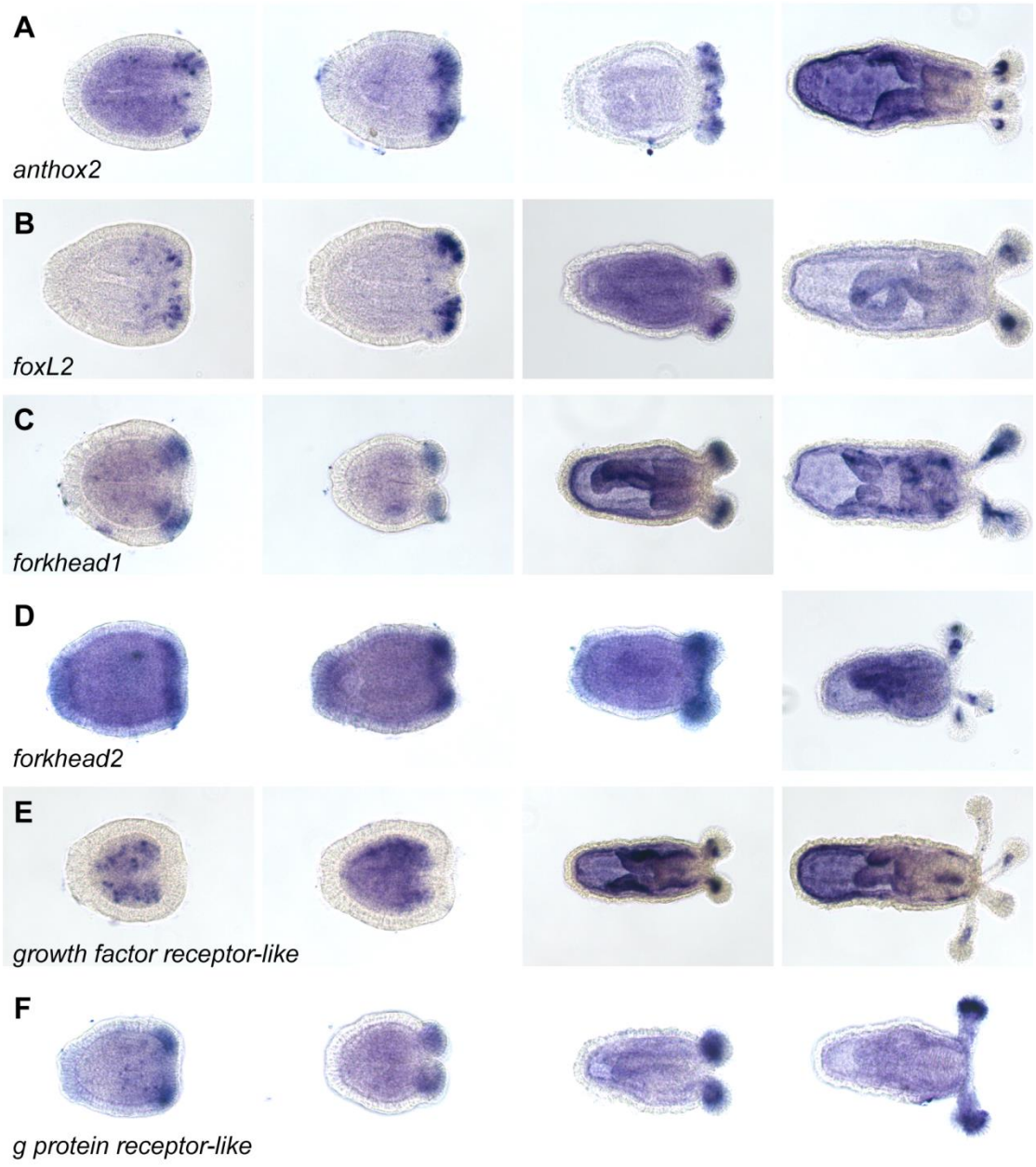
A
anthox2
B
foxL2
C
forkhead1
D
forkhead2
E
growth factor receptor-like
F
g protein receptor-like

Figure 2.17

Table 2.2: Tentacle domain markers identified in the microarray screen

Sequence name	**Accession**	**Primer pair for *in situ* probe**
Anthox2	AF085283.1	CATGTCTTCGTCCTTCTACATTGACT AGGTTGCCCCGAATATAGTACATT
FoxL2	JGI: 82873608	ATTAACTGTGTCACACACAAGCGC TTCATGTACGGGTATACAGGAGGTAC
Forkhead1	XM_001630267.1	CACCGCACCACTGCAGCAAT CCTGCGACGGAAATTCCCCT
Forkhead2	XM_001638841.1	GGATGATGCAAAGCAAGCGA TCTCAGAGGGATGTTTAGCCGA
Growth factor receptor-like	XM_001637818	CTTGCACTCATTGACCGACATG ACGATTGGATTGCGTGGTTG
G protein receptor-like	XM_001636348.1	ATGTCCACAAACACAAGCACCTC AGAAAATCTTGTCGGCGGTCT

Table 2.3: *In situ* hybridization primer pairs

Sequence name	**Accession**	**Primer pair for *in situ* probe**
OtxB	FJ824850	AAGAGCTGGGGGCCACGGATTACATC TATCTCGGCGCCATGGAATGCACG
Notch	JN982705	GCATGGGCTTTGCTTGGATT CAGTTACTCCCAGTGTATCCAGGTCT
Delta	JN982706	ATGCAGCTACTACCACTCCAGCCA GACACGCGCCATCAAAGCAA
HES3	JN982709	GGCCGTTGACTGCATCGATA TGTGCTGACGATAGTCGTCTGC

the remaining two, one contained a growth factor receptor domain (*growth factor receptor-like*; XM_001637818; Figure 2.17E) and the other contained a G protein receptor domain (*g protein receptor-like*; XM_001636348.1; Figure 2.17F). Most of these genes were expressed early in some or all of the oral placodal ectoderm before bud formation, and then exhibited bud-specific expression when the tentacle primordia formed (Figure 2.17A-D,F). However, *growth factor receptor-like* was expressed ubiquitously in the endoderm until the growing tentacle stage, when it also became expressed in the tips of the tentacle endoderm (Figure 2.17D). When we screened these genes for changes in their expression patterns after DAPT treatment, none were altered (Table 2.1), suggesting that tentacle patterning was not disrupted following inhibition of Notch signaling. From the expression patterns of these genes as well as those previously published in the literature, we propose a model for tentacle patterning whereby the oral tissue is progressively subdivided into tentacle competent and non-competent domains (Figure 2.18).

Figure 2.18 – Model for the transcriptional patterning of tentacles

A conceptual model for tentacle patterning in which oral cells are subdivided into tentacle-competent and non-competent domains. In early planulae, genes such as *FoxB* (Magie et al., 2005), *Wnt1* (Kusserow et al., 2005), and *Notch* (Marlow et al., 2012), are expressed orally (*blue*). At the oral placode stage, genes such as *WntA* (Kusserow et al., 2005), *forkhead2*, and *Delta* (Marlow et al., 2012) are expressed broadly in the oral placode (*green*). Once budded, planula larvae express a subset of genes in the buds, such as *PaxA* (Magie et al., 2005) (*green*), between the buds, such as *homeobrain* (Mazza et al., 2010) (*red*), and encircling the buds, such as *Delta* (Marlow et al., 2012) (*orange*). Patterning becomes more complicated at the primary polyp stage, when some genes are expressed along the length of the tentacle, such as *muscle LIM* and *Rx* (Martindale et al., 2004; Mazza et al., 2010) (*green*), or at the tips of the tentacles like *sprouty* (Matus et al., 2007) (*yellow*).

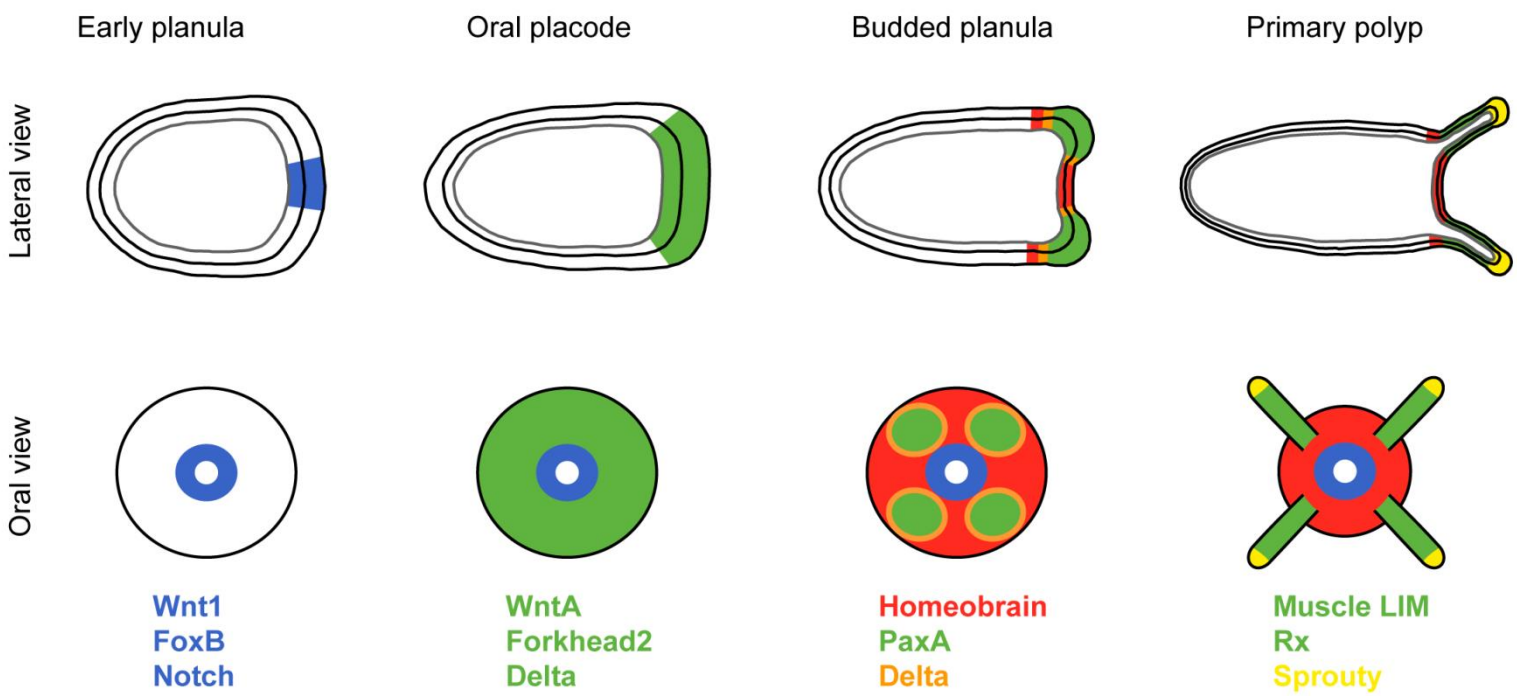
Early planula
Oral placode
Budded planula
Primary polyp
Lateral view
Oral view
Wnt1
FoxB
Notch
WntA
Forkhead2
Delta
Homeobrain
PaxA
Delta
Muscle LIM
Rx
Sprouty

Figure 2.18

Discussion

A new model for pre-bilaterian appendage development

Our results establish a novel model for tentacle morphogenesis in *Nematostella*. The initial step in tentacle development is formation of a thickened ectodermal placode at the oral pole of the animal, approximately five days after fertilization at 16°C (Figure 2.1A, Figure 2.4A,E). This placode is progressively subdivided into four distinct tentacle domains (Figure 2.1B, Figure 2.4B,F), presumably through the spatially-restricted expression of key effector genes (Figures 2.17 and 2.18). Once the tentacle buds are thus formed, Notch signaling activity is required to trigger apico-basal thinning of the tentacular ectoderm (Figure 2.11), radically increasing the surface area of the presumptive tentacle. Actin dynamics are required for this process to occur in both the body column and oral ectoderm (Figure 2.5), and cell proliferation occurs stochastically along the length of the tentacle throughout development (Figure 2.13C-D"). Cell lineage-tracing experiments further reveal a concomitant axial rearrangement of cell clones from irregular and isometric (Figure 2.7A,B and Figure 2.8A,B) to linear morphologies (Figure 2.7C,D and Figure 2.8C,D) during tentacle outgrowth. We propose that these changes in epithelial architecture of the oral ectoderm contribute to elongation of the tentacles. Intriguingly, although elongation of the main body column appears to involve oriented cell division (Figure 2.10E-H), we did not observe oriented cell division in the tentacles (Figure 2.10J-M).

Currently, we do not have enough molecular data from *Nematostella* appendage development or from other basal metazoans to make a comparison to bilaterian

appendage development. Even though arthropod appendages and vertebrate limbs are not homologous, both exhibit *distalless*/*Dlx* expression at the presumptive distal portion of the appendage (Angelini and Kaufman, 2005; Kraus and Lufkin, 2006). The published RNA expression pattern of the *Nematostella Dlx* homolog does not show expression at the tentacle tips or in any tentacle tissue during development (Ryan et al., 2007). Our current data would not support a model where *Nematostella* tentacles are homologous to any of the bilaterians appendages, but more data from *Nematostella* as well as other basal metazoan species is still needed.

Notch signaling and tentacle elongation

Pharmacological inhibitor studies with DAPT indicate a key role for Notch signaling in tentacle elongation (Figure 2.11). Consistent with this, Notch pathway components are expressed in the oral and tentacle bud ectoderm prior to and during metamorphosis (Marlow et al., 2012), and signaling through this pathway is generally known to affect downstream transcription (Petcherski and Kimble, 2000; Wu et al., 2000a; Artavanis-Tsakonas and Muskavitch, 2010). When we inhibited Notch signaling, the tentacle bud expression of *OtxB* was disrupted (Figure 2.14). Additionally, Notch signaling restricts *PaxA* expression to the tentacle primordia (Marlow et al., 2012). These results indicate that Notch signaling directly or indirectly leads to the specific tentacle expression patterns of these genes.

However, our results do not support the hypothesis that Notch signaling is required for global tentacle patterning since many other tentacle markers were

unaffected by Notch inhibition (Table 2.1). A previous study of Notch signaling in *Nematostella* reported fused tentacles and an expanded tentacle field (based on *PaxA* expression) following 72 hours of DAPT treatment (10 μM in 1% DMSO) in three days post-fertilization planulae raised at 25°C. In contrast, we used eight day old planula larvae raised at 16°C, and treated them with a tenth of the concentration of DMSO but a higher concentration of DAPT for 48 hours. Given these differences, our data do not support a general expansion of the tentacle field following DAPT treatment, since numerous tentacle markers did not change their expression pattern and our animals developed four tentacle buds which failed to elongate (Figures 2.11 and 2.14; Table 2.1).

Nematostella and *Hydra* tentacle development likely occur through different mechanisms

In hydrozoans, tentacle development has mainly been studied in adult animals, in regeneration, and in the asexual budding of polyps, but not during embryonic development. *Hydra* polyps replace all of the cells in their bodies with cells derived from their i-cells and from constantly dividing epithelial cells (David and Campbell, 1972; David and Murphy, 1977; Bode and David, 1978). This is unlikely the case in *Nematostella*, where i-cells have not been identified. Another hallmark of *Hydra* tentacle development and maintenance is a distinct border at the tentacle zone. This is delineated by an absence of cell division and sharply defined gene expression domains (Holstein et al., 1991; Smith et al., 1999; Bode, 2001). Based on our EdU staining

results as well as known expression patterns, we do not see the same evidence for a 'tentacle zone' in *Nematostella* during development or adult maintenance (Figure 2.3). Furthermore, in *Hydra*, activation of canonical Wnt signaling is sufficient to cause tentacle outgrowth along the body column (Hassel et al., 1993; Broun et al., 2005). In contrast, recent studies in *Nematostella* show that ectopic activation of canonical Wnt signaling can only induce tentacle and oral fates at the aboral pole of developing animals, not along the body column (Trevino et al., 2011). Additionally, we have demonstrated that Notch signaling is required for tentacle elongation in *Nematostella* (Figure 2.11). Notch signaling in *Hydra* is important for stem cell development and detachment of the asexual bud from the parent animal (Kasbauer et al., 2007; Munder et al., 2010), but its role in embryonic tentacle development is unknown. While more data is needed from *Hydra* embryonic development, these previous results provide further evidence that the tentacle development program may be very different between *Hydra* and *Nematostella*.

Epithelial placodes as a common theme in organ and appendage outgrowth

It is well established that thickened epithelial placodes (similar to those described herein) play a role in the development of various tissues and organs of bilaterian organisms. The imaginal discs of *Drosophila*, for example, are larval primordia that give rise to all the appendages of the adult body (Cohen, 1993). These structures all develop as pseudostratified epithelial placodes prior to undergoing radical metamorphic cell shape changes that result in elongation of the larval epithelia into their adult forms

(Fristrom, 1988). Placodes are also central to development of outgrowths in vertebrate systems, including hair follicles, teeth, feathers, ears, and the lens of the eye among others (Baker and Bronner-Fraser, 2001; Pispa and Thesleff, 2003; Streit, 2007). Remarkably, it remains poorly understood why thickened epithelial primordia are such a common theme in animal development. We have now shown that a similar mechanism occurs during appendage morphogenesis of a basal metazoan, indicating deep evolutionary constraints that favor this cellular mechanism, regardless of its molecular basis in each lineage.

There are two potential scenarios for the evolution of placodal development. The first is that placodal development is a conserved feature inherited from the common cnidarian-bilaterian ancestor. In this situation, *Hydra* might represent a derived situation where the placode-dependent mechanism for tentacle development has been lost. Investigation of additional cnidarian species, especially anthozoans, would be needed to support this contention. The second possibility is that the appearance of epithelial placodes throughout Metazoa is a product of convergent evolution; appearing independently in multiple lineages. Currently, the sensory placodes of vertebrates are the best studied in the light of evolution, yet prior to data from chordates and urochordates, these were thought to be a vertebrate innovation (Graham and Shimeld, 2013). The evolution of mechanisms to control the development of integumental placodes (which give rise to the ectodermal appendages of vertebrates) has not been addressed, although there do seem to be common molecular themes (Mikkola, 2007). Nevertheless, more invertebrate and basal metazoan species would need to be examined before there is sufficient data to support a definitive hypothesis.

Regardless of the evolutionary scenario, the widespread appearance of placodes in animal embryos indicates a crucial utility in formation and patterning of secondary outgrowths of the main body axis. This raises the question of why placodal development is such an important mechanism. Using a thickened placode where the cells are packed closely together may allow for high density patterning of a large primordial structure in a relatively small space. Once the pattern is formed, morphogenesis of the epithelium through changes in apico-basal cell thickness could then directly expand the primordium into a larger structure, organ or outgrowth.

Chapter 3: Disruption of epithelial integrity and cell polarity by VirA, a bacterial effector protein

Abstract

Bacterial pathogens have evolved a variety of protein tools that allow them to evade the host immune system and hijack endogenous processes for their own infection and replication. *Shigella flexneri* injects a host of these effector proteins into cells during its pathogenesis that are known to alter the cytoskeleton and intracellular signaling among other processes. However, the function of virulence factor, VirA, which is known to be vital for effective infection and spreading, remains controversial. While most previous studies have been conducted *in vitro* or with cell culture assays, the function of VirA in an epithelial context remains unknown. Here, we demonstrate that VirA expression disrupts epithelial cell polarity with no discernible effects on microtubule stability. We show that transgenic *Drosophila* expressing VirA results in a mislocalization of polarity proteins, cell rounding, and loss of epithelial integrity. A strikingly similar effect is observed after expression of VirA in the chick neural tube epithelium, implicating a conserved activity of VirA from arthropods to vertebrates. Further, we show a potential defect in vesicle trafficking by examining Rab11 localization in epithelia expressing VirA, suggesting a mechanism for loss of polarity and tissue architecture. Our results reveal a novel cellular mechanism for VirA in disruption of cell polarity leading to a breakdown of epithelial integrity, which may facilitate the infection and spreading of *Shigella* in the human intestinal epithelium.

Introduction

The maintenance of epithelial integrity and polarity is essential for barrier function and assists in resistance to pathogens. Bacteria have evolved the ability to penetrate and hijack this endogenous barrier through the secretion of various effector proteins. *Shigella flexneri* infects the human intestinal epithelium after ingestion of contaminated food or water and is a paramount problem for public health, especially in developing countries, claiming around 700,000 lives worldwide every year (WHO, 2005). VirA, a *Shigella* effector protein, is known to be vital for effective infection and spreading of the bacteria in mammalian cells (Uchiya et al., 1995). However, the cellular mechanism by which it assists in the infection of the human gut remains unclear.

Shigella bacteria are initially transported across the host intestinal epithelium by microfold cells (M cells), which are specialized immune cells that constantly sample the gut contents for antigens (Wassef et al., 1989; Sansonetti et al., 1996). After passing through the M cell to the basal side of the epithelium, the bacteria are engulfed by macrophages. *Shigella* induces macrophage death, allowing the bacteria to infect through the basolateral membrane of the epithelial cells, ultimately resulting in breakdown of the epithelial barrier and diarrhea (Mounier et al., 1992; Zychlinsky et al., 1992). Using a type III secretion system, *Shigella* injects effector proteins into host cells that can alter the cytoskeleton, innate immune response, and the host cell transcriptome, enabling the bacteria to replicate and spread (reviewed in Schroeder and Hilbi, 2008).

VirA was initially reported to be a cysteine protease that cleaved microtubules by binding to Tubulin heterodimers, thus assisting the bacteria in intercellular movement

(Yoshida et al., 2002; Yoshida et al., 2006). More recent reports have refuted this claim (Davis et al., 2008; Germane et al., 2008) and suggested other functions including potential binding to GM130 (a golgi membrane protein), activation of calpain and inactivation of Rab1 (Clements et al., 2011; Bergounioux et al., 2012; Dong et al., 2012). However, these studies only examined the function of VirA *in vitro* and using cell culture assays. None explored the function of VirA in the context of an *in vivo* tissue system, where VirA would act in the human intestine.

Here, using *Drosophila* and vertebrate systems, we examined the function of VirA in epithelial tissue *in vivo*. We confirmed in both mammalian cells and *Drosophila* tissue that VirA expression does not abolish polymerized microtubules. However, it does affect tissue integrity and cell polarity. We validated the use of *Drosophila* as a pathogenesis model by observing similar phenotypes in two vertebrate systems. Additionally, we show that VirA expression correlates with a mislocalizaton of Rab11, potentially suggesting a function of VirA in vesicle trafficking. Finally by utilizing an *in vivo* epithelial system, our studies uncover a novel cellular function of VirA in *Shigella* pathogenesis by disrupting tissue integrity and cell polarity, which could lead to breakdown of the host gut epithelium aiding in infection.

Materials and Methods

Fly stocks and genetics

To generate VirA transgenic *Drosophila*, VirA (gift from the Sasakawa Lab) was cloned into the *PUAS-T* vector to produce a fusion with Green Fluorescent Protein (GFP; Brand and Perrimon, 1993). Transgenic lines were obtained by standard methods (Genetic Services, Cambridge MA). For this study, w; UAS-VirA-GFP/TM6B was used. Other transgenic lines used in this study were obtained from Bloomington *Drosophila* Stock Center: yw, flpout Gal4; MKRS-Flp/TM6B; w; GMR-Gal4; UAS-GFP; and UAS-p35.

Immunofluorescence and imaging

To induce the expression of VirA clones, w; UAS-VirA-GFP/TM6B was crossed to yw,flpout Gal4; MRKS-Flp/TM6B. Larval progeny were heat shocked for 5 or 10 minutes at 37°C. 24 hours after heat shock, wandering third instar larvae were dissected, fixed, and stained by the standard protocol (Meyer et al., 2011). Expression of VirA in the eye disc was driven by the GMR promoter, and wandering third instar larvae were dissected, fixed, and stained by the standard protocol. Primary antibodies included mouse anti-α-Tubulin (1:1000, Sigma), mouse anti-Rab11 (1:200, BD Biosciences), mouse anti-Discs Large (1:500, C. Goodman), and mouse anti-Armadillo (1:100, E. Wieschaus). Secondary antibody was goat anti-mouse IgG Alexa Fluor 647 (1:500, Molecular Probes). F-Actin was stained by Alexa Fluor 546 phalloidin (1:250;

Molecular Probes). Salivary glands and eye imaginal discs were mounted on glass slides in glycerol and imaged on a Leica SP5 confocal microscope.

HeLa transfection, culture, and imaging

VirA was cloned into the eGFP-C1 vector (Invitrogen) to produce a fusion protein with GFP under the control of the CMV promoter. Plasmid DNA was transfected into HeLa cells using FuGENE HD (Promega), and cells were cultured in TransfectaGRO (Corning) for 24, 30, or 48 hours. Cells were rinsed once with PBS and fixed in 4% paraformaldehyde for 30 minutes at room temperature. After fixation, cells were permeabilized with 0.2% TritionX-100 in PBS for 5 minutes, rinsed 4 times with PBS, and subsequently stained. Primary (anti-αTubulin; 1:1000; Sigma) and secondary antibodies (goat anti-mouse IgG Alexa Fluor 647; 1:500; Molecular Probes) were incubated in PBS with 3% BSA. Alexa Fluor 546 phalloidin (1:250; Molecular probes) was applied in PBS with 0.1% TritionX-100. Cells were mounted with glycerol with a coverslip and imaged on a Leica SP5 confocal microscope.

Chick embryo electroporation and imaging

VirA was cloned in the pCAGGS vector (gift from O. Pourquie), which put VirA and zsGreen (separated by an IRES sequence) under the control of the chick β-actin promoter. *Gallus gallus* eggs (purchased from commercial sources) were incubated for

48 hours at 37°C. A hole was cut in the eggshell and the plasmid DNA was injected into the lumen of the neural tube. DNA was electroporated into one side of the neural tube using an electrode with three pulses of 20 V for 50 milliseconds each with 100 milliseconds between pulses. Eggs were covered with parafilm and further cultured for five hours. Embryos were removed from the yolk and fixed in 4% paraformaldehyde for two hours at room temperature. They were subsequently washed in PBS + 0.1% TritionX-100 (PBT), incubated with Alexa Fluor 546 phalloidin in PBT (Invitrogen; 1:100), and washed again (in PBT). Embryos were mounted on slides with spacers and imaged on a Leica SP5 confocal microscope. The cell rounding phenotype was quantified by counting the number of apically rounded zsGreen expressing cells in control and VirA embryos.

Results and Discussion

VirA expression does not disrupt microtubules *in vivo*

To address the previously reported, controversial microtubule-severing function of VirA (Yoshida et al., 2002; Yoshida et al., 2006), we transiently expressed VirA in mammalian cell culture. HeLa cells were transfected with a plasmid containing VirA fused to Green Fluorescent Protein (GFP) or only GFP under the control of the CMV promoter. After 24 hours of post-transfection culture, both control and VirA expressing HeLa cells contained numerous polymerized microtubules (Figure 3.1A-B"). To ensure that our culture duration was sufficient, we also examined HeLa cultures 48 hours after transfection and still observed polymerized microtubules in the control and VirA expressing cells (Figure 3.1C-D"). These results support the previous reports that suggest VirA does not deplete mammalian cells of microtubules (Davis et al., 2008; Germane et al., 2008; Germane and Spiller, 2011; Bergounioux et al., 2012; Dong et al., 2012).

Further, we sought to confirm these results using an *in vivo* tissue instead of cell culture. The *Drosophila* salivary gland provides a tractable system to express proteins of interest within the epithelial tissue context. We induced expression of the VirA::GFP fusion protein or GFP alone using the Gal4-UAS system (Brand and Perrimon, 1993). This system was under further temporal control by employing heat shock FLPout to induce random clonal expression (Golic, 1991; Pignoni and Zipursky, 1997). We heat shocked the larvae 24 hours before dissection of wandering third instar larval salivary

Figure 3.1 – VirA expression does not disrupt microtubule architecture in HeLa cells

(A-D) HeLa cells transiently transfected with GFP (A,C; Control) or VirA::GFP (B,D; VirA) under the control of a CMV promoter and cultured for 24 (A,B) or 48 (C,D) hours after transfection. GFP positive cells (*green*) are shown stained with anti-αTubulin (αTub, *red*). VirA expression does not disrupt the polymerization of microtubules compared to controls (A'-D'). Enlarged images from A'-D' show polymerized microtubules in these cells (A"-D", *yellow arrows*). Scale bar in A represents 25 μm.

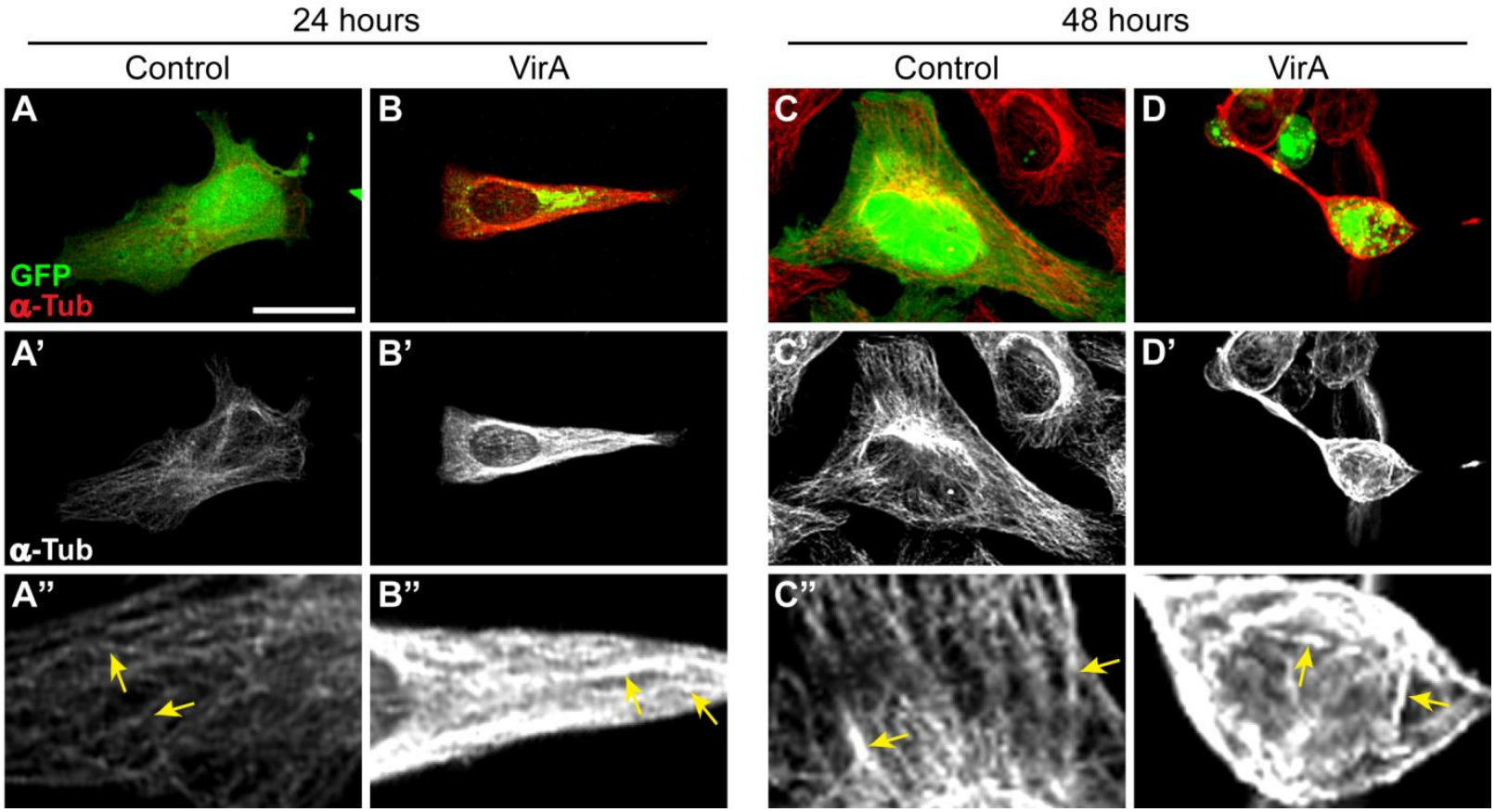
24 hours
48 hours
Control
VirA
Control
VirA
A
B
C
D
GFP
α-Tub
A'
B'
C'
D'
α-Tub
A''
B''
C''

Figure 3.1

glands. In the post-mitotic, endoreplicating salivary gland cells, there is a meshwork of polymerized Tubulin at the basal periphery of the cells. This meshwork still exists in the VirA expressing salivary gland cells where we can observe polymerized microtubules (Figure 3.2A-B"). These data support the proposed model that VirA does not sever microtubules (Davis et al., 2008; Germane et al., 2008; Germane and Spiller, 2011; Bergounioux et al., 2012; Dong et al., 2012). Further, we demonstrate this in an *in vivo* tissue context.

VirA expression disrupts epithelial architecture and cell polarity *in vivo*

While VirA expression did not cause a loss of microtubules in *Drosophila* epithelia, we did notice a striking loss of normal tissue architecture. When clone induction resulted in only a few VirA::GFP expressing cells, the overall salivary gland tubular structure, with large cubodial cells surrounding a central lumen, was maintained (Figure 3.3A-A', B-B'). However, when the majority of cells in the salivary gland expressed VirA::GFP, the tissue architecture was completely lost including an absence of the lumen (Figure 3.3C-C'). Additionally, these VirA::GFP expressing cells contained F-Actin rich structures in the cytoplasm (Figure 3.3A",B",C"). Previously, VirA was reported to inactivate Rab1 GTPase, important for ER-to-golgi trafficking, which might explain the accumulation of these structures (Dong et al., 2012). Some of these Actin rich structures can also be seen in the non-GFP cells of the VirA::GFP salivary glands. If the larvae are not heat shocked, these Actin rich structures can still be seen in many of the VirA::GFP salivary glands, which are absent in the controls (Figure 3.4),

Figure 3.2 – VirA expression does not disrupt microtubule architecture *in vivo*

(A-B) Surface view of salivary glands clonally expressing GFP (A, Control, *green*) or VirA::GFP (B, VirA, *green*) stained for anti-αTubulin (αTub, *blue*) and F-Actin (*red*). Cells in the salivary gland expressing GFP or VirA still contained polymerized microtubules (A',B'). Examples are denoted by yellow arrow in A" and B". Scale bar in A represents 50 μm.

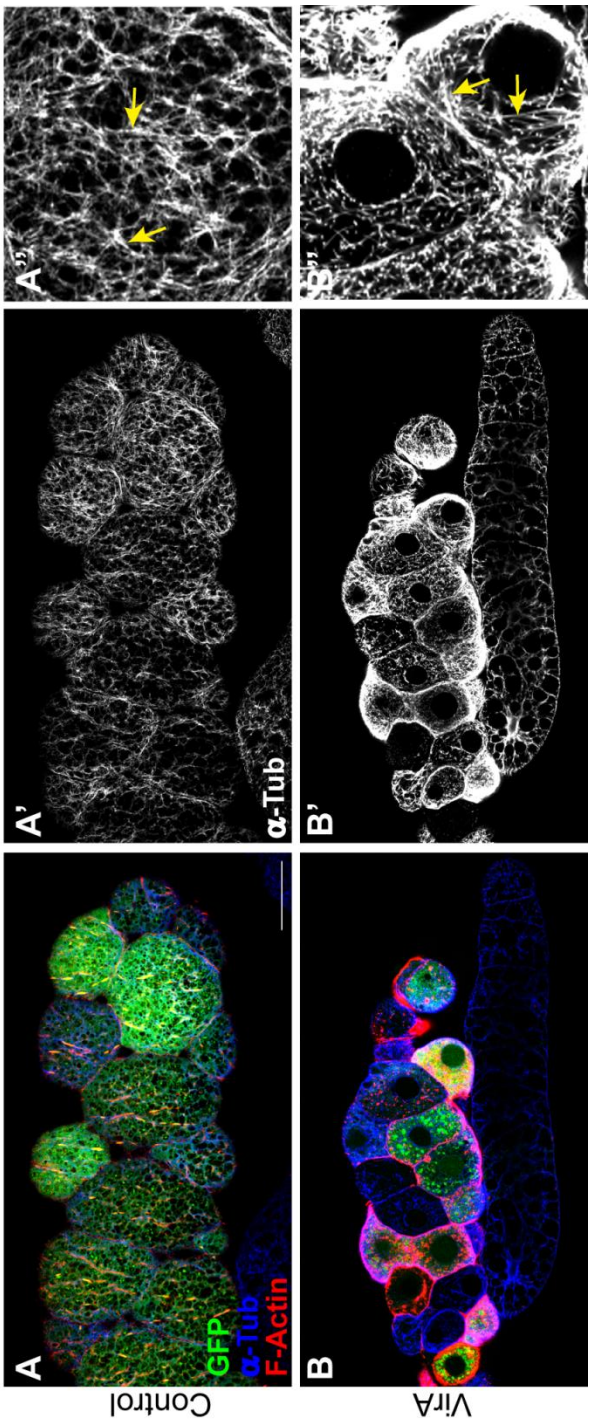

Figure 3.2

Figure 3.3 – Disruption of tissue architecture in *Drosophila* salivary glands expressing VirA

(A-C) GFP (A, Control, *green*) or VirA::GFP (B-C, VirA, *green*) expression was clonally induced in the salivary gland, and they were stained for F-Actin (*red*). Salivary glands with only a few VirA expressing cells (B) retained their tissue structure, while glands with many VirA expressing cells (C) lost tissue architecture and the lumen (*yellow dotted line* in A',B',C'). Cells expressing VirA also contained numerous Actin rich structures (*yellow arrows* in B",C"). Scale bar in A represents 100 μm.

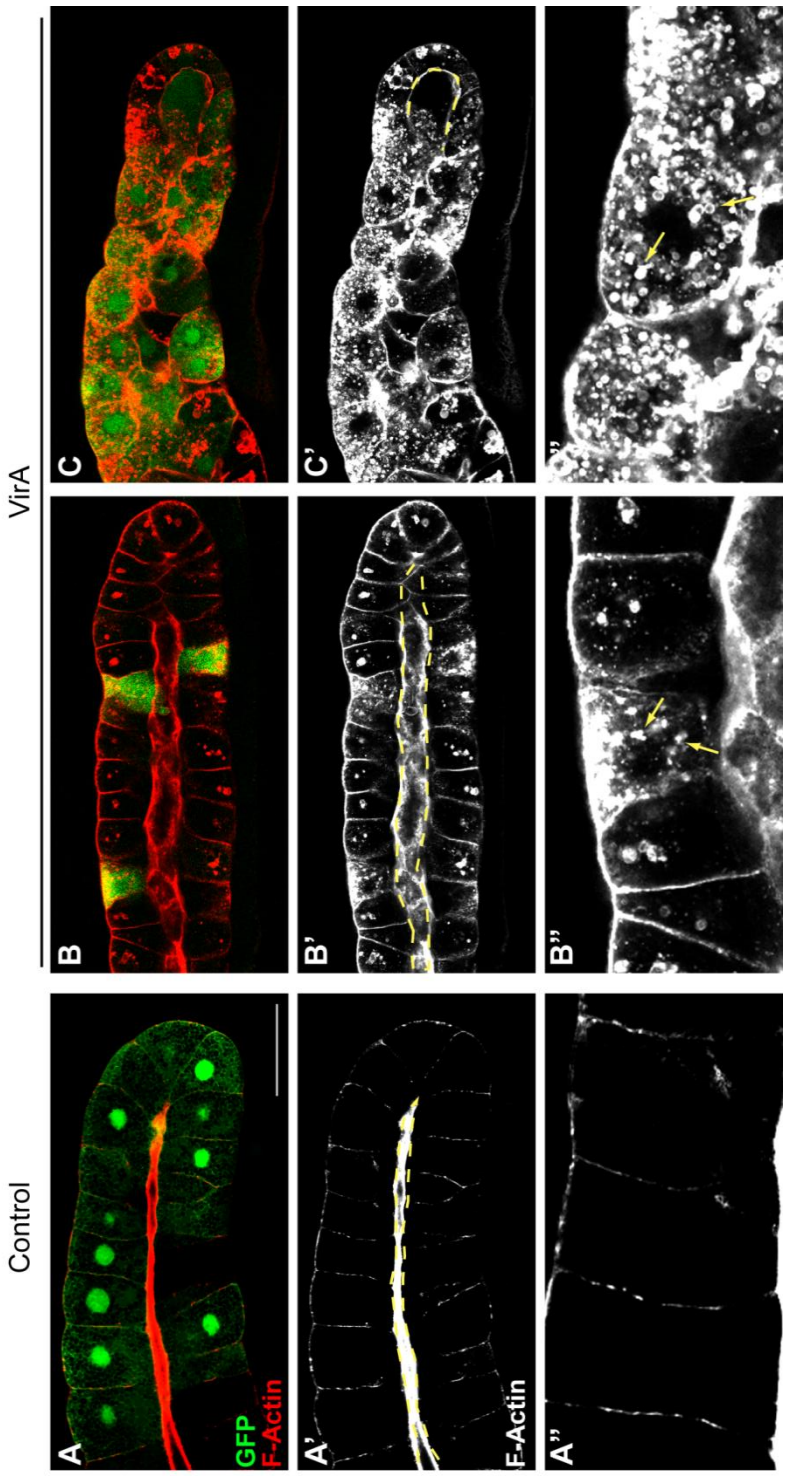

Figure 3.3

Figure 3.4 – Background expression of VirA in salivary glands without heat shock

(A-C) Salivary glands from yw, flpout Gal4; UAS-GFP; MKRS-Flp (Control, A) or yw, flpout Gal4; UAS-VirA-GFP; MKRS-Flp (VirA, B-C) larvae that have not been heat shocked. Glands were stained with phalloidin (F-Actin*, red*) and Hoechst (*blue*). Some of the VirA glands showed actin rich structures to varying degrees even the in absence of induction of expression (*yellow arrows*). Scale bar in A represents 50 μm.

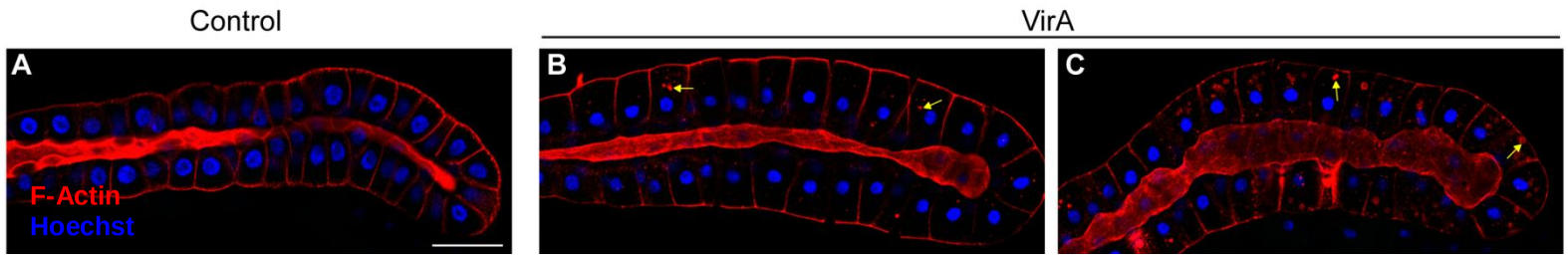

Figure 3.4

suggesting that there is a low level of background VirA expression in these salivary glands.

To confirm the loss of tissue architecture in a separate epithelial context, we additionally expressed VirA::GFP in the post mitotic cells of the *Drosophila* eye imaginal disc using the GMR promoter and Gal4/UAS system (Moses and Rubin, 1991; Brand and Perrimon, 1993). In this system, we also observed a loss of normal epithelial architecture (Figure 3.5A-H'). Behind the morphogenetic furrow, VirA expressing cells lost their pseudostratified epithelial structure, rounded, and even apically extruded from the tissue, accumulating in the lumen between the two layers of the imaginal disc (Figure 3.5C,D,G,H). Since we observed this disruption of normal epithelial architecture, we were interested to explore if cell polarity was maintained during this process. To address this question, we assayed cell polarity markers for their localization in the VirA expressing eye discs. Discs Large (Dlg), a well-known apical polarity protein, localized to the septate junctions in control discs (Figure 3.5A-C'). However, Dlg localization was disrupted in the GMR domain where VirA::GFP was expressed (Figure 3.5B-D'). Similarly, Armadillo (Arm), the *Drosophila* homolog of β-Catenin, localized to the apical adherens junctions in control discs (Figure 3.5E-G'). This localization was disrupted in the GMR domain of the VirA::GFP eye discs (Figure 3.5F-H'). These results reveal a potential tissue level function of VirA that was not previously identified in cell culture assays. Our data suggest that VirA expression causes a loss of normal tissue architecture in both the salivary gland and eye disc, and this is accompanied by the loss of cell polarity (Dlg and Arm localization) in the eye disc.

Figure 3.5 – Disruption of tissue architecture and cell polarity in *Drosophila* eye imaginal discs expression VirA

(A-H) GFP (A,C,E,G; Control; *green*) or VirA::GFP (B,D,F,H; VirA; *green*) expression was driven with the GMR promoter posterior to the furrow in the eye imaginal disc. Not only did VirA expression cause a loss of normal tissue architecture, but also caused the loss of localization of the polarity markers Discs Large (A-D', *red*) and Armadillo (E-H', *red*). Yellow brackets denote areas of GFP positive expression. Anterior side of discs is oriented to the left. Scale bars in A, C, E, and G represent 25 μm.

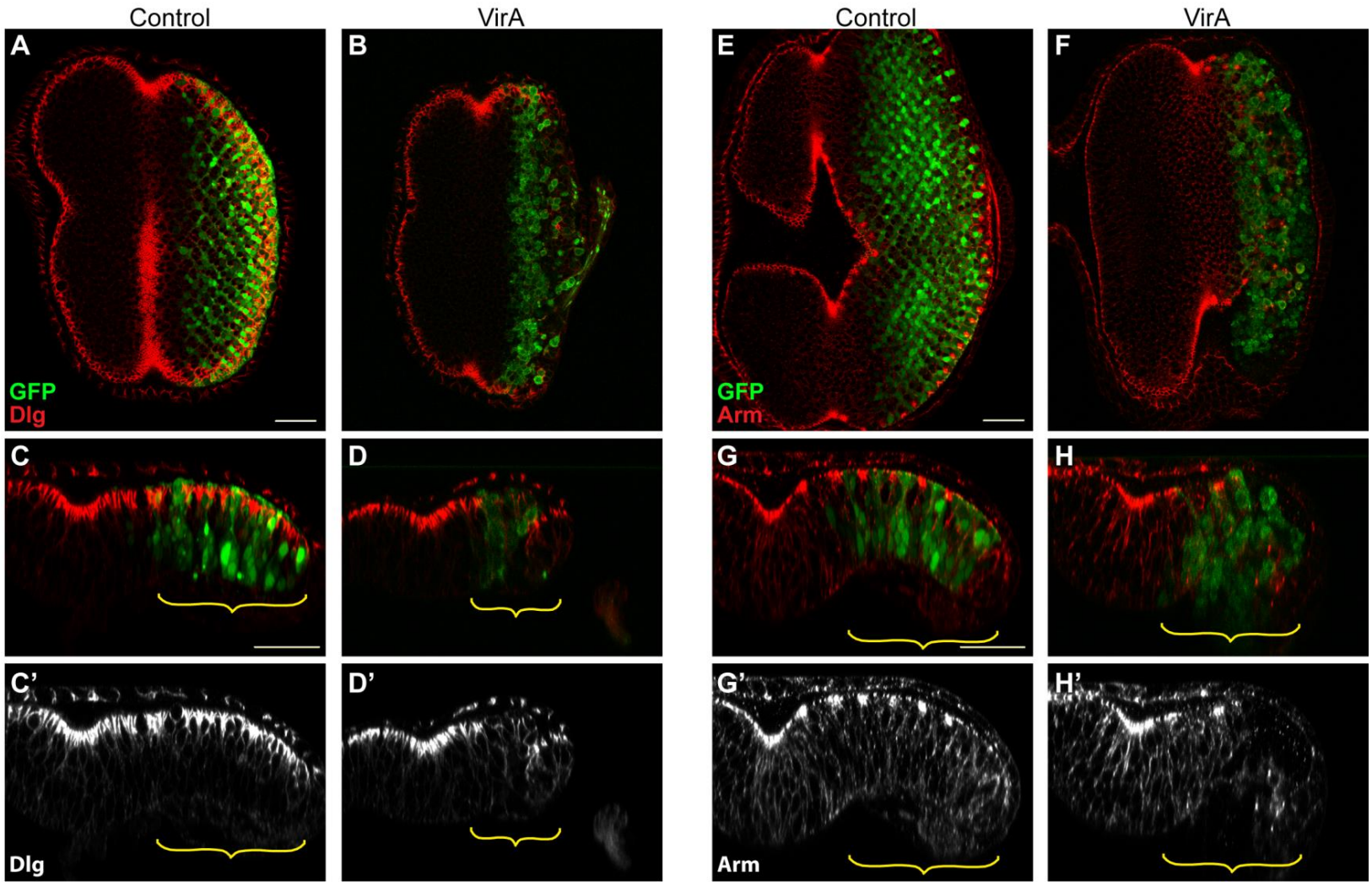
Control
VirA
Control
VirA
A
B
E
F
GFP
Dlg
GFP
Arm
C
D
G
H
C'
D'
G'
H'
Dlg
Arm

Figure 3.5

VirA expression results in cell rounding *in vivo*

To validate the use of *Drosophila* as a pathogenesis model and to rule out *Drosophila* specific phenotypes, we expressed VirA in two distinct vertebrate systems and observed the resulting cellular phenotypes. As described previously, we transiently expressed GFP or VirA::GFP in HeLa cells. After 24 hours of culture, the VirA::GFP expressing cells appeared largely similar to the control cells (Figure 3.1A-B; quantified in Figure 3.6E). While the majority of VirA::GFP cells appeared similar to controls after 30 hours of culture, a subset of the VirA::GFP expressing cells displayed a rounded morphology (Figure 3.6A-B, quantified in E). By 48 hours of culture, the majority of the VirA::GFP expressing cells exhibited a rounded phenotype (Figure 3.6C-D, quantified in E). This rounding of the cells was very similar to the phenotype we observed in the *Drosophila* tissue systems, particularly in the eye imaginal disc where cells rounded before apically extruding from the epithelium (Figure 3.5).

Additionally, we expressed VirA in a vertebrate epithelium *in vivo*. The chick neural tube is amenable to electroporation of plasmid DNA constructs. In our construct, VirA and zsGreen or zsGreen alone was expressed under the control of the chick β-Actin promoter. Interestingly, the VirA expressing cells rounded up at the apical side of the epithelium, a strikingly similar phenotype to the *Drosophila* eye imaginal disc (Figure 3.7A-B', quantified in C, compare to Figure 3.5). These results from two different vertebrate systems recapitulate our results from *Drosophila* that VirA expression results in rounded cells and validates the use of *Drosophila* as a pathogenesis model.

Figure 3.6 – VirA expression results in cell rounding in HeLa cells

(A-E) HeLa cells were transiently transfected with GFP (A,C; Control; *green*) or VirA::GFP (B,D; VirA; green) and cultured for 30 (A-B) or 48 (C-D) hours. Cells were stained for anti-αTubulin (αTub, *blue*) and F-Actin (*red*). Most of the VirA expressing cells were rounded by 48 hours of culture (D). Quantification of the percentage of rounded GFP positive cells for control (*grey*) and VirA (*black*) after 24, 30, and 48 hours of culture is shown in E. Scale bar in A represents 15 μm.

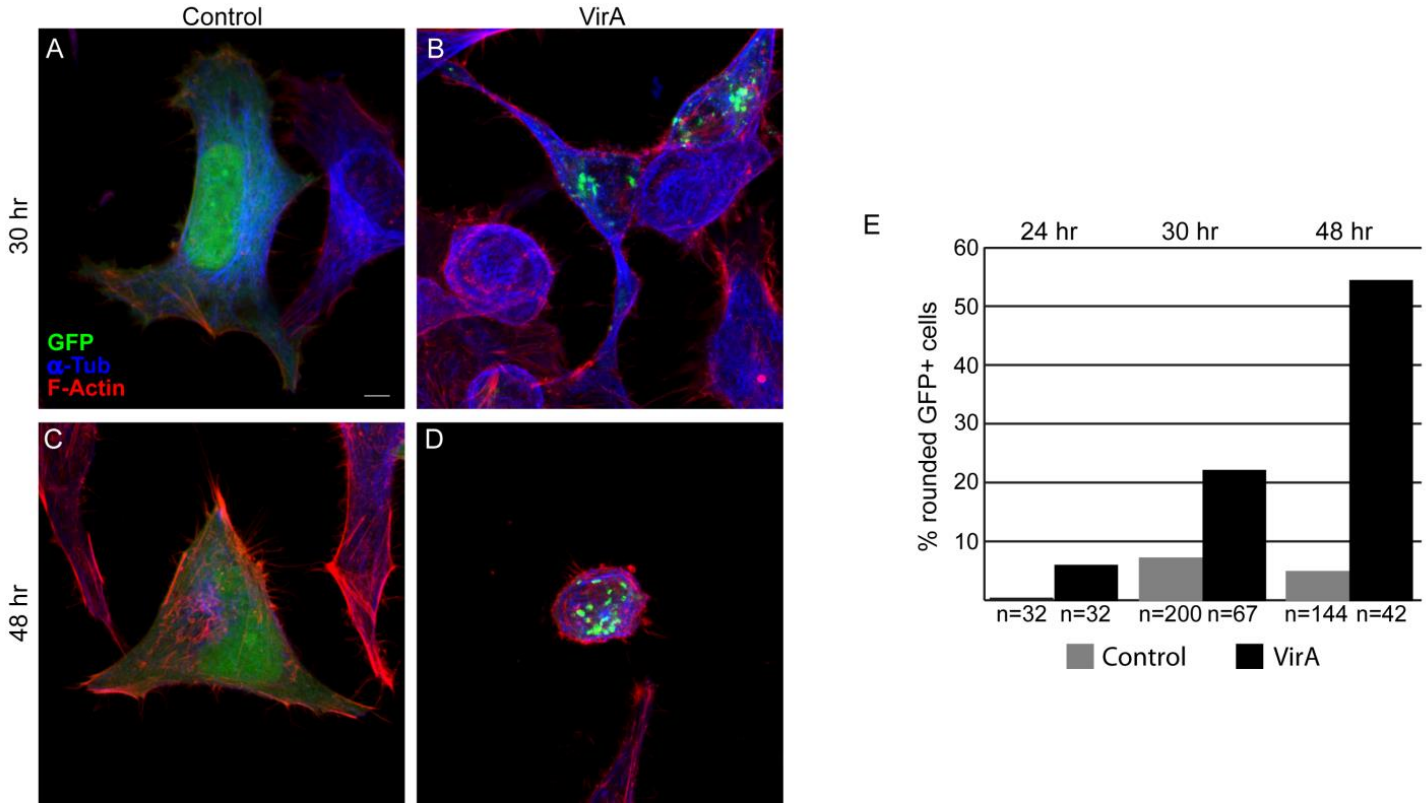
Control
VirA
A
B
C
D
30 hr
48 hr
GFP
α-Tub
F-Actin
E
24 hr
30 hr
48 hr
% rounded GFP+ cells
60
50
40
30
20
10
n=32
n=32
n=200
n=67
n=144
n=42
Control
VirA

Figure 3.6

Figure 3.7 – VirA expression results in apical cell rounding in chick neural tube

(A-C) Chick embryonic neural tube was electroporated with a construct expressing zsGreen (A, A'; Control; *green*) or VirA and zsGreen (B, B'; VirA; *green*). The embryos were also stained for F-Actin (*red*). Control cells expressing zsGreen largely exhibit the pseudostratified epithelial structure of the neural tube, while VirA expressing cells round up at the apical side of the epithelium. Quantification of the percentage of apically rounded zsGreen positive cells for control (*grey*) and VirA (*black*) embryos is shown in C. Scale bar in A represents 25 μm.

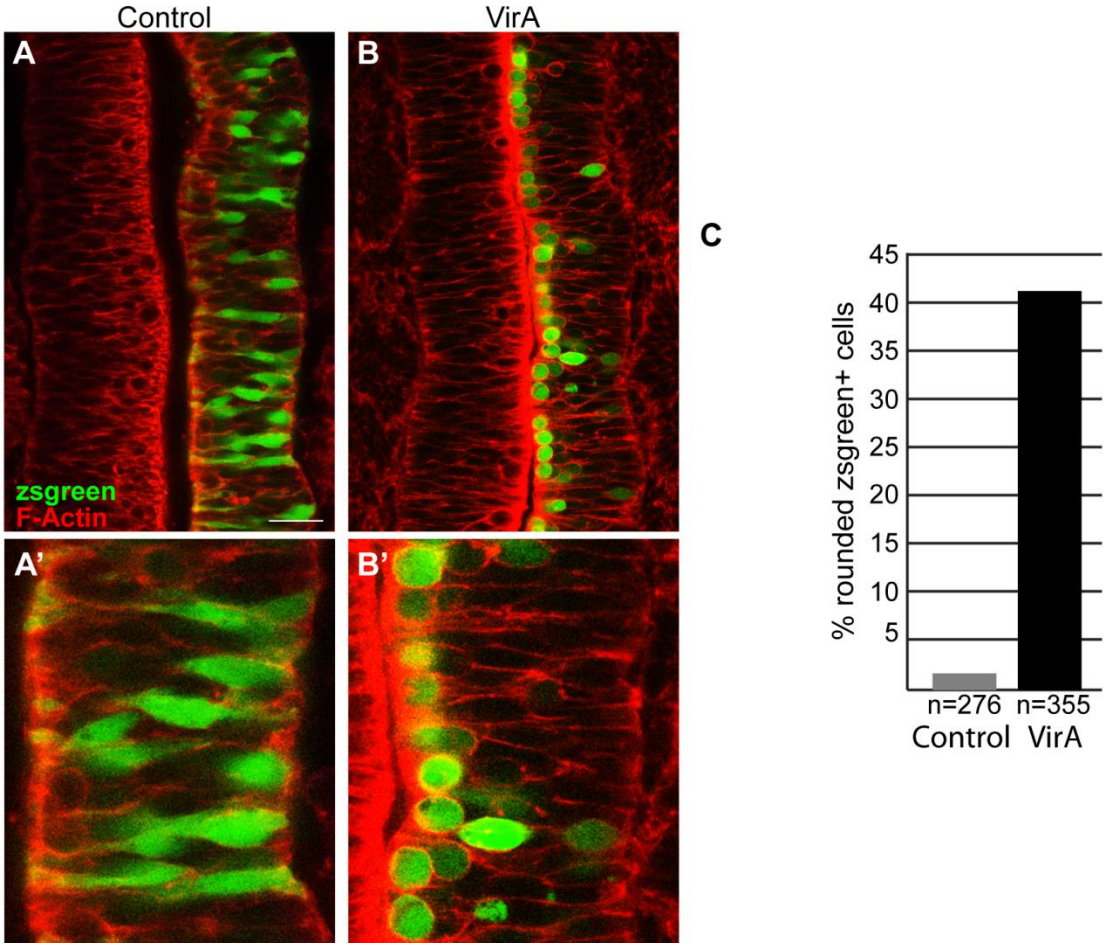
Control
VirA
A
B
zsgreen
F-Actin
A'
B'
C
% rounded zsgreen+ cells
45
40
35
30
25
20
15
10
5
n=276
n=355
Control
VirA

Figure 3.7

Rab11 localization is altered in VirA expressing cells

The establishment and maintenance of epithelial polarity and integrity requires localization of distinct proteins to specific sites in the cell. Thus, vesicle trafficking is essential for maintaining and regulating proper epithelial structure. Since the disruption of epithelial architecture was accompanied by the loss cell polarity (Figure 3.5), we were interested to examine if there was a defect in vesicle trafficking in VirA expressing epithelial cells. Rab GTPases are well known regulators of vesicle trafficking in eukaryotic cells. Rab11 has been shown to be important for targeting recycling endosomes to the apical surface (Calhoun and Goldenring, 1996; Ren et al., 1998; Casanova et al., 1999) and has roles in epithelial adhesion and integrity (Langevin et al., 2005; Lock and Stow, 2005; Desclozeaux et al., 2008; Roeth et al., 2009; Xu et al., 2011). We again induced clonal expression of VirA::GFP or GFP alone in the *Drosophila* salivary gland. Control salivary glands exhibited peripheral staining of Rab11 near the apical plasma membrane (Figure 3.8A,A',C,C'; Zhang et al., 2007). Interestingly, gland cells overexpressing VirA::GFP had strongly increased Rab11 antibody signal that was no longer restricted to the apical periphery of the cells (Figure 3.8B,B',D,D').

To confirm this mislocalization of Rab11 in another epithelial context, we additionally examined Rab11 localization in the eye imaginal disc. As previously described, we expressed VirA::GFP or GFP under the control of the GMR promoter. In control discs, there was punctate staining for Rab11 in the GFP expressing cells (Figure 3.9A-B'). However, VirA::GFP expression resulted in increased staining with numerous and aggregating clusters of Rab11 positive puncta (Figure 3.9C-D'). To rule out the

Figure 3.8 – Mislocalization of Rab11 in *Drosophila* salivary glands expressing VirA

(A-D) Salivary glands clonally expressing GFP (A,C; Control; *green*) or VirA::GFP (B,D; VirA; *green*) stained for Rab11 (*blue*) and F-Actin (*red*). Normal localization (A',C') was lost in the VirA expressing glands, and Rab11 signal was increased (B',D'). Scale bar in A represents 50 μm.

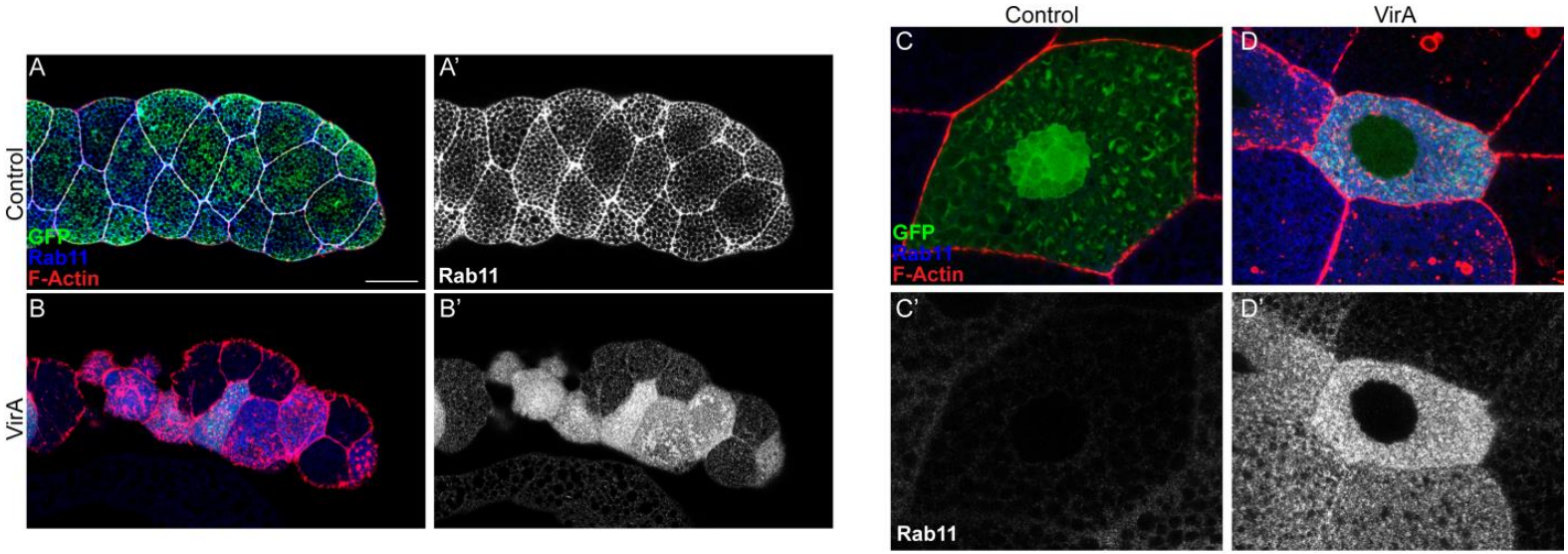
Control
VirA
A
A'
B
B'
C
D
C'
D'
GFP
Rab11
F-Actin
Rab11
GFP
Rab11
F-Actin
Rab11

Figure 3.8

Figure 3.9 – Rab11 mislocalization in the *Drosophila* eye imaginal disc following VirA expression

(A-F) GFP (A-B; Control; *green*), VirA::GFP (C-D; VirA; *green*), and VirA::GFP, p35 (E-F; VirA, p35; *green*) were expressed in the GMR domain of the eye disc. Discs were stained for Rab11 (*blue*) and F-Actin (*red*). Top panels show the eye disc while the bottom panels show a magnified portion from the top panel. VirA::GFP and VirA::GFP, p35 discs showed increased Rab11 staining. The discs are oriented with posterior to the right. Scale bar in A represents 25 μm.

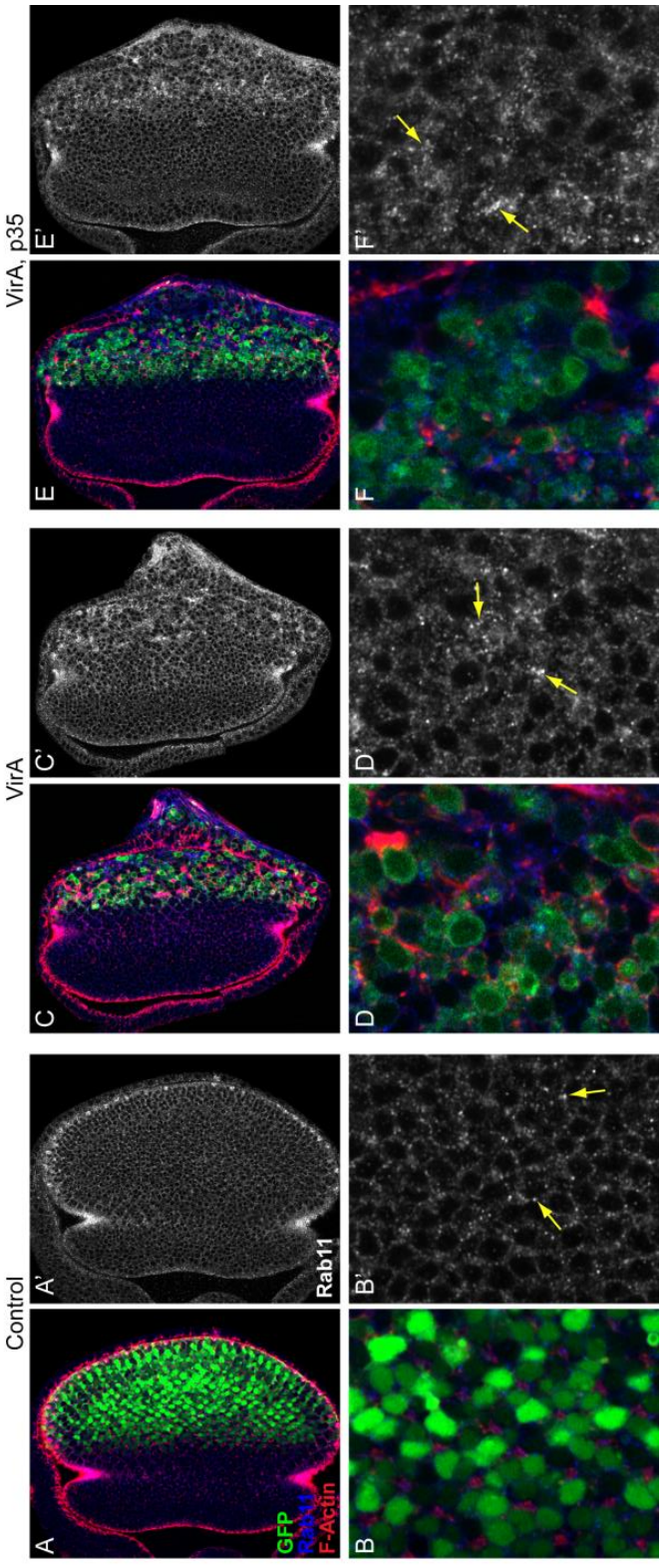

Figure 3.9

possibility that this phenotype was caused by cell death, we co-expressed p35 with VirA::GFP in the GMR domain. In this condition, we still observed the same accumulation of Rab11 (Figure 3.9E-F'). These results both suggest that *in vivo* VirA expression causes mislocalization and possibly accumulation of Rab11, which may alter the trafficking of proteins near the membrane. Consistent with our results, a recent study reported the data from an *in vitro* GTP hydrolysis enzymatic assay using VirA and various Rab proteins, which shows that Rab11 could act as a substrate for VirA (Dong et al., 2012). Further, Rab11 mediated trafficking is known to be important for E-cadherin targeting and recycling at the apical junctions and has been implicated in cell polarity and tissue integrity (Langevin et al., 2005; Lock and Stow, 2005; Desclozeaux et al., 2008; Xu et al., 2011; Nakanishi et al., 2012). This suggests a mechanism where VirA may act as a Rab11 GAP to alter cell polarity and adhesion, ultimately leading to compromised epithelial integrity.

Conclusions

While a few recent studies have investigated potential molecular mechanisms of VirA, outside of severing microtubules, the tissue level functions have been largely overlooked. This is the first and only study that examines the function of VirA in an *in vivo* tissue. Our data suggest a novel function of VirA where its expression leads to disruption of cell polarity and tissue integrity. Both key apical polarity proteins, Armadillo (β-catenin) and Discs large, were no longer correctly localized after VirA expression (Figure 3.5). We also show the localization of Rab11 was disrupted in VirA expressing salivary gland cells and the eye imaginal disc (Figures 3.8 and 3.9). The loss of cell polarity caused by VirA expression might be accomplished by defects in Rab11 trafficking of polarity or adhesion proteins to the apical plasma membrane (Desclozeaux et al., 2008; Roeth et al., 2009). Ultimately, this could lead to a breakdown of the epithelial architecture and integrity, assisting in the infection and spreading during *Shigella* pathogenesis.

Chapter 4: Discussion

The evolution of multicellularity and epithelial tissue was a crucial innovation that potentiated the diversity of animal body plans we see in the natural world. The polarized, adherent tissue architecture must be established and maintained during development and homeostasis. Loss of polarity or integrity during either of these processes can be catastrophic for the organism leading to developmental defects or disease. Epithelial architecture is maintained through dynamic regulation by a multitude of cellular processes including intracellular transport, cytoskeleton modulation, and cell adhesion during epithelial morphogenesis as well as adult homeostasis. While studies from model systems and cell culture have contributed to our understanding of these processes, many questions remain unanswered. Our efforts to uncover ancient mechanisms of epithelial morphogenesis in a basal metazoan and how normal epithelial architecture can be altered during pathogenesis have contributed new insights to these processes and in the field of epithelial biology.

Ancient mechanisms of epithelial morphogenesis

Studies of epithelial morphogenesis in *Drosophila*, chick, *Xenopus*, and mouse have laid the foundation for cellular and molecular mechanisms that are involved during development (reviewed in Schock and Perrimon, 2002). However, these few systems are not a total representation of the diversity of animals, and do not include more basal organisms, which may provide insight into the evolution of these developmental mechanisms. Our study (Chapter 2) explores ancient mechanisms of development in a

basal metazoan model, *Nematostella vectensis*. Using the tentacle as a model of an organ or appendage, we have identified ancient cellular mechanisms that drive morphogenesis in this simple system. Our work not only described this process for the first time, but also lays the basis for future studies in tentacle development, addition, and regeneration (Fritz et al., 2013).

Cellular and molecular mechanisms of morphogenesis

We uncovered cellular mechanisms that play a role during elongation of both the body column and tentacles during development. Cell shape changes in the ectoderm from columnar to flattened correlate with elongation of both the body column and tentacles (Figure 2.4). We demonstrate by drug treatment that this conversion requires Actin dynamics (Figure 2.6). The flattening of the ectodermal epithelial cells can expand the surface area of the tissue. However, in both the body column and tentacles, it is directed specifically into elongation. By labeling cells and exploring their behavior during development, we observed elongating cell clones (Figures 2.7 and 2.8), suggesting cell rearrangements are involved in directing the tissue expansion into elongation. Additionally, we observed oriented cell division in the body column during elongation, where divisions were biased along the oral-aboral axis (Figure 2.10). These cellular processes are very similar to the mechanisms that are involved during morphogenetic events of bilaterian organisms, such as *Xenopus* epiboly, *Drosophila* germ band extension, and ascidian notochord development (Keller, 1980; Irvine and Wieschaus, 1994; Munro and Odell, 2002; da Silva and Vincent, 2007).

While we were able to identify cellular mechanisms that function during body axis and tentacle elongation, we still do not know what underpins the initiation or regulation of these processes. One interesting candidate is the planar cell polarity (PCP) pathway, also known as non-canonical Wnt signaling, since it is independent of β-catenin. First identified in *Drosophila* and later studied in vertebrates, the PCP pathway has been implicated in the regulation of oriented cell division, cell rearrangements, and axis elongation during development (Gubb and Garcia-Bellido, 1982; Nubler-Jung et al., 1987; Jessen et al., 2002; Park and Moon, 2002; Wallingford and Harland, 2002; Gong et al., 2004; Baena-Lopez et al., 2005; Ciruna et al., 2006; Mao et al., 2011; reviewed in Gray et al., 2011). In this pathway, interaction of Frizzled and Dishevelled lead to the activation of downstream kinases including RhoA, c-Jun N-terminal Kinase (JNK), and Rho-associated protein kinase (ROCK) (reviewed in Simons and Mlodzik, 2008). Modulation of the Actin cytoskeleton is known to be regulated by RhoA downstream of PCP signaling in *Drosophila* and vertebrates (Fanto et al., 2000; Winter et al., 2001; Marlow et al., 2002). Polarity across a field of cells can be achieved by asymmetrical localization of the core PCP components: Frizzled, Dishevelled, Strabismus/Van Gogh, Diego, and Prickle (reviewed in Gray et al., 2011). Recently, this pathway has been explored in two cnidarians, *Hydra* and *Clytia*, suggesting its conservation from cnidarians to mammals (Philipp et al., 2009; Momose et al., 2012). In *Hydra* when the pathway is inhibited by drug treatment, asexual bud and tentacle evagination was disrupted; these processes are normally accompanied by lateral cell intercalation and Actin reorganization (Philipp et al., 2009). Similarly in *Clytia*, when PCP signaling was

inhibited by a morpholino against Strabismus, embryo elongation was inhibited, which was accompanied by a lack of normal cell intercalation (Momose et al., 2012).

The *Nematostella* genome contains the PCP components, but no functional studies have been done during *Nematostella* development (Guder et al., 2006; Lee et al., 2006; Rigo-Watermeier et al., 2012). Thus, it would be interesting to explore the functions of this pathway during *Nematostella* body column and tentacle elongation. To explore if PCP signaling is required for proper cell intercalations, oriented cell division, or actin dynamics during elongation, we could inhibit the pathway using drug treatment (SP600125, inhibits JNK) or antisense morpholinos against PCP pathway members, such as Strabismus (Han et al., 2001; Philipp et al., 2009; Momose et al., 2012). Our imaging assays, clonal analysis or quantification of the orientation of cell division could be repeated at various stages during elongation after PCP signaling inhibition. Additionally, to confirm the phenotypes are caused by the PCP pathway, canonical Wnt signaling can be activated as a control by using drug treatment (alsterpaullone; Lahusen et al., 2003; Broun et al., 2005) or expression of dominant negative proteins (DN-Glycogen synthase kinase 3; Pierce and Kimelman, 1995).

Placodes as a mechanism for development

Our results emphasize the use of placodes as a common mode of development across a diverse group of animals. These thickened, epithelial, primordial structures are observed in animals from cnidarians to humans. The *Drosophila* imaginal discs are a prime example of these in invertebrates (Fristrom, 1988; Cohen, 1993). Placodes are also involved in the development of structures in vertebrates, including hair follicles,

teeth, feathers, the inner ear, and the lens of the eye to name a few (Baker and Bronner-Fraser, 2001; Pispa and Thesleff, 2003; Streit, 2007). The sensory placodes of vertebrates are the best molecularly characterized, but more data from chordates and urochordates is emerging (reviewed in Graham and Shimeld, 2013). However, the evolution of these structures outside of vertebrates remains unclear (reviewed in Graham and Shimeld, 2013, Patthey et al., 2014, and Schlosser et al., 2014). Further, both the evolution of and cellular mechanisms that underlie integumental placodes (ectodermal appendages) remain largely unknown (reviewed in Mikkola, 2007 and Biggs and Mikkola, 2014). While the vertebrate examples are more complicated and involve the interaction of mesenchymal cells, placodes remain a common feature of developmental mechanisms across diverse species. It remains unknown and underappreciated as to why these seem to be important during development. We propose the model that when the epithelial cells are thickened, the cells are packed more closely together. This would allow for patterning of the primordia to occur over a relatively small area. Once molecularly patterned, epithelial morphogenesis by a variety of cellular mechanisms could elaborate this into the adult structure.

Tentacle patterning

Through our unbiased microarray approach, as well as from the literature, we identified a potential mechanism of sequential patterning of the oral ectoderm into tentacle competent and non-competent regions (Figure 2.18). However, further studies will be needed to verify and characterize the role of these genes in patterning and development. In order to study these processes as well as others in later stages of

development, past the embryonic stage, the creation of new tools for inducible gene expression and loss- and gain-of-function studies will be essential (discussed below). Generation of transgenic animals has been reported (Renfer et al., 2010; Nakanishi et al., 2012), as well as the use of antisense morpholinos (Rentzsch et al., 2008; Genikhovich and Technau, 2011; Nakanishi et al., 2012; Sinigaglia et al., 2013; Wolenski et al., 2013) and expression of mRNA or dominant negative constructs (Tsukita and Furuse, 2002; Rentzsch et al., 2006; Rentzsch et al., 2008; Kumburegama et al., 2011; Layden et al., 2012; Marlow et al., 2012; Rottinger et al., 2012; Layden et al., 2013). However, these technologies currently do not persist long enough to affect gene function late or do not allow inducible expression to avoid early developmental toxicity.

Subsequent tentacle addition

While our study has examined how the first four tentacles form during development, it would also be interesting to examine the patterning and morphogenesis of the subsequent tentacles. These are added as the animal begins feeding and growing overall in size. Are similar cellular mechanisms involved? It would be necessary to analyze the morphology of these subsequent tentacle buds to see if they similarly begin as thickened, pseudostratified epithelial that flatten as the tentacle elongates. Also, we could explore the gene expression patterns of known tentacle markers during tentacle initiation and elongation, including the ones identified from our microarray analysis.

Tentacle regeneration

Nematostella has an amazing capacity for regeneration (Reitzel et al., 2007). While there have been limited studies on animal regeneration in *Nematostella*, nothing is currently known about tentacle regeneration. Following amputation of the whole oral section of the body, cell proliferation is increased, and this proliferation is necessary for regeneration of the oral structures (Passamaneck and Martindale, 2012; Bossert et al., 2013). Therefore, we could characterize patterns of cell proliferation after amputation of a tentacle to examine if proliferation similarly upregulated. Also, are there cell shape changes or cytoskeletal rearrangements during regeneration of a tentacle? For both tentacle and head amputation, it would be interesting to explore the patterns of gene expression for tentacle marker genes to see if the same developmental program is redeployed or if regeneration involves a new molecular mechanism.

Generation of genetic tools

To establish *Nematostella* as a tractable genetic system, more tools to carry out functional experiments will be required. Both mouse and *Drosophila* have systems for inducible gene expression including heat shock/FlpOut (Golic and Lindquist, 1989; Golic, 1991; Chou and Perrimon, 1992; Struhl and Basler, 1993; Xu and Rubin, 1993; reviewed in Branda and Dymecki, 2004 and McGuire et al., 2004), Gal4/UAS (Brand and Perrimon, 1993) and Lox/CRE (Gu et al., 1993). By the creation of transgenic *Nematostella* carrying members of these systems, it may be possible to develop a method for inducible gene expression. New technologies are rapidly being developed

and employed in model organisms for genome editing including transcription activator-like effector nucleases (TALENs; Miller et al., 2011; Wood et al., 2011) and the clustered regulatory interspaced short palindromic repeat (CRISPR)-Cas system (Cong et al., 2013; Mali et al., 2013). If any of these systems could be applied to *Nematostella*, we could generate both knock-in and knock-out strategies. Current efforts in our lab are to develop methods for inducible expression, genome editing, and gain- and loss-of-function studies, which will help to drive the field forward.

Hijacking of vesicle trafficking as a mechanism of pathogenesis

Epithelial tissues are not only essential for the formation of a diversity of structures and body plans, but also the maintenance of their architecture during homeostasis is important for the prevention of pathogenesis, such as bacterial infections and cancer. During infection, bacteria secrete a host of effector proteins that can hijack endogenous processes for their own replication, survival, and spreading. In our study, we used the *Shigella* effector protein, VirA, to examine its effect on epithelial architecture. VirA is known to be essential for the effective infection and spreading of *Shigella*, however, its function in this process still remains unclear (Uchiya et al., 1995). The previous studies examining VirA function have only used *in vitro* and cell culture assays (Clements et al., 2011; Bergounioux et al., 2012; Dong et al., 2012). We are the first to express VirA in an epithelial tissue, and our results from three different systems in two separate organisms highlight the importance of using an *in vivo* model. In the *Drosophila* salivary gland, eye imaginal disc, and chick neural tube, expression of VirA

caused rounding of the epithelial cells (Figures 3.4, 3.5, and 3.7). Additionally in *Drosophila*, VirA expression resulted in a loss of normal epithelial architecture, an accumulation of Actin-rich structures, and a loss of polarity markers, Armadillo and β-catenin (Figures 3.3 and 3.5). These results suggest a function for VirA in polarity or vesicle trafficking, which is supported by the mislocalization of Rab11 in tissue expressing VirA (Figures 3.8 and 3.9).

Bacteria effector proteins accomplish a variety of functions during pathogenesis, including modulation of host tissue integrity (reviewed in Kim et al., 2010). Proteins secreted by *Clostridium difficile* and *Vibrio cholera*, among others, are known to accomplish this through modulation of the tight junctions (Wu et al., 2000b; Nusrat et al., 2001; Chen et al., 2002). Other pathogens, such as *Bacteroides fragilis*, alter tissue architecture by targeting the adherens junctions (Wu et al., 1998). Further, other bacterial effectors proteins modulate intracellular trafficking by activating or inactivating Rab proteins (reviewed in Ham et al., 2011). Nevertheless, most of these studies have been conducted in cell culture, and more *in vivo* tissue studies will be required to confirm these functions.

Overall, our results propose a model where VirA may contribute to *Shigella* pathogenesis by altering cell polarity or adhesion, ultimately causing loss of normal intestinal epithelial architecture and integrity, which could facilitate the invasion of more bacteria. This may be achieved by modulation of vesicle trafficking through Rab 11. Rab11, which localizes to recycling endosomes, is known to function in cell polarity, adhesion, and tissue integrity through the targeting and recycling of E-cadherin to the adherens junctions (Langevin et al., 2005; Lock and Stow, 2005; Desclozeaux et al.,

2008; Roeth et al., 2009; Xu et al., 2011). By mis-localizing or inactivating Rab11, VirA could cause disruption of the adherens junctions, which may lead to a loss of cell polarity and tissue architecture.

It is still unclear as to the mechanism of how VirA expression leads to alteration of Rab11 localization and disruption of polarity in epithelial cells. A drawback of our current approach is we are overexpressing VirA at high levels, potentially a non-physiological condition. However, it is still possible that with lower levels of expression VirA could have an impact on the junctional architecture or polarity to at least 'loosen up' the epithelium. More studies will be necessary to determine the mechanisms that underlie this function. Biochemical experiments could be done to determine if the interaction between VirA and Rab11 is direct or not. Further, VirA modulation of Rab11 localization could be confirmed in a vertebrate model, such as the chick neural tube. A promising hypothesis is that VirA may act as a Rab11 GAP to inactive it. *In vitro* data reported by Dong et al. (2012) suggest that Rab11 is a potential substrate for VirA GAP activity. Genetic experiments in *Drosophila* expressing dominant negative or constitutively active Rab11 mutants may also shed light on the molecular function of VirA.

Much is still unclear about the function of effector proteins during bacterial pathogenesis of a host tissue. What is known has largely only been examined through *in vitro* and cell culture assays. In contrast, our pioneering *in vivo* studies take advantage of tractable, *in vivo* systems to examine the effects of bacterial effectors. Our studies have contributed novel insight into the cellular and tissue level mechanisms that contribute to bacterial pathogenesis.

Concluding Remarks

As a critical innovation in the evolution of metazoans, epithelial tissues have allowed for the diversification of organs and body plans. The maintenance of polarity and integrity in epithelia play key roles in morphogenesis during development and homeostasis in preventing disease and infection. The efforts to understand these processes have largely come from studies in bilaterian model systems and cell culture assays. This dissertation focused on adding to these efforts in two largely unexplored contexts: 1) Ancient mechanisms of epithelial morphogenesis in a basal metazoan and 2) Modulation of epithelial polarity and integrity during bacterial pathogenesis. In an effort to uncover ancient mechanisms involved in epithelial morphogenesis, we used *Nematostella* tentacle development as a model for outgrowth formation. Our results established the initial study of this process and identified molecular and cellular mechanisms involved during development. Additional studies of tentacle development, addition, and regeneration will build from our initial results. To explore the modulation of epithelial architecture during bacteria pathogenesis, we expressed VirA, a *Shigella* effector protein, in *Drosophila* and vertebrate tissue. Our study is the first to explore the function of VirA in epithelial tissue. Our data suggest a novel mechanism for VirA function in disruption of cell polarity and tissue integrity during *Shigella* pathogenesis. The results stemming from our unique approach highlight the importance of *in vivo* experiments in studying the mechanisms of bacterial pathogenesis. Combined, our efforts to understand mechanisms of tissue morphogenesis, polarity, and integrity have contributed evolutionary and mechanistic insights in the fields of developmental biology, pathogenesis and epithelial biology.

References

Angelini, D. R. and Kaufman, T. C. (2005) 'Functional analyses in the milkweed bug Oncopeltus fasciatus (Hemiptera) support a role for Wnt signaling in body segmentation but not appendage development', *Dev Biol* 283(2): 409-23.

Artavanis-Tsakonas, S. and Muskavitch, M. A. (2010) 'Notch: the past, the present, and the future', *Curr Top Dev Biol* 92: 1-29.

Baena-Lopez, L. A., Baonza, A. and Garcia-Bellido, A. (2005) 'The orientation of cell divisions determines the shape of Drosophila organs', *Curr Biol* 15(18): 1640-4.

Baker, C. V. and Bronner-Fraser, M. (2001) 'Vertebrate cranial placodes I. Embryonic induction', *Dev Biol* 232(1): 1-61.

Barr, F. and Lambright, D. G. (2010) 'Rab GEFs and GAPs', *Curr Opin Cell Biol* 22(4): 461-70.

Benjamini, Y. and Hochberg, Y. (1995) 'Controlling the false discovery rate: a practical and powerful approach to multiple testing', *Journal of the Royal Statistical Society Series B* 57: 289-300.

Bergounioux, J., Elisee, R., Prunier, A. L., Donnadieu, F., Sperandio, B., Sansonetti, P. and Arbibe, L. (2012) 'Calpain activation by the Shigella flexneri effector VirA regulates key steps in the formation and life of the bacterium's epithelial niche', *Cell Host Microbe* 11(3): 240-52.

Biggs, L. C. and Mikkola, M. L. (2014) 'Early inductive events in ectodermal appendage morphogenesis', *Semin Cell Dev Biol*.

Bilder, D. (2001) 'PDZ proteins and polarity: functions from the fly', *Trends Genet* 17(9): 511-9.

Bilder, D., Li, M. and Perrimon, N. (2000) 'Cooperative regulation of cell polarity and growth by Drosophila tumor suppressors', *Science* 289(5476): 113-6.

Bilder, D. and Perrimon, N. (2000) 'Localization of apical epithelial determinants by the basolateral PDZ protein Scribble', *Nature* 403(6770): 676-80.

Blumer, J., Rey, J., Dehmelt, L., Mazel, T., Wu, Y. W., Bastiaens, P., Goody, R. S. and Itzen, A. (2013) 'RabGEFs are a major determinant for specific Rab membrane targeting', *J Cell Biol* 200(3): 287-300.

Bode, H. R. (1996) 'The interstitial cell lineage of hydra: a stem cell system that arose early in evolution', *J Cell Sci* 109 (Pt 6): 1155-64.

Bode, H. R. (2001) 'Role of Hox genes in axial patterning in Hydra', *Am. Zool.* 41(621-628).

Bode, H. R. and David, C. N. (1978) 'Regulation of a multipotent stem cell, the interstitial cell of *hydra*', *Prog Biophys Mol Biol* 33(2): 189-206.

Bosch, T. C. G. and David, C. N. (1987) 'Stem cells of *Hydra magnipapillata* can differentiate into somatic cells and germ line cells', *Dev. Biol.* 121: 182-191.

Bossert, P. E., Dunn, M. P. and Thomsen, G. H. (2013) 'A staging system for the regeneration of a polyp from the aboral physa of the anthozoan Cnidarian Nematostella vectensis', *Dev Dyn* 242(11): 1320-31.

Bottger, A., Strasser, D., Alexandrova, O., Levin, A., Fischer, S., Lasi, M., Rudd, S. and David, C. N. (2006) 'Genetic screen for signal peptides in Hydra reveals

novel secreted proteins and evidence for non-classical protein secretion', *Eur J Cell Biol* 85(9-10): 1107-17.

Bouillon, J. (1994) Embranchement des cnidaires (Cnidaria). in P. P. Grassé (ed.) *Traité de Zoologie. Cnidaires, Cténaires*. Paris: Masson.

Brand, A. H. and Perrimon, N. (1993) 'Targeted gene expression as a means of altering cell fates and generating dominant phenotypes', *Development* 118(2): 401-15.

Branda, C. S. and Dymecki, S. M. (2004) 'Talking about a revolution: The impact of site-specific recombinases on genetic analyses in mice', *Dev Cell* 6(1): 7-28.

Broun, M. and Bode, H. R. (2002) 'Characterization of the head organizer in hydra', *Development* 129(4): 875-84.

Broun, M., Gee, L., Reinhardt, B. and Bode, H. R. (2005) 'Formation of the head organizer in hydra involves the canonical Wnt pathway', *Development* 132(12): 2907-16.

Calhoun, B. C. and Goldenring, J. R. (1996) 'Rab proteins in gastric parietal cells: evidence for the membrane recycling hypothesis', *Yale J Biol Med* 69(1): 1-8.

Campbell, R. D. (1967a) 'Tissue dynamics of steady state growth in *Hydra littoralis*. I. Patterns of cell division', *Dev Biol* 15(5): 487-502.

Campbell, R. D. (1967b) 'Tissue dynamics of steady state growth in *Hydra littoralis*. II. Patterns of tissue movement', *J Morphol* 121(1): 19-28.

Carre, D. and Carre, C. (2000) 'Origin of germ cells, sex determination, and sex inversion in medusae of the genus Clytia (Hydrozoa, leptomedusae): the influence of temperature', *J Exp Zool* 287(3): 233-42.

Casanova, J. E., Wang, X., Kumar, R., Bhartur, S. G., Navarre, J., Woodrum, J. E., Altschuler, Y., Ray, G. S. and Goldenring, J. R. (1999) 'Association of Rab25 and Rab11a with the apical recycling system of polarized Madin-Darby canine kidney cells', *Mol Biol Cell* 10(1): 47-61.

Casella, J. F., Flanagan, M. D. and Lin, S. (1981) 'Cytochalasin D inhibits actin polymerization and induces depolymerization of actin filaments formed during platelet shape change', *Nature* 293(5830): 302-5.

Chapman, J. A., Kirkness, E. F., Simakov, O., Hampson, S. E., Mitros, T., Weinmaier, T., Rattei, T., Balasubramanian, P. G., Borman, J., Busam, D. et al. (2010) 'The dynamic genome of Hydra', *Nature* 464(7288): 592-6.

Chavrier, P., Parton, R. G., Hauri, H. P., Simons, K. and Zerial, M. (1990) 'Localization of low molecular weight GTP binding proteins to exocytic and endocytic compartments', *Cell* 62(2): 317-29.

Chen, M. L., Pothoulakis, C. and LaMont, J. T. (2002) 'Protein kinase C signaling regulates ZO-1 translocation and increased paracellular flux of T84 colonocytes exposed to Clostridium difficile toxin A', *J Biol Chem* 277(6): 4247-54.

Chou, T. B. and Perrimon, N. (1992) 'Use of a yeast site-specific recombinase to produce female germline chimeras in Drosophila', *Genetics* 131(3): 643-53.

Chourrout, D., Delsuc, F., Chourrout, P., Edvardsen, R. B., Rentzsch, F., Renfer, E., Jensen, M. F., Zhu, B., de Jong, P., Steele, R. E. et al. (2006) 'Minimal ProtoHox cluster inferred from bilaterian and cnidarian Hox complements', *Nature* 442(7103): 684-7.

Ciruna, B., Jenny, A., Lee, D., Mlodzik, M. and Schier, A. F. (2006) 'Planar cell polarity signalling couples cell division and morphogenesis during neurulation', *Nature* 439(7073): 220-4.

Clements, A., Smollett, K., Lee, S. F., Hartland, E. L., Lowe, M. and Frankel, G. (2011) 'EspG of enteropathogenic and enterohemorrhagic E. coli binds the Golgi matrix protein GM130 and disrupts the Golgi structure and function', *Cell Microbiol* 13(9): 1429-39.

Cohen, S. M. (1993) Imaginal disc development. in M. Bate and A. Martinez Arias (eds.) *The development of Drosophila melanogaster*, vol. II. Cold Spring Harbor, NY: Cold Spring Harbor Laboratory Press.

Collins, A. G. (1998) 'Evaluating multiple alternative hypotheses for the origin of Bilateria: an analysis of 18S rRNA molecular evidence', *Proc Natl Acad Sci U S A* 95(26): 15458-63.

Collins, A. G. (2002) 'Phylogeny of Medusozoa and the evolution of cnidarian life cycles', *J Evol Biol* 15: 418-432.

Collins, A. G., Schuchert, P., Marques, A. C., Jankowski, T., Medina, M. and Schierwater, B. (2006) 'Medusozoan phylogeny and character evolution clarified by new large and small subunit rDNA data and an assessment of the utility of phylogenetic mixture models', *Syst Biol* 55(1): 97-115.

Concha, M. L. and Adams, R. J. (1998) 'Oriented cell divisions and cellular morphogenesis in the zebrafish gastrula and neurula: a time-lapse analysis', *Development* 125(6): 983-94.

Cong, L., Ran, F. A., Cox, D., Lin, S., Barretto, R., Habib, N., Hsu, P. D., Wu, X., Jiang, W., Marraffini, L. A. et al. (2013) 'Multiplex genome engineering using CRISPR/Cas systems', *Science* 339(6121): 819-23.

da Silva, S. M. and Vincent, J. P. (2007) 'Oriented cell divisions in the extending germband of Drosophila', *Development* 134(17): 3049-54.

Daly, M., Brugler, M. R., Cartwright, P., Collins, A. G., Dawson, M. N., Fautin, D. G., France, S. C., Mcfadden, C. S., Opresko, D. M., Rodriguez, E. et al. (2007) 'The phylum Cnidaria: A review of phylogenetic patterns and diversity 300 years after Linnaeus', *Zootaxa*(1668): 127-182.

David, C. N. and Campbell, R. D. (1972) 'Cell cycle kinetics and development of *Hydra attenuata*. I. Epithelial cells', *J Cell Sci* 11(2): 557-68.

David, C. N. and Challoner, D. (1974) 'Distribution of interstitial cells and differentiating nematocytes in nests in *Hydra attenuata*', *Integr Comp Biol* 14: 537-542.

David, C. N. and Gierer, A. (1974) 'Cell cycle kinetics and development of *Hydra attenuata*. III. Nerve and nematocyte differentiation', *J Cell Sci* 16(2): 359-75.

David, C. N. and Murphy, S. (1977) 'Characterization of interstitial stem cells in hydra by cloning', *Dev Biol* 58(2): 372-83.

Davis, J., Wang, J., Tropea, J. E., Zhang, D., Dauter, Z., Waugh, D. S. and Wlodawer, A. (2008) 'Novel fold of VirA, a type III secretion system effector protein from Shigella flexneri', *Protein Sci* 17(12): 2167-73.

Delprato, A., Merithew, E. and Lambright, D. G. (2004) 'Structure, exchange determinants, and family-wide rab specificity of the tandem helical bundle and Vps9 domains of Rabex-5', *Cell* 118(5): 607-17.

Delva, E., Tucker, D. K. and Kowalczyk, A. P. (2009) 'The desmosome', *Cold Spring Harb Perspect Biol* 1(2): a002543.

Denker, E., Manuel, M., Leclere, L., Le Guyader, H. and Rabet, N. (2008) 'Ordered progression of nematogenesis from stem cells through differentiation stages in the tentacle bulb of *Clytia hemisphaerica* (Hydrozoa, Cnidaria)', *Dev Biol* 315(1): 99-113.

Desclozeaux, M., Venturato, J., Wylie, F. G., Kay, J. G., Joseph, S. R., Le, H. T. and Stow, J. L. (2008) 'Active Rab11 and functional recycling endosome are required for E-cadherin trafficking and lumen formation during epithelial morphogenesis', *Am J Physiol Cell Physiol* 295(2): C545-56.

Dong, N., Zhu, Y., Lu, Q., Hu, L., Zheng, Y. and Shao, F. (2012) 'Structurally distinct bacterial TBC-like GAPs link Arf GTPase to Rab1 inactivation to counteract host defenses', *Cell* 150(5): 1029-41.

Dovey, H. F., John, V., Anderson, J. P., Chen, L. Z., de Saint Andrieu, P., Fang, L. Y., Freedman, S. B., Folmer, B., Goldbach, E., Holsztynska, E. J. et al. (2001) 'Functional gamma-secretase inhibitors reduce beta-amyloid peptide levels in brain', *J Neurochem* 76(1): 173-81.

Dubel, S., Hoffmeister, S. A. and Schaller, H. C. (1987) 'Differentiation pathways of ectodermal epithelial cells in hydra', *Differentiation* 35(3): 181-9.

Dunn, C. W., Hejnol, A., Matus, D. Q., Pang, K., Browne, W. E., Smith, S. A., Seaver, E., Rouse, G. W., Obst, M., Edgecombe, G. D. et al. (2008) 'Broad phylogenomic sampling improves resolution of the animal tree of life', *Nature* 452(7188): 745-9.

DuPont, H. L., Levine, M. M., Hornick, R. B. and Formal, S. B. (1989) 'Inoculum size in shigellosis and implications for expected mode of transmission', *J Infect Dis* 159(6): 1126-8.

Elliott, S. J., Krejany, E. O., Mellies, J. L., Robins-Browne, R. M., Sasakawa, C. and Kaper, J. B. (2001) 'EspG, a novel type III system-secreted protein from enteropathogenic Escherichia coli with similarities to VirA of Shigella flexneri', *Infect Immun* 69(6): 4027-33.

Erwin, D. H. (2009) 'Early origin of the bilaterian developmental toolkit', *Philos Trans R Soc Lond B Biol Sci* 364(1527): 2253-61.

Fanto, M., Weber, U., Strutt, D. I. and Mlodzik, M. (2000) 'Nuclear signaling by Rac and Rho GTPases is required in the establishment of epithelial planar polarity in the Drosophila eye', *Curr Biol* 10(16): 979-88.

Finnerty, J. R. (2003) 'The origins of axial patterning in the metazoa: how old is bilateral symmetry?', *Int J Dev Biol* 47(7-8): 523-9.

Finnerty, J. R. and Martindale, M. Q. (1999) 'Ancient origins of axial patterning genes: Hox genes and ParaHox genes in the Cnidaria', *Evol Dev* 1(1): 16-23.

Finnerty, J. R., Paulson, D., Burton, P., Pang, K. and Martindale, M. Q. (2003) 'Early evolution of a homeobox gene: the parahox gene Gsx in the Cnidaria and the Bilateria', *Evol Dev* 5(4): 331-45.

Franch-Marro, X., Martin, N., Averof, M. and Casanova, J. (2006) 'Association of tracheal placodes with leg primordia in *Drosophila* and implications for the origin of insect tracheal systems', *Development* 133(5): 785-90.

Fristrom, D. (1988) 'The cellular basis of epithelial morphogenesis. A review', *Tissue Cell* 20(5): 645-90.

Fritz, A. E., Ikmi, A., Seidel, C., Paulson, A. and Gibson, M. C. (2013) 'Mechanisms of tentacle morphogenesis in the sea anemone Nematostella vectensis', *Development* 140(10): 2212-23.

Fritzenwanker, J. H. and Technau, U. (2002a) 'Induction of gametogenesis in the basal cnidarian *Nematostella vectensis* (Anthozoa)', *Dev Genes Evol* 212(2): 99-103.

Fritzenwanker, J. H. and Technau, U. (2002b) 'Induction of gametogenesis in the basal cnidarian Nematostella vectensis(Anthozoa)', *Dev Genes Evol* 212(2): 99-103.

Gelei, J. (1925) 'Über die Sprossbildung bei *Hydra grisea*', *Wilhelm Roux's Arch. Dev. Biol* 105: 633-654.

Geling, A., Steiner, H., Willem, M., Bally-Cuif, L. and Haass, C. (2002) 'A gamma-secretase inhibitor blocks Notch signaling in vivo and causes a severe neurogenic phenotype in zebrafish', *EMBO Rep* 3(7): 688-94.

Genikhovich, G. and Technau, U. (2009a) 'Anti-acetylated tubulin antibody staining and phalloidin staining in the starlet sea anemone Nematostella vectensis', *CSH Protoc* 2009(9): pdb prot5283.

Genikhovich, G. and Technau, U. (2009b) 'In situ hybridization of starlet sea anemone (Nematostella vectensis) embryos, larvae, and polyps', *CSH Protoc* 2009(9): pdb prot5282.

Genikhovich, G. and Technau, U. (2011) 'Complex functions of Mef2 splice variants in the differentiation of endoderm and of a neuronal cell type in a sea anemone', *Development* 138(22): 4911-9.

Genova, J. L. and Fehon, R. G. (2003) 'Neuroglian, Gliotactin, and the Na+/K+ ATPase are essential for septate junction function in Drosophila', *J Cell Biol* 161(5): 979-89.

Gerhart, J. (1999) '1998 Warkany lecture: signaling pathways in development', *Teratology* 60(4): 226-39.

Germane, K. L., Ohi, R., Goldberg, M. B. and Spiller, B. W. (2008) 'Structural and functional studies indicate that Shigella VirA is not a protease and does not directly destabilize microtubules', *Biochemistry* 47(39): 10241-3.

Germane, K. L. and Spiller, B. W. (2011) 'Structural and functional studies indicate that the EPEC effector, EspG, directly binds p21-activated kinase', *Biochemistry* 50(6): 917-9.

Gerondopoulos, A., Langemeyer, L., Liang, J. R., Linford, A. and Barr, F. A. (2012) 'BLOC-3 mutated in Hermansky-Pudlak syndrome is a Rab32/38 guanine nucleotide exchange factor', *Curr Biol* 22(22): 2135-9.

Golic, K. G. (1991) 'Site-specific recombination between homologous chromosomes in Drosophila', *Science* 252(5008): 958-61.

Golic, K. G. and Lindquist, S. (1989) 'The FLP recombinase of yeast catalyzes site-specific recombination in the Drosophila genome', *Cell* 59(3): 499-509.

Gong, Y., Mo, C. and Fraser, S. E. (2004) 'Planar cell polarity signalling controls cell division orientation during zebrafish gastrulation', *Nature* 430(7000): 689-93.

Graf, L. and Gierer, A. (1980) 'Size, shape and orientation of cells in budding hydra and regulation of regeneration in cell aggregates', *Wilhelm Roux's Arch. Dev. Biol* 188: 141-151.

Graham, A. and Shimeld, S. M. (2013) 'The origin and evolution of the ectodermal placodes', *J Anat* 222(1): 32-40.

Gray, R. S., Roszko, I. and Solnica-Krezel, L. (2011) 'Planar cell polarity: coordinating morphogenetic cell behaviors with embryonic polarity', *Dev Cell* 21(1): 120-33.

Gu, H., Zou, Y. R. and Rajewsky, K. (1993) 'Independent control of immunoglobulin switch recombination at individual switch regions evidenced through Cre-loxP-mediated gene targeting', *Cell* 73(6): 1155-64.

Gubb, D. and Garcia-Bellido, A. (1982) 'A genetic analysis of the determination of cuticular polarity during development in Drosophila melanogaster', *J Embryol Exp Morphol* 68: 37-57.

Guder, C., Philipp, I., Lengfeld, T., Watanabe, H., Hobmayer, B. and Holstein, T. W. (2006) 'The Wnt code: cnidarians signal the way', *Oncogene* 25(57): 7450-60.

Haas, A. K., Yoshimura, S., Stephens, D. J., Preisinger, C., Fuchs, E. and Barr, F. A. (2007) 'Analysis of GTPase-activating proteins: Rab1 and Rab43 are key Rabs required to maintain a functional Golgi complex in human cells', *J Cell Sci* 120(Pt 17): 2997-3010.

Ham, H., Sreelatha, A. and Orth, K. (2011) 'Manipulation of host membranes by bacterial effectors', *Nat Rev Microbiol* 9(9): 635-46.

Han, Z., Boyle, D. L., Chang, L., Bennett, B., Karin, M., Yang, L., Manning, A. M. and Firestein, G. S. (2001) 'c-Jun N-terminal kinase is required for

metalloproteinase expression and joint destruction in inflammatory arthritis', *J Clin Invest* 108(1): 73-81.

Hand, C. and Unlinger, K. R. (1992) 'The culture, sexual and asexual reproduction, and growth of the sea anemone *Nematostella vectensis*', *Biol Bull* 182: 169-176.

Hassel, M., Albert, K. and Hofheinz, S. (1993) 'Pattern formation in *Hydra vulgaris* is controlled by lithium-sensitive processes', *Dev Biol* 156(2): 362-71.

Hejnol, A., Obst, M., Stamatakis, A., Ott, M., Rouse, G. W., Edgecombe, G. D., Martinez, P., Baguna, J., Bailly, X., Jondelius, U. et al. (2009) 'Assessing the root of bilaterian animals with scalable phylogenomic methods', *Proc Biol Sci* 276(1677): 4261-70.

Holstein, T. W., Hobmayer, E. and David, C. N. (1991) 'Pattern of epithelial cell cycling in hydra', *Dev Biol* 148(2): 602-11.

Houliston, E., Momose, T. and Manuel, M. (2010) 'Clytia hemisphaerica: a jellyfish cousin joins the laboratory', *Trends Genet* 26(4): 159-67.

Hynes, R. O. and Zhao, Q. (2000) 'The evolution of cell adhesion', *J Cell Biol* 150(2): F89-96.

Irvine, K. D. and Wieschaus, E. (1994) 'Cell intercalation during Drosophila germband extension and its regulation by pair-rule segmentation genes', *Development* 120(4): 827-41.

Jessen, J. R., Topczewski, J., Bingham, S., Sepich, D. S., Marlow, F., Chandrasekhar, A. and Solnica-Krezel, L. (2002) 'Zebrafish trilobite identifies new roles for Strabismus in gastrulation and neuronal movements', *Nat Cell Biol* 4(8): 610-5.

Kasbauer, T., Towb, P., Alexandrova, O., David, C. N., Dall'armi, E., Staudigl, A., Stiening, B. and Bottger, A. (2007) 'The Notch signaling pathway in the cnidarian Hydra', *Dev Biol* 303(1): 376-90.

Kayal, E., Roure, B., Philippe, H., Collins, A. G. and Lavrov, D. V. (2013) 'Cnidarian phylogenetic relationships as revealed by mitogenomics', *BMC Evol Biol* 13: 5.

Keller, R., Shih, J. and Sater, A. (1992) 'The cellular basis of the convergence and extension of the Xenopus neural plate', *Dev Dyn* 193(3): 199-217.

Keller, R. E. (1978) 'Time-lapse cinemicrographic analysis of superficial cell behavior during and prior to gastrulation in *Xenopus laevis*', *J. Morph.* 157: 223-248.

Keller, R. E. (1980) 'The cellular basis of epiboly: an SEM study of deep-cell rearrangement during gastrulation in *Xenopus laevis*', *J Embryol Exp Morphol* 60: 201-34.

Kim, J., Kim, W. and Cunningham, C. W. (1999) 'A new perspective on lower metazoan relationships from 18S rDNA sequences', *Mol Biol Evol* 16(3): 423-7.

Kim, M., Ashida, H., Ogawa, M., Yoshikawa, Y., Mimuro, H. and Sasakawa, C. (2010) 'Bacterial interactions with the host epithelium', *Cell Host Microbe* 8(1): 20-35.

Knust, E. and Bossinger, O. (2002) 'Composition and formation of intercellular junctions in epithelial cells', *Science* 298(5600): 1955-9.

Kraus, P. and Lufkin, T. (2006) 'Dlx homeobox gene control of mammalian limb and craniofacial development', *Am J Med Genet A* 140(13): 1366-74.

Kumburegama, S., Wijesena, N., Xu, R. and Wikramanayake, A. H. (2011) 'Strabismus-mediated primary archenteron invagination is uncoupled from

Wnt/beta-catenin-dependent endoderm cell fate specification in Nematostella vectensis (Anthozoa, Cnidaria): Implications for the evolution of gastrulation', *Evodevo* 2(1): 2.

Kusserow, A., Pang, K., Sturm, C., Hrouda, M., Lentfer, J., Schmidt, H. A., Technau, U., von Haeseler, A., Hobmayer, B., Martindale, M. Q. et al. (2005) 'Unexpected complexity of the Wnt gene family in a sea anemone', *Nature* 433(7022): 156-60.

Lahusen, T., De Siervi, A., Kunick, C. and Senderowicz, A. M. (2003) 'Alsterpaullone, a novel cyclin-dependent kinase inhibitor, induces apoptosis by activation of caspase-9 due to perturbation in mitochondrial membrane potential', *Mol Carcinog* 36(4): 183-94.

Lamb, R. S., Ward, R. E., Schweizer, L. and Fehon, R. G. (1998) 'Drosophila coracle, a member of the protein 4.1 superfamily, has essential structural functions in the septate junctions and developmental functions in embryonic and adult epithelial cells', *Mol Biol Cell* 9(12): 3505-19.

Langevin, J., Morgan, M. J., Sibarita, J. B., Aresta, S., Murthy, M., Schwarz, T., Camonis, J. and Bellaiche, Y. (2005) 'Drosophila exocyst components Sec5, Sec6, and Sec15 regulate DE-Cadherin trafficking from recycling endosomes to the plasma membrane', *Dev Cell* 9(3): 365-76.

Layden, M. J., Boekhout, M. and Martindale, M. Q. (2012) 'Nematostella vectensis achaete-scute homolog NvashA regulates embryonic ectodermal neurogenesis and represents an ancient component of the metazoan neural specification pathway', *Development* 139(5): 1013-22.

Layden, M. J., Rottinger, E., Wolenski, F. S., Gilmore, T. D. and Martindale, M. Q. (2013) 'Microinjection of mRNA or morpholinos for reverse genetic analysis in the starlet sea anemone, Nematostella vectensis', *Nat Protoc* 8(5): 924-34.

Lee, P. N., Pang, K., Matus, D. Q. and Martindale, M. Q. (2006) 'A WNT of things to come: evolution of Wnt signaling and polarity in cnidarians', *Semin Cell Dev Biol* 17(2): 157-67.

Lock, J. G. and Stow, J. L. (2005) 'Rab11 in recycling endosomes regulates the sorting and basolateral transport of E-cadherin', *Mol Biol Cell* 16(4): 1744-55.

Macara, I. G. (2004) 'Parsing the polarity code', *Nat Rev Mol Cell Biol* 5(3): 220-31.

Magie, C. R., Daly, M. and Martindale, M. Q. (2007) 'Gastrulation in the cnidarian Nematostella vectensis occurs via invagination not ingression', *Dev Biol* 305(2): 483-97.

Magie, C. R., Pang, K. and Martindale, M. Q. (2005) 'Genomic inventory and expression of Sox and Fox genes in the cnidarian Nematostella vectensis', *Dev Genes Evol* 215(12): 618-30.

Mali, P., Yang, L., Esvelt, K. M., Aach, J., Guell, M., DiCarlo, J. E., Norville, J. E. and Church, G. M. (2013) 'RNA-guided human genome engineering via Cas9', *Science* 339(6121): 823-6.

Manni, L., Lane, N. J., Joly, J. S., Gasparini, F., Tiozzo, S., Caicci, F., Zaniolo, G. and Burighel, P. (2004) 'Neurogenic and non-neurogenic placodes in ascidians', *J Exp Zool B Mol Dev Evol* 302(5): 483-504.

Mao, Y., Tournier, A. L., Bates, P. A., Gale, J. E., Tapon, N. and Thompson, B. J. (2011) 'Planar polarization of the atypical myosin Dachs orients cell divisions in Drosophila', *Genes Dev* 25(2): 131-6.

Marlow, F., Topczewski, J., Sepich, D. and Solnica-Krezel, L. (2002) 'Zebrafish Rho kinase 2 acts downstream of Wnt11 to mediate cell polarity and effective convergence and extension movements', *Curr Biol* 12(11): 876-84.

Marlow, H., Roettinger, E., Boekhout, M. and Martindale, M. Q. (2012) 'Functional roles of Notch signaling in the cnidarian *Nematostella vectensis*', *Dev Biol* 362(2): 295-308.

Marlow, H. Q., Srivastava, M., Matus, D. Q., Rokhsar, D. and Martindale, M. Q. (2009) 'Anatomy and development of the nervous system of Nematostella vectensis, an anthozoan cnidarian', *Dev Neurobiol* 69(4): 235-54.

Marques, A. C. and Collins, A. G. (2004) 'Cladistic analysis of Medusozoa and cnidarian evolution', *Invert Biol* 12323-42.

Martin, V. J., Littlefield, C. L., Archer, W. E. and Bode, H. R. (1997) 'Embryogenesis in hydra', *Biol Bull* 192(3): 345-63.

Martindale, M. Q., Pang, K. and Finnerty, J. R. (2004) 'Investigating the origins of triploblasty: 'mesodermal' gene expression in a diploblastic animal, the sea anemone Nematostella vectensis (phylum, Cnidaria; class, Anthozoa)', *Development* 131(10): 2463-74.

Matsui, Y., Kikuchi, A., Araki, S., Hata, Y., Kondo, J., Teranishi, Y. and Takai, Y. (1990) 'Molecular cloning and characterization of a novel type of regulatory

protein (GDI) for smg p25A, a ras p21-like GTP-binding protein', *Mol Cell Biol* 10(8): 4116-22.

Matus, D. Q., Magie, C. R., Pang, K., Martindale, M. Q. and Thomsen, G. H. (2008) 'The Hedgehog gene family of the cnidarian, Nematostella vectensis, and implications for understanding metazoan Hedgehog pathway evolution', *Dev Biol* 313(2): 501-18.

Matus, D. Q., Thomsen, G. H. and Martindale, M. Q. (2007) 'FGF signaling in gastrulation and neural development in Nematostella vectensis, an anthozoan cnidarian', *Dev Genes Evol* 217(2): 137-48.

Mazza, M. E., Pang, K., Martindale, M. Q. and Finnerty, J. R. (2007) 'Genomic organization, gene structure, and developmental expression of three clustered otx genes in the sea anemone *Nematostella vectensis*', *J Exp Zool B Mol Dev Evol* 308(4): 494-506.

Mazza, M. E., Pang, K., Reitzel, A. M., Martindale, M. Q. and Finnerty, J. R. (2010) 'A conserved cluster of three PRD-class homeobox genes (homeobrain, rx and orthopedia) in the Cnidaria and Protostomia', *Evodevo* 1(1): 3.

McGuire, S. E., Roman, G. and Davis, R. L. (2004) 'Gene expression systems in Drosophila: a synthesis of time and space', *Trends Genet* 20(8): 384-91.

Meyer, E. J., Ikmi, A. and Gibson, M. C. (2011) 'Interkinetic nuclear migration is a broadly conserved feature of cell division in pseudostratified epithelia', *Curr Biol* 21(6): 485-91.

Mikkola, M. L. (2007) 'Genetic basis of skin appendage development', *Semin Cell Dev Biol* 18(2): 225-36.

Miller, J. C., Tan, S., Qiao, G., Barlow, K. A., Wang, J., Xia, D. F., Meng, X., Paschon, D. E., Leung, E., Hinkley, S. J. et al. (2011) 'A TALE nuclease architecture for efficient genome editing', *Nat Biotechnol* 29(2): 143-8.

Momose, T., Kraus, Y. and Houliston, E. (2012) 'A conserved function for Strabismus in establishing planar cell polarity in the ciliated ectoderm during cnidarian larval development', *Development* 139(23): 4374-82.

Moses, K. and Rubin, G. M. (1991) 'Glass encodes a site-specific DNA-binding protein that is regulated in response to positional signals in the developing Drosophila eye', *Genes Dev* 5(4): 583-93.

Mounier, J., Vasselon, T., Hellio, R., Lesourd, M. and Sansonetti, P. J. (1992) 'Shigella flexneri enters human colonic Caco-2 epithelial cells through the basolateral pole', *Infect Immun* 60(1): 237-48.

Munder, S., Kasbauer, T., Prexl, A., Aufschnaiter, R., Zhang, X., Towb, P. and Bottger, A. (2010) 'Notch signalling defines critical boundary during budding in Hydra', *Dev Biol* 344(1): 331-45.

Munro, E. M. and Odell, G. M. (2002) 'Polarized basolateral cell motility underlies invagination and convergent extension of the ascidian notochord', *Development* 129(1): 13-24.

Nakanishi, N., Renfer, E., Technau, U. and Rentzsch, F. (2012) 'Nervous systems of the sea anemone Nematostella vectensis are generated by ectoderm and endoderm and shaped by distinct mechanisms', *Development* 139(2): 347-57.

Nielsen, C., Scharff, N. and Eibye-Jacobsen, D. (1996) 'Cladistic analyses of the animal kingdom', *Biological Journal of the Linnean Society* 57(4): 385-410.

Nubler-Jung, K., Bonitz, R. and Sonnenschein, M. (1987) 'Cell polarity during wound healing in an insect epidermis', *Development* 100(1): 163-70.

Nusrat, A., von Eichel-Streiber, C., Turner, J. R., Verkade, P., Madara, J. L. and Parkos, C. A. (2001) 'Clostridium difficile toxins disrupt epithelial barrier function by altering membrane microdomain localization of tight junction proteins', *Infect Immun* 69(3): 1329-36.

Ohya, T., Miaczynska, M., Coskun, U., Lommer, B., Runge, A., Drechsel, D., Kalaidzidis, Y. and Zerial, M. (2009) 'Reconstitution of Rab- and SNARE-dependent membrane fusion by synthetic endosomes', *Nature* 459(7250): 1091-7.

Park, M. and Moon, R. T. (2002) 'The planar cell-polarity gene stbm regulates cell behaviour and cell fate in vertebrate embryos', *Nat Cell Biol* 4(1): 20-5.

Parsot, C. (2009) 'Shigella type III secretion effectors: how, where, when, for what purposes?', *Curr Opin Microbiol* 12(1): 110-6.

Passamaneck, Y. J. and Martindale, M. Q. (2012) 'Cell proliferation is necessary for the regeneration of oral structures in the anthozoan cnidarian Nematostella vectensis', *BMC Dev Biol* 12: 34.

Patthey, C., Schlosser, G. and Shimeld, S. M. (2014) 'The evolutionary history of vertebrate cranial placodes - I: Cell type evolution', *Dev Biol*.

Pereira-Leal, J. B. and Seabra, M. C. (2001) 'Evolution of the Rab family of small GTP-binding proteins', *J Mol Biol* 313(4): 889-901.

Petcherski, A. G. and Kimble, J. (2000) 'Mastermind is a putative activator for Notch', *Curr Biol* 10(13): R471-3.

Peterson, K. J. and Eernisse, D. J. (2001) 'Animal phylogeny and the ancestry of bilaterians: inferences from morphology and 18S rDNA gene sequences', *Evol Dev* 3(3): 170-205.

Phelan, P. and Starich, T. A. (2001) 'Innexins get into the gap', *Bioessays* 23(5): 388-96.

Philipp, I., Aufschnaiter, R., Ozbek, S., Pontasch, S., Jenewein, M., Watanabe, H., Rentzsch, F., Holstein, T. W. and Hobmayer, B. (2009) 'Wnt/beta-catenin and noncanonical Wnt signaling interact in tissue evagination in the simple eumetazoan Hydra', *Proc Natl Acad Sci U S A* 106(11): 4290-5.

Pierce, S. B. and Kimelman, D. (1995) 'Regulation of Spemann organizer formation by the intracellular kinase Xgsk-3', *Development* 121(3): 755-65.

Pignoni, F. and Zipursky, S. L. (1997) 'Induction of Drosophila eye development by decapentaplegic', *Development* 124(2): 271-8.

Pires-daSilva, A. and Sommer, R. J. (2003) 'The evolution of signalling pathways in animal development', *Nat Rev Genet* 4(1): 39-49.

Pispa, J. and Thesleff, I. (2003) 'Mechanisms of ectodermal organogenesis', *Dev Biol* 262(2): 195-205.

Putnam, N. H., Srivastava, M., Hellsten, U., Dirks, B., Chapman, J., Salamov, A., Terry, A., Shapiro, H., Lindquist, E., Kapitonov, V. V. et al. (2007) 'Sea anemone genome reveals ancestral eumetazoan gene repertoire and genomic organization', *Science* 317(5834): 86-94.

Reitzel, A. M., Burton, P. M., Krone, C. and Finnerty, J. R. (2007) 'Comparison of developmental trajectories in the starlet sea anemone *Nemaostella vectensis*:

embryogenesis, regeneration, and two forms of asexual fission', *Invert Biol* 126(2): 99-112.

Ren, M., Xu, G., Zeng, J., De Lemos-Chiarandini, C., Adesnik, M. and Sabatini, D. D. (1998) 'Hydrolysis of GTP on rab11 is required for the direct delivery of transferrin from the pericentriolar recycling compartment to the cell surface but not from sorting endosomes', *Proc Natl Acad Sci U S A* 95(11): 6187-92.

Renfer, E., Amon-Hassenzahl, A., Steinmetz, P. R. and Technau, U. (2010) 'A muscle-specific transgenic reporter line of the sea anemone, Nematostella vectensis', *Proc Natl Acad Sci U S A* 107(1): 104-8.

Rentzsch, F., Anton, R., Saina, M., Hammerschmidt, M., Holstein, T. W. and Technau, U. (2006) 'Asymmetric expression of the BMP antagonists chordin and gremlin in the sea anemone Nematostella vectensis: implications for the evolution of axial patterning', *Dev Biol* 296(2): 375-87.

Rentzsch, F., Fritzenwanker, J. H., Scholz, C. B. and Technau, U. (2008) 'FGF signalling controls formation of the apical sensory organ in the cnidarian Nematostella vectensis', *Development* 135(10): 1761-9.

Rigo-Watermeier, T., Kraft, B., Ritthaler, M., Wallkamm, V., Holstein, T. and Wedlich, D. (2012) 'Functional conservation of Nematostella Wnts in canonical and noncanonical Wnt-signaling', *Biol Open* 1(1): 43-51.

Roeth, J. F., Sawyer, J. K., Wilner, D. A. and Peifer, M. (2009) 'Rab11 helps maintain apical crumbs and adherens junctions in the Drosophila embryonic ectoderm', *PLoS One* 4(10): e7634.

Roosen-Runge, E. C. (1970) 'Life cycle of the hydromedusa *Philidium gregarium* (A. Agassiz, 1862) in the laboratory', *Biol Bull* 139: 203-221.

Rottinger, E., Dahlin, P. and Martindale, M. Q. (2012) 'A framework for the establishment of a cnidarian gene regulatory network for "endomesoderm" specification: the inputs of ss-catenin/TCF signaling', *PLoS Genet* 8(12): e1003164.

Ryan, J. F., Burton, P. M., Mazza, M. E., Kwong, G. K., Mullikin, J. C. and Finnerty, J. R. (2006) 'The cnidarian-bilaterian ancestor possessed at least 56 homeoboxes: evidence from the starlet sea anemone, *Nematostella vectensis*', *Genome Biol* 7(7): R64.

Ryan, J. F., Mazza, M. E., Pang, K., Matus, D. Q., Baxevanis, A. D., Martindale, M. Q. and Finnerty, J. R. (2007) 'Pre-bilaterian origins of the Hox cluster and the Hox code: evidence from the sea anemone, Nematostella vectensis', *PLoS One* 2(1): e153.

Ryan, J. F., Pang, K., Schnitzler, C. E., Nguyen, A. D., Moreland, R. T., Simmons, D. K., Koch, B. J., Francis, W. R., Havlak, P., Smith, S. A. et al. (2013) 'The genome of the ctenophore Mnemiopsis leidyi and its implications for cell type evolution', *Science* 342(6164): 1242592.

Saina, M., Genikhovich, G., Renfer, E. and Technau, U. (2009) 'BMPs and chordin regulate patterning of the directive axis in a sea anemone', *Proc Natl Acad Sci U S A* 106(44): 18592-7.

Sansonetti, P. J., Arondel, J., Cantey, J. R., Prevost, M. C. and Huerre, M. (1996) 'Infection of rabbit Peyer's patches by Shigella flexneri: effect of adhesive or

invasive bacterial phenotypes on follicle-associated epithelium', *Infect Immun* 64(7): 2752-64.

Schlosser, G., Patthey, C. and Shimeld, S. M. (2014) 'The evolutionary history of vertebrate cranial placodes II. Evolution of ectodermal patterning', *Dev Biol*.

Schock, F. and Perrimon, N. (2002) 'Molecular mechanisms of epithelial morphogenesis', *Annu Rev Cell Dev Biol* 18: 463-93.

Schram, F. R. (1991) Cladistic analysis of metazoan phyla and the placement of fossil problematica. in E. M. Simonetta and S. Conway-Morris (eds.) *The early evolution of metazoa and the significance of problematic taxa*. Cambridge: Cambridge University Press.

Schroeder, G. N. and Hilbi, H. (2008) 'Molecular pathogenesis of Shigella spp.: controlling host cell signaling, invasion, and death by type III secretion', *Clin Microbiol Rev* 21(1): 134-56.

Schwartz, S. L., Cao, C., Pylypenko, O., Rak, A. and Wandinger-Ness, A. (2007) 'Rab GTPases at a glance', *J Cell Sci* 120(Pt 22): 3905-10.

Shih, J. and Keller, R. (1992) 'Cell motility driving mediolateral intercalation in explants of Xenopus laevis', *Development* 116(4): 901-14.

Shimizu, H., Bode, P. M. and Bode, H. R. (1995) 'Patterns of oriented cell division during the steady-state morphogenesis of the body column in hydra', *Dev Dyn* 204(4): 349-57.

Shirane, M. and Nakayama, K. I. (2006) 'Protrudin induces neurite formation by directional membrane trafficking', *Science* 314(5800): 818-21.

Simons, M. and Mlodzik, M. (2008) 'Planar cell polarity signaling: from fly development to human disease', *Annu Rev Genet* 42: 517-40.

Sinigaglia, C., Busengdal, H., Leclere, L., Technau, U. and Rentzsch, F. (2013) 'The bilaterian head patterning gene six3/6 controls aboral domain development in a cnidarian', *PLoS Biol* 11(2): e1001488.

Sivars, U., Aivazian, D. and Pfeffer, S. R. (2003) 'Yip3 catalyses the dissociation of endosomal Rab-GDI complexes', *Nature* 425(6960): 856-9.

Smith, K. M., Gee, L., Blitz, I. L. and Bode, H. R. (1999) 'CnOtx, a member of the Otx gene family, has a role in cell movement in hydra', *Dev Biol* 212(2): 392-404.

Smith, K. M., Gee, L. and Bode, H. R. (2000) 'HyAlx, an aristaless-related gene, is involved in tentacle formation in hydra', *Development* 127(22): 4743-52.

Smollett, K., Shaw, R. K., Garmendia, J., Knutton, S. and Frankel, G. (2006) 'Function and distribution of EspG2, a type III secretion system effector of enteropathogenic Escherichia coli', *Microbes Infect* 8(8): 2220-7.

Smyth, G. K. (2004) 'Linear models and empirical bayes methods for assessing differential expression in microarray experiments', *Stat Appl Genet Mol Biol* 3: Article3.

Soldati, T., Shapiro, A. D., Svejstrup, A. B. and Pfeffer, S. R. (1994) 'Membrane targeting of the small GTPase Rab9 is accompanied by nucleotide exchange', *Nature* 369(6475): 76-8.

Stefanik, D. J., Friedman, L. E. and Finnerty, J. R. (2013) 'Collecting, rearing, spawning and inducing regeneration of the starlet sea anemone, Nematostella vectensis', *Nat Protoc* 8(5): 916-23.

Stenmark, H. (2009) 'Rab GTPases as coordinators of vesicle traffic', *Nat Rev Mol Cell Biol* 10(8): 513-25.

Streit, A. (2007) 'The preplacodal region: an ectodermal domain with multipotential progenitors that contribute to sense organs and cranial sensory ganglia', *Int J Dev Biol* 51(6-7): 447-61.

Stroupe, C. and Brunger, A. T. (2000) 'Crystal structures of a Rab protein in its inactive and active conformations', *J Mol Biol* 304(4): 585-98.

Struhl, G. and Basler, K. (1993) 'Organizing activity of wingless protein in Drosophila', *Cell* 72(4): 527-40.

Sullivan, J. C. and Finnerty, J. R. (2007) 'A surprising abundance of human disease genes in a simple "basal" animal, the starlet sea anemone (Nematostella vectensis)', *Genome* 50(7): 689-92.

Sullivan, J. C., Reitzel, A. M. and Finnerty, J. R. (2008) 'Upgrades to StellaBase facilitate medical and genetic studies on the starlet sea anemone, *Nematostella vectensis*', *Nucleic Acids Res* 36(Database issue): D607-11.

Sullivan, J. C., Ryan, J. F., Watson, J. A., Webb, J., Mullikin, J. C., Rokhsar, D. and Finnerty, J. R. (2006) 'StellaBase: the *Nematostella vectensis* Genomics Database', *Nucleic Acids Res* 34(Database issue): D495-9.

Szczepanek, S., Cikala, M. and David, C. N. (2002) 'Poly-gamma-glutamate synthesis during formation of nematocyst capsules in Hydra', *J Cell Sci* 115(Pt 4): 745-51.

Takahashi, T., Hatta, M., Yum, S., Gee, L., Ohtani, M., Fujisawa, T. and Bode, H. R. (2005) 'Hym-301, a novel peptide, regulates the number of tentacles formed in hydra', *Development* 132(9): 2225-34.

Technau, U. (2010) 'The sea anemone *Nematostella vectensis* as a model system for the study of the evolutionary origin of triploblasty and bilaterality', paper given at a conference on 'Willi-Henning Symposium on Phylogenetics and Evolution', University of Hohenheim.

Tepass, U. (1996) 'Crumbs, a component of the apical membrane, is required for zonula adherens formation in primary epithelia of Drosophila', *Dev Biol* 177(1): 217-25.

Tepass, U. and Hartenstein, V. (1994) 'The development of cellular junctions in the Drosophila embryo', *Dev Biol* 161(2): 563-96.

Tepass, U., Tanentzapf, G., Ward, R. and Fehon, R. (2001) 'Epithelial cell polarity and cell junctions in Drosophila', *Annu Rev Genet* 35: 747-84.

Trevino, M., Stefanik, D. J., Rodriguez, R., Harmon, S. and Burton, P. M. (2011) 'Induction of canonical Wnt signaling by alsterpaullone is sufficient for oral tissue fate during regeneration and embryogenesis in *Nematostella vectensis*', *Developmental Dynamics* 240: 2673-2679.

Tsukita, S. and Furuse, M. (2002) 'Claudin-based barrier in simple and stratified cellular sheets', *Curr Opin Cell Biol* 14(5): 531-6.

Tsukita, S., Furuse, M. and Itoh, M. (2001) 'Multifunctional strands in tight junctions', *Nat Rev Mol Cell Biol* 2(4): 285-93.

Uchiya, K., Tobe, T., Komatsu, K., Suzuki, T., Watarai, M., Fukuda, I., Yoshikawa, M. and Sasakawa, C. (1995) 'Identification of a novel virulence gene, virA, on the large plasmid of Shigella, involved in invasion and intercellular spreading', *Mol Microbiol* 17(2): 241-50.

Ullrich, O., Horiuchi, H., Bucci, C. and Zerial, M. (1994) 'Membrane association of Rab5 mediated by GDP-dissociation inhibitor and accompanied by GDP/GTP exchange', *Nature* 368(6467): 157-60.

Ullrich, O., Stenmark, H., Alexandrov, K., Huber, L. A., Kaibuchi, K., Sasaki, T., Takai, Y. and Zerial, M. (1993) 'Rab GDP dissociation inhibitor as a general regulator for the membrane association of rab proteins', *J Biol Chem* 268(24): 18143-50.

Verlhac, M. H., Villeneuve, A., Amiel, A., Chang, P., Momose, T. and Houliston, E. (2010) *Clytia hemisphaerica*: A cnidarian model for studing oogenesis. in M. H. Verlhac and A. Villeneuve (eds.) *Oogenesis: The universial process*. Chichester, UK: John Wiley & Sons, Ltd.

Wallingford, J. B. and Harland, R. M. (2002) 'Neural tube closure requires Dishevelled-dependent convergent extension of the midline', *Development* 129(24): 5815-25.

Wassef, J. S., Keren, D. F. and Mailloux, J. L. (1989) 'Role of M cells in initial antigen uptake and in ulcer formation in the rabbit intestinal loop model of shigellosis', *Infect Immun* 57(3): 858-63.

Wei, Y. and Mikawa, T. (2000) 'Formation of the avian primitive streak from spatially restricted blastoderm: evidence for polarized cell division in the elongating streak', *Development* 127(1): 87-96.

WHO (2005) Guidelines for the control of shigellosis, including epidemics due to *Shigella dysenteriae* type 1. Geneva, Switzerland: WHO Press.

Wikramanayake, A. H., Hong, M., Lee, P. N., Pang, K., Byrum, C. A., Bince, J. M., Xu, R. and Martindale, M. Q. (2003) 'An ancient role for nuclear beta-catenin in the evolution of axial polarity and germ layer segregation', *Nature* 426(6965): 446-50.

Winter, C. G., Wang, B., Ballew, A., Royou, A., Karess, R., Axelrod, J. D. and Luo, L. (2001) 'Drosophila Rho-associated kinase (Drok) links Frizzled-mediated planar cell polarity signaling to the actin cytoskeleton', *Cell* 105(1): 81-91.

Wodarz, A., Ramrath, A., Grimm, A. and Knust, E. (2000) 'Drosophila atypical protein kinase C associates with Bazooka and controls polarity of epithelia and neuroblasts', *J Cell Biol* 150(6): 1361-74.

Wolenski, F. S., Bradham, C. A., Finnerty, J. R. and Gilmore, T. D. (2013) 'NF-kappaB is required for cnidocyte development in the sea anemone Nematostella vectensis', *Dev Biol* 373(1): 205-15.

Wood, A. J., Lo, T. W., Zeitler, B., Pickle, C. S., Ralston, E. J., Lee, A. H., Amora, R., Miller, J. C., Leung, E., Meng, X. et al. (2011) 'Targeted genome editing across species using ZFNs and TALENs', *Science* 333(6040): 307.

Wu, L., Aster, J. C., Blacklow, S. C., Lake, R., Artavanis-Tsakonas, S. and Griffin, J. D. (2000a) 'MAML1, a human homologue of *Drosophila* mastermind, is a transcriptional co-activator for NOTCH receptors', *Nat Genet* 26(4): 484-9.

Wu, S., Lim, K. C., Huang, J., Saidi, R. F. and Sears, C. L. (1998) 'Bacteroides fragilis enterotoxin cleaves the zonula adherens protein, E-cadherin', *Proc Natl Acad Sci U S A* 95(25): 14979-84.

Wu, Z., Nybom, P. and Magnusson, K. E. (2000b) 'Distinct effects of Vibrio cholerae haemagglutinin/protease on the structure and localization of the tight junction-associated proteins occludin and ZO-1', *Cell Microbiol* 2(1): 11-7.

Xu, J., Lan, L., Bogard, N., Mattione, C. and Cohen, R. S. (2011) 'Rab11 is required for epithelial cell viability, terminal differentiation, and suppression of tumor-like growth in the Drosophila egg chamber', *PLoS One* 6(5): e20180.

Xu, T. and Rubin, G. M. (1993) 'Analysis of genetic mosaics in developing and adult Drosophila tissues', *Development* 117(4): 1223-37.

Yaross, M. S., Westerfield, J., Javois, L. C. and Bode, H. R. (1986) 'Nerve cells in hydra: monoclonal antibodies identify two lineages with distinct mechanisms for their incorporation into head tissue', *Dev Biol* 114(1): 225-37.

Yoshida, S., Handa, Y., Suzuki, T., Ogawa, M., Suzuki, M., Tamai, A., Abe, A., Katayama, E. and Sasakawa, C. (2006) 'Microtubule-severing activity of Shigella is pivotal for intercellular spreading', *Science* 314(5801): 985-9.

Yoshida, S., Katayama, E., Kuwae, A., Mimuro, H., Suzuki, T. and Sasakawa, C. (2002) 'Shigella deliver an effector protein to trigger host microtubule destabilization, which promotes Rac1 activity and efficient bacterial internalization', *EMBO J* 21(12): 2923-35.

Zarnescu, D. C. and Thomas, G. H. (1999) 'Apical spectrin is essential for epithelial morphogenesis but not apicobasal polarity in Drosophila', *J Cell Biol* 146(5): 1075-86.

Zerial, M. and McBride, H. (2001) 'Rab proteins as membrane organizers', *Nat Rev Mol Cell Biol* 2(2): 107-17.

Zhang, J., Schulze, K. L., Hiesinger, P. R., Suyama, K., Wang, S., Fish, M., Acar, M., Hoskins, R. A., Bellen, H. J. and Scott, M. P. (2007) 'Thirty-one flavors of Drosophila rab proteins', *Genetics* 176(2): 1307-22.

Zrzavy, J., Mihulka, S., Kepka, P., Bezdek, A. and Tietz, D. (1998) 'Phylogeny of the Metazoa based on morphological and 18S ribosomal DNA evidence', *Cladistics* 14: 249–285.

Zychlinsky, A., Prevost, M. C. and Sansonetti, P. J. (1992) 'Shigella flexneri induces apoptosis in infected macrophages', *Nature* 358(6382): 167-9.